

***CRYPTOSPORIDIUM* DETECTION THROUGH ANTIBODY  
IMMOBILIZATION ON A SOLID SURFACE**

by

Rony Das

B.Sc., Bangladesh University of Engineering and Technology, 2007

A THESIS SUBMITTED IN PARTIAL FULFILLMENT  
OF THE REQUIREMENTS FOR THE DEGREE OF

MASTER OF APPLIED SCIENCE

in

The College of Graduate Studies

(Civil Engineering)

THE UNIVERSITY OF BRITISH COLUMBIA  
(Okanagan)

August 2010

© Rony Das, 2010

## Abstract

Current detection of pathogenic organisms in water relies on the use of indicators (turbidity, *Escherichia coli*, total coliforms, fecal coliforms etc.) or time consuming assays that can only be done in a specialized laboratory. In this research a simple assay was developed for rapid and sensitive recovery and identification of waterborne pathogens from environmental samples. The assay developed involves capturing target pathogens onto an activated capture surface, exposing the capture surface to antibody conjugated micro-retroreflectors, and then inserting the capture surface into an inexpensive, simple reader to detect the retroreflection signal to confirm the presence of target pathogens.

Antibody (capture molecule: IgG and IgM) fragments specific to *Cryptosporidium*, as a model waterborne pathogen, were produced and immobilized site specifically and randomly onto gold-coated surfaces as well as corner cube micro-retroreflectors (ccμRR). A shear test performed to determine the critical shear stress that antigen-antibody bonds are able to endure showed that the organism-antibody bond could resist up to a shear stress of 126 dyne/cm<sup>2</sup> and beyond this critical value immobilized *Cryptosporidium* oocysts were lost from the system. Capture tests were designed to determine the optimum operating conditions of the parallel flow sampling device using IgG-Fab', IgG-Fab, and IgM-Fab' activated surfaces. Capture efficiencies did not differ significantly within the range of flow rate used (14 – 42 mL/min), but improvement was noticed when the cell depth was decreased from 250 μm to 125 μm. Site specifically oriented IgG-Fab' activated surfaces resulted in significantly better capture efficiencies than surface with randomly immobilized IgG-Fab fragments. The capture efficiency of IgG-Fab' activated surfaces was significantly different than that of IgM-Fab' immobilized surfaces. There

was no significant difference in capture efficiency using the surfaces activated with dilutions (1:8, 1:4, 1:2, and 1:1.5) of antibody fragments originally made of 500 $\mu$ g of IgG<sub>1</sub> antibody. The use of BSA as a blocking agent improved the reproducibility of the capture efficiency. Cc $\mu$ RR were suspended in solution and activated with IgG-Fab' to use as a recognition molecule. The current set up of the detector system is capable of detecting the presence and absence of a large number of cc $\mu$ RR attached on the solid surface.

# Table of Contents

<b>Abstract</b> .....	ii
<b>Table of Contents</b> .....	iv
<b>List of Tables</b> .....	vi
<b>List of Figures</b> .....	vii
<b>Acknowledgements</b> .....	viii
<b>Dedication</b> .....	ix
<b>Chapter 1: Introduction</b> .....	1
<b>1.1 Background and motivation</b> .....	1
<b>1.2 Objectives</b> .....	2
<b>1.3 Thesis organization</b> .....	3
<b>Chapter 2: Literature Review</b> .....	5
<b>2.1 Sample collection and concentration</b> .....	6
2.1.1 Flocculation and sedimentation .....	6
2.1.1.1 Calcium carbonate flocculation .....	6
2.1.1.2 Ferric sulphate and aluminum sulphate flocculation .....	7
2.1.2 Filtration .....	10
2.1.3 Continuous flow centrifugation .....	16
<b>2.2 Re-concentration and purification</b> .....	18
2.2.1 Density gradient separation .....	18
2.2.2 Immunomagnetic separation (IMS).....	20
<b>2.3 Detection</b> .....	24
2.3.1 Immunofluorescent assay .....	24
2.3.2 Flow cytometry.....	28
<b>2.4 Antibody chemistry</b> .....	30
<b>2.5 Immobilization of antibodies onto solid surfaces</b> .....	32
<b>Chapter 3: Materials and Methods</b> .....	40
<b>3.1 Source of <i>Cryptosporidium</i> oocysts and antibodies</b> .....	40
<b>3.2 Preparation of antibody fragments</b> .....	40
3.2.1 Preparation of IgG <sub>1</sub> -Fab' antibody fragments.....	40

3.2.2 Preparation of IgG <sub>1</sub> -Fab antibody fragments.....	41
3.2.3 Preparation of IgM-Fab' antibody fragments.....	42
<b>3.3 Gold coated slide preparation .....</b>	<b>42</b>
<b>3.4 Antibody fragment immobilization.....</b>	<b>42</b>
<b>3.5 Preparation of <i>Cryptosporidium parvum</i> oocysts.....</b>	<b>43</b>
<b>3.6 Design of shear test .....</b>	<b>44</b>
<b>3.7 Design of capture tests .....</b>	<b>45</b>
<b>3.8 Implementation of retroreflectors.....</b>	<b>47</b>
3.8.1 Retroreflector cube release .....	47
3.8.2 Retroreflector activation.....	48
<b>3.9 Detector system.....</b>	<b>48</b>
<b>3.10 Statistical analysis.....</b>	<b>50</b>
<b>Chapter 4: Results and Discussion .....</b>	<b>51</b>
<b>4.1 Shear test results.....</b>	<b>51</b>
<b>4.2 Capture test results.....</b>	<b>53</b>
4.2.1 IgG-Fab'.....	55
4.2.2 IgM-Fab'.....	57
4.2.3 IgG-Fab .....	59
4.2.4 Effect of antibody type .....	59
4.2.5 Effect of antibody fragments .....	60
4.2.6 Effect of antibody loading .....	60
<b>4.3 Blocking using BSA .....</b>	<b>62</b>
<b>4.4 Implementation of retroreflectors.....</b>	<b>63</b>
<b>4.5 Detection system .....</b>	<b>65</b>
<b>4.6 Discussion.....</b>	<b>70</b>
<b>Chapter 5: Conclusions and Recommendations.....</b>	<b>74</b>
<b>5.1 General .....</b>	<b>74</b>
<b>5.2 Limitations of the study .....</b>	<b>75</b>
<b>5.3 Future recommendations .....</b>	<b>76</b>
<b>References.....</b>	<b>78</b>
<b>Appendices .....</b>	<b>91</b>
<b>Appendix A.....</b>	<b>91</b>
<b>Appendix B.....</b>	<b>92</b>

## List of Tables

Table 2.1: Summary of steps for <i>Cryptosporidium</i> detection .....	5
Table 2.2: Flocculation used for concentration of <i>Cryptosporidium</i> oocysts.....	9
Table 2.3: Filtration used for concentration of <i>Cryptosporidium</i> oocysts.....	11
Table 2.4: Commercially available <i>Cryptosporidium</i> specific antibodies.....	26
Table 2.5: Site specific antibody immobilization strategies.....	34
Table 3.1: Hydrodynamic experimental variables of capture tests.....	47
Table 4.1: Summary of capture test results (direct microscopic observation).....	54
Table 4.2: Capture test results with different antibody concentration.....	61
Table B.1: Shear test results .....	92
Table B.2: Capture test results for surface activation using IgG-Fab' fragments .....	93
Table B.3: Capture test results for surface activation using IgM-Fab' fragments .....	94
Table B.4: Capture test results for surface activation using IgG -Fab fragments.....	95
Table B.5: Sample raw data of capture test at 1:8 dilution.....	96

## List of Figures

Figure 2.1: Schematic diagram of IgG and its fragments.....	31
Figure 2.2: Schematic representation of mouse IgM.....	32
Figure 3.1: Fragmentation of IgG <sub>1</sub> to Fab'.....	41
Figure 3.2: Shear test and capture test setup .....	45
Figure 3.3: Detector system.....	49
Figure 3.4: Schematic of detector system configuration .....	49
Figure 4.1: Microscopic image used for Matlab analysis.....	51
Figure 4.2: Matlab output (Histogram) .....	52
Figure 4.3: Example of total while pixel count before and after the shear experiment at 81 mL/min flow rate and 250 $\mu$ m cell depth .....	52
Figure 4.4: Capture efficiency of different antibody fragments under different treatment conditions .....	54
Figure 4.5: <i>Cryptosporidium</i> recovery with respect to the flow rate (IgG-Fab').....	56
Figure 4.6: <i>Cryptosporidium</i> recovery with respect to the depth of flow cell (IgG-Fab').....	56
Figure 4.7: <i>Cryptosporidium</i> recovery with respect to the shear stress (IgG-Fab').....	57
Figure 4.8: <i>Cryptosporidium</i> recovery with respect to the flow rate (IgM-Fab') .....	58
Figure 4.9: <i>Cryptosporidium</i> recovery with respect to the depth of flow cell (IgM-Fab') .....	58
Figure 4.10: <i>Cryptosporidium</i> recovery with respect to the shear stress (IgM-Fab') .....	59
Figure 4.11: Optimization of antibody concentration .....	62
Figure 4.12: Unreleased retroreflector on wafer (8X magnification).....	64
Figure 4.13: Wafer after retroreflector was released (8X magnification) .....	64
Figure 4.14: Property of retroreflector .....	65
Figure 4.15: Preliminary Signal detection configuration .....	66
Figure 4.16: Modified setup of the signal detector system.....	68
Figure 4.17: Image of slide with retroreflectors while laser was off.....	69
Figure 4.18: Image of retroreflectors with clear edge .....	69

## **Acknowledgements**

I would like to offer enduring gratitude to my supervisor Dr. Deborah J. Roberts for her guidance and support throughout my tenure at the University of British Columbia. I would also like to extend gratitude to my committee members, Dr. Mina Hoorfar, Dr. Jonathan Holzman, and Dr. Deanna Gibson for their advice and time.

Deanna Ericson and Danny Trommelen have been an integral part in completion of this work. Deanna fabricated the gold surfaces during the experiments and Danny assisted in counting the capture test slides. Both of them assisted in the development of the detection system. I would like to thank the entire Dr. Roberts lab group for their advice throughout the project and specifically Yeyuan Xiao for his help in performing experiments. Sina Jomeh has provided valuable help and discussions over the years.

I would like to thank all my friends and family for their help and encouragement throughout my entire life. My parents have provided unwavering support and belief in me as I moved across the continent and entered graduate school.

My most heartfelt appreciation goes out to my wife, Snigdha for providing me with the motivation to complete my research.

## **Dedication**

**To my parents and wife**

# Chapter 1: Introduction

## 1.1 Background and motivation

*Cryptosporidium* is an obligate intracellular, protozoan parasite of great public health significance as it is ubiquitous in source waters throughout the world and resistant to standard water treatment processes (Korich et al. 1990; Robertson et al. 1992; Steiner et al., 1997; Karanis et al. 2007). Ingestion of a low dose (median infectious dose of 132 viable oocysts) can cause cryptosporidiosis to healthy individuals (Dupont et al. 1995). Currently, there is no specific treatment for cryptosporidiosis. The infection can be life-threatening to immune-suppressed patients and may also cause serious gastrointestinal illness to healthy people (Goldstein et al. 1996). Steiner et al., 1997;

Millions of environmentally resistant oocysts, which can stay viable in fresh water up to 6 months, can be shed from infected individuals (Thomas et al. 2000). Many outbreaks of cryptosporidiosis have been reported all around the world caused by contaminated drinking and recreational water supplies (Karanis et al. 2007). Of these, the most infamous outbreak was in Milwaukee, Wisconsin, USA in 1993; more than 400,000 people were infected, of which 4,400 were hospitalized and 69 died (Mackenzie et al. 1994; Corso et al. 2003). In most of the cases, the key cause was reported to be the failure of a water treatment plant process (Mackenzie et al. 1994; Karanis et al. 2007). A method for monitoring *Cryptosporidium* in treated water by plant operators on a regular basis is required to protect the public.

Most water facilities rely on turbidity and total coliform as surrogates for regular monitoring of *Cryptosporidium* in source water. But, consistent co-occurrence of these surrogates and *Cryptosporidium* oocysts is not confirmed (Nieminski et al., 2000).

Routine analysis and monitoring of waterborne *Cryptosporidium* is complicated for several reasons. Their small size (4 – 6µm), inability to *in vitro* culture, presence in low concentration in water sources are the most challenging parameters. A large volume of water must be sampled to increase the probability of detection. Turbidity is another important factor that affects the detection of *Cryptosporidium* from environmental water samples. Various inorganic particles such as clay, silt, and organic matter, for example algae, impart turbidity to water and are responsible for filter clogging, adversely affecting purification steps and subsequent detection.

The current methods are time-consuming, labor-intensive, insensitive, expensive, and require well-trained personnel and highly equipped lab facilities. The turnaround time is also relatively long ( $\geq 24$  hrs). These quantitative methods are a challenge to implement for routine (daily) monitoring. Therefore, a simple in house and near real time (turnaround time  $< 24$  hrs) method is needed for the detection of *Cryptosporidium* spp. for frequent analysis of environmental samples.

## **1.2 Objectives**

The overall objective of this research is to develop a sensitive and near real time system for the detection of *Cryptosporidium* in drinking water. The detection tool consists of a sampling cell with capture surface activated with *Cryptosporidium* specific capture molecules. *Cryptosporidium* specific antibodies will be used as a capture molecule to prepare the capture surface in this research. The sampling cell is then installed in an online system for continuous monitoring or connected to a batch of water and allowed to capture *Cryptosporidium* from the suspension for a specified time period on the antibody activated surface. After sampling, the capture surface is placed in a solution of corner cube micro-retroreflectors (ccµRR: 2 – 5 micron cubes with 3 mirrored sides, conjugated with the same

or a second capture molecule) that will bind to the captured oocysts. The surface is then rinsed and put in a detector system that measures the presence of the organisms and the position on the surface by the image analysis of the reflected light from the ccμRR. This method is expected to be near real time taking one day for complete analysis. The specific objectives of this thesis are:

- To select an anti-*Cryptosporidium* spp. antibody as capture molecule based on the specificity and avidity using current literature.
- To select a strategy to immobilize antibody onto a solid surface.
- To determine the antibody type and fragment to be used in preparing the capture surface.
- To determine the optimum operating conditions (flow rate and cell depth) of the sample cell.
- To optimize antibody loading on the solid surface with respect to *Cryptosporidium* capture efficiency.
- To activate suspended ccμRR.
- To develop a signal detector system to detect captured *Cryptosporidium* spp. using surface activated micro-retroreflectors.

### **1.3 Thesis organization**

The thesis is organized into five chapters. Chapter 1: Introduction gives the background and motivation of this research. The objectives of this work are also outlined in this chapter. The literature involving the current detection methods for *Cryptosporidium* spp. in environmental samples is reviewed in Chapter 2: Literature Review. The efficiency of various *Cryptosporidium* specific antibodies and immobilization strategies of these antibodies onto solid surfaces are also reviewed. Chapter 3: Materials and Methods deals

with the materials and methods used in the experiments. This chapter is followed by the Results and discussion chapter (Chapter 4). Key outcomes this research is summarized in the final chapter (Chapter 5: Conclusions and Recommendations). The limitations of this research and the recommendations for the future research are also included in this chapter. The references cited are presented in Chapter 6. Part of this research has been submitted for publication, and some of the current work is still under preparation for publication.

## Chapter 2: Literature Review

A number of reviews have been published addressing different aspects of the detection of pathogens such as methods for concentration, purification, and detection of different waterborne parasites separately (Quintero-Betancourt et al. 2002; Wohlsen et al. 2004; Zarlenga and Trout 2004; Wohlsen and Katouli 2008). Table 2.1 presents a summary of the different steps required for *Cryptosporidium* detection, typical recovery efficiency, and minimum processing time required for each step. The reported sampling and concentration time varies from 0.5 – 4.5 hours depending on the type of sampling technique used, the volume of water sampled, and the sample water quality. A wide range of average recovery efficiency (15 – 85%) was reported in the concentration stage. Depending on the technique used, the time for analysis could be up to 2.5 hours for sample reconcentration, purification, and detection. A maximum average recovery of equal to or more than 95% was achievable. Each method is critically evaluated below with respect to the complexity, recovery efficiency and time of analysis.

**Table 2.1: Summary of steps for *Cryptosporidium* detection**

Step	Method	Typical recovery efficiency range (%)	Minimum processing time (hours)
Sampling and concentration	Flocculation	45 – 75	4.5
	Filtration	15 – 80	0.5
	Continuous flow centrifugation	30 – 85	1.0
Reconcentration and purification	Density gradient separation	60 – 70	0.3
	Immunomagnetic separation	85 – 95	1.5
Detection	Immunofluorescence assay	95 – 99	2.5
	Flow cytometry	95 – 99	1.5

## **2.1 Sample collection and concentration**

*Cryptosporidium* spp. is ubiquitous in many water sources, but present in low numbers. The sampling technique used must concentrate *Cryptosporidium* oocysts from a large volume of sample to increase the probability and sensitivity of detection. A number of methods such as centrifugation, sedimentation, filtration etc. have been employed to concentrate *Cryptosporidium* spp. and are reviewed in the following sections:

### 2.1.1 Flocculation and sedimentation

Although *Cryptosporidium* spp. will settle out from water due to gravity, direct sedimentation is uneconomical due to the time required to sediment these small particles. In order to expedite the sedimentation process, the addition of flocculants (materials that encourage the formation of large particles (floc) from water samples) has been suggested by Vesey et al. (1993a). The flocculant such as calcium carbonate, aluminum sulphate, ferric sulphate etc. is added to a sample and the developed floc is allowed to settle for a specified time period (four hours or overnight). The supernatant is discarded carefully and undisturbed precipitate is dissolved with acid solution. The sample is then usually concentrated by centrifugation.

#### 2.1.1.1 Calcium carbonate flocculation

The procedure of Vesey et al. (1993a) included the addition of calcium chloride and sodium bicarbonate solutions (100 mL of 1 M solutions each) to a 10 L sample. After mixing, sodium hydroxide (1 M) was used to adjust the pH of the sample to 10. The sample was then left to settle out at room temperature for four hours. The supernatant liquid was then aspirated leaving the calcium carbonate residue undisturbed. The residue was then dissolved in 200 mL 10% (w/v) sulphamic acid solution. The sample was further concentrated by centrifugation and ready for enumeration. Greinert et al. (2004)

recommended the use of a 1% concentration of  $\text{NaHCO}_3$  (1 M) and  $\text{CaCl}_2$  (1 M) as the optimum dose for oocyst recovery, an increase in concentration above this optimum level increased the amount of precipitate while decreasing oocyst recovery efficiency.

Flocculation using calcium carbonate has been considered as quite an efficient means of concentrating *Cryptosporidium* in water since first proposed by Vesey et al. (1993a) who obtained a 73.7% (69.0 – 76.9%) mean recovery in a seeding experiment ( $61 \text{ oocysts L}^{-1}$ ) of 10 L tap-water samples. Recoveries from river water were in a similar range as the tap water. Using the same method, Campbell et al. (1994) achieved a recovery range of 66.0 – 93.4% (mean recovery 74.8%) for  $5 \times 10^5 \text{ oocysts.L}^{-1}$  in tap-water samples. Shepherd and Wyn-Jones (1995) evaluated different concentration techniques (cartridge filtration, membrane filtration, and flocculation) and concluded that calcium carbonate produced a high *Cryptosporidium* oocysts recovery (tap water mean 72.9 % and river water mean 41.9%) the most consistently. Later, Shepherd and Wyn-Jones (1996) reproduced the same mean recovery rate (73.6%) using tap-water and a higher recovery range (65.3 – 76.0%) for river water of low turbidity. Lower mean recovery rates (65.2% mean recovery for  $1 \times 10^6 \text{ oocysts L}^{-1}$  spiked in tap-water replicates) were achieved by Karanis and Kimura (2002). For lower oocyst numbers ( $2.5 \times 10^5 \text{ L}^{-1}$ ), the mean recovery rate was reduced significantly to 38.8%. In an experiment to evaluate techniques for detection of *Cryptosporidium* spp. oocysts in swimming pool filter backwash water, Greinert et al. (2004) used calcium carbonate flocculation to concentrate a 1 L filter backwash water sample and observed mean recovery of 48.3% ( $\pm 2.6\%$ ).

#### 2.1.1.2 Ferric sulphate and aluminum sulphate flocculation

A procedure developed by Karanis et al. (2002) included mixing the sample with ferric sulphate solution (9.37 g ferric sulphate per liter distilled  $\text{H}_2\text{O}$ ) and adjusting the pH of

the mixed solution to 6.0. Overnight incubation (approximately 24 hours) of the sample at room temperature ensured floc formation and precipitation. The resulting pellets (200 mL) were carefully separated from the supernatant by centrifugation at 2000 x g for 10 min (4 °C). The sample was then re-suspended and centrifuged two additional times. The final pellets (1 mL) were re-suspended in 1 mL citric acid buffer (8.4 g citric acid monohydrate, 17.64 g tri-sodium-citrate-dihydrate, distilled H<sub>2</sub>O up to 100 mL; pH 4.7) and mixed by vortexing every 15 minutes for one hour. The sample was then washed twice with distilled water at 2000 x g for 10 min. Oocysts in the final pellet (1 mL) were then ready for enumeration. Concentration via aluminum sulphate flocculation required the addition of 2 mL of aluminum sulphate solution (10.13 g aluminum sulphate per 100 mL distilled H<sub>2</sub>O) to 1 L of sample. The pH of the mixed solution was adjusted to pH 5.4 – 5.8. The rest of the concentration procedure using aluminum sulphate was same as that of ferric sulphate flocculation.

Vesey et al. (1993a) reported less than 10% recovery during flocculation of seeded oocysts using ferric sulphate as flocculent while adjusting the pH to 9.0. In contrast, Karanis and Kimura (2002) estimated higher recovery rates (more than 50%) when the pH was adjusted to 6.0 and also effectively recovered oocysts in solutions containing as low as 2.5 oocysts L<sup>-1</sup> and 1 oocyst L<sup>-1</sup>. Tsushima et al. (2003) reported the same oocyst recovery using ferric sulphate flocculation. Similar recovery efficiency (58 – 68%) was reported by Vesey et al. (1993a) and Karanis and Kimura (2002) using aluminum sulphate as the flocculant at different concentrations of seeded oocysts. Stanfield et al. (2000) compared recovery efficiencies using three flocculation techniques in a seeded untreated water sample and concluded that aluminum sulphate and ferric sulphate produced better recoveries than calcium carbonate. Ferric sulphate flocculation was better than aluminum sulphate in terms of simplicity in operation, because the flocs were

smaller and easier to collect and analyze. They obtained an optimal recovery more than 80% for both the flocculants with turbidity levels in between 6 to 15 NTU. They recorded a significant decrease in mean recovery (less than 50%) when the turbidity levels in the water were higher than 20 NTU.

The efficiency of a flocculant and subsequent oocyst recovery by flocculation typically depended on the pH along with other physical and chemical factors. Shepherd and Wyn-Jones (1996) suggested that flocculation followed by centrifugation at 5000 x g resulted in better oocyst recovery efficiency than concentration by centrifugation at 1500 x g. Vesey et al. (1993a) claimed that calcium carbonate flocculation produced the highest recovery over the other metallic flocculation; however, experiments by Karanis and Kimura (2002) revealed that the highest recovery was achieved by ferric chloride flocculation followed by aluminum sulphate and calcium chloride flocculation. After an epidemiological study of environmental water samples in Hokkaido, Japan, Tsushima et al. (2001) concluded that 1.7 – 330 times more oocysts were detected by flocculation (ferric sulphate) than by filtration. Though investigators assessed different modifications of the concentration procedures proposed by Vesey et al. (1993a) and used different enumeration techniques, more than 40% recovery was reported by various investigators using flocculation as a means of concentration (Table 2.2).

**Table 2.2: Flocculation used for concentration of *Cryptosporidium* oocysts**

Flocculent	Source	Recovery (%)		Spike con. (oocysts/L)
		Range	Mean (S.D.)	
Calcium Carbonate	Vesey et al. 1993a	69.0 – 76.9 <sup>b</sup>	73.3 <sup>b</sup>	1.00 × 10 <sup>3</sup>
		69.0 – 79.0 <sup>c</sup>	75.6 <sup>c</sup>	6.08 × 10 <sup>2</sup>
	Campbell et al. 1994	66.0 – 93.4 <sup>b</sup>	74.8 <sup>b</sup>	5.00 × 10 <sup>5</sup>
	Shepherd and Wyn-Jones 1995	70.8 – 75.2 <sup>b</sup>	72.9 <sup>b</sup>	5.00 × 10 <sup>1</sup>
		32.9 – 52.4 <sup>c</sup>	41.9 <sup>c</sup>	6.68 × 10 <sup>1</sup>
	Shepherd and Wyn-Jones 1996	66.0 – 80.7 <sup>b</sup>	73.6 <sup>b</sup>	7.50 × 10 <sup>1</sup>
65.3 – 76.0 <sup>c</sup>		71.3 <sup>c</sup>	7.50 × 10 <sup>1</sup>	

Flocculent	Source	Recovery (%)		Spike con. (oocysts/L)
		Range	Mean (S.D.)	
	Skerrett and Holland 2000	32.0 – 49.0 <sup>a</sup>	37.6 (± 6.1) <sup>a</sup>	1.00 × 10 <sup>3</sup>
	Karanis and Kimura 2002		38.8 (± 12.1)	2.50 × 10 <sup>5</sup>
	Greinert et al. 2004		0.67 (± 0.2) <sup>a</sup>	3.50 × 10 <sup>1</sup>
	Stanfield et al. 2000		64.1 <sup>c</sup>	1.00 × 10 <sup>3</sup>
			60.6 <sup>c</sup>	1.00 × 10 <sup>3</sup>
Ferric Sulphate	Vesey et al. 1993a		< 10 <sup>b</sup>	1.00 × 10 <sup>3</sup>
	Karanis and Kimura 2002		68.1 (± 2.0) <sup>b</sup>	1.00 × 10 <sup>6</sup>
	Stanfield et al. 2000		74.1 <sup>c</sup>	1.00 × 10 <sup>3</sup>
Aluminum Sulphate	Vesey et al. 1993a		59 <sup>b</sup>	1.00 × 10 <sup>3</sup>
	Karanis and Kimura 2002		58.1 (± 17.0)	2.50 × 10 <sup>5</sup>
	Stanfield et al. 2000		75.0 <sup>c</sup>	1.00 × 10 <sup>3</sup>
			95.4 <sup>c</sup>	1.00 × 10 <sup>3</sup>

<sup>a</sup> distilled water; <sup>b</sup> tap water; <sup>c</sup> untreated water

In summary, flocculation followed by sedimentation can be used to concentrate *Cryptosporidium* oocysts, but requires careful chemical addition and pH adjustment of the solution to a level that may cause a significant reduction in oocyst viability (Campbell et al. 1994). The level of turbidity and subsequent precipitation of foreign particles other than oocysts adversely affects oocyst recovery. Careful selection of flocculants based on water types, turbidity, and hydrophobic and electrostatic properties of oocysts cell surface that interfere in the recovery efficiency of flocculation (Hsu et al. 2001c), is necessary to achieve optimal recovery.

### 2.1.2 Filtration

Filtration is used to concentrate *Cryptosporidium* spp. in the *United States Environmental Protection Agency* (USEPA) Method 1622/1623; Standard Operating Protocol (SOP) for monitoring of *Cryptosporidium* oocysts in treated water supply. The primary mechanisms that are involved during filtration to concentrate *Cryptosporidium* from water samples are mechanical entrapment and hydrophobic interactions. Wide ranges (0 – 93%) of recovery efficiencies have been reported using various filter types, pore sizes, and modifications of

the basic filtration process (Table 2.3). Different membrane filter matrices of various filter materials, such as polycarbonate membrane, cellulose acetate membrane, cellulose nitrate membrane, polyethylsulfone and various sizes, for example micro-filtration (0.1 – 10.0  $\mu\text{m}$ ) and ultra-filtration (UF: 0.001 – 0.1  $\mu\text{m}$ ) have been used for the concentration of *Cryptosporidium*.

**Table 2.3: Filtration used for concentration of *Cryptosporidium* oocysts**

Filter Type	Nominal pore size ( $\mu\text{m}$ )	Recovery (%)		Source
		Range	Mean (SD)	
Polypropylene cartridge filter	1.0	25.0 – 81.0 <sup>a</sup>	50 <sup>a</sup>	Rose et al. 1986
	1.0		8 (13) <sup>c</sup>	Nieminski et al. 1995
	1.0	9.6 – 16.5	13.3	Shepherd and Wyn-Jones 1995
		3.0 – 16.5	10.8	
	15.0	4.5 – 16.1 <sup>a</sup>	11.2 <sup>a</sup>	Shepherd and Wyn-Jones 1996
		3.9 – 14.2 <sup>b</sup>	9.4 <sup>b</sup>	
	1.0		9.8 (4.5) <sup>a</sup>	Hsu et al. 2001b
			9.3 (3.3) <sup>b</sup>	
3.0 – 16.5		10.8		
Polycarbonate membrane filter	1.0	5 – 20		Ongerth and Stibbs 1987
	2.0	18.6 – 34.3	26.2 (5.5)	Hansen and Ongerth 1991
	2.0		9 (4)	Nieminski et al. 1995
	2.0	4.4 – 7.0	6.0	Shepherd and Wyn-Jones 1995
		3.6 – 7.2	5.6	
	2.0	24.0 – 32.0 <sup>a</sup>	27.2 <sup>a</sup>	Shepherd and Wyn-Jones 1996
		32.0 – 38.7 <sup>b</sup>	36.0 <sup>b</sup>	
	3.0		17.5 (3.2) <sup>a</sup>	Hsu et al. 2001b
		16.0 (1.7) <sup>b</sup>		
Cellulose acetate membrane filter	1.2	24.5 – 55.7	37.8	Shepherd and Wyn-Jones 1995
		23.6 – 33.0	26.6	
	1.2	32.0 – 44.0 <sup>a</sup>	39.7 <sup>a</sup>	Shepherd and Wyn-Jones 1996
		32.0 – 42.7 <sup>b</sup>	38.1 <sup>b</sup>	
	1.2	12 – 19 <sup>a</sup>	16.2 (2.8) <sup>a</sup>	Wohlsen et al. 2004
		0 – 14 <sup>b</sup>	3.2 (6.1) <sup>b</sup>	
Cellulose nitrate membrane filter	3.0	19.3 – 31.6	24.1	Shepherd and Wyn-Jones 1995
		5.4 – 8.4	7.1	

Filter Type	Nominal pore size (µm)	Recovery (%)		Source
		Range	Mean (SD)	
	5.0	6.1 – 14.6	10.3	Shepherd and Wyn-Jones 1995
		3.6 – 5.4	4.6	
	3.0	24.0 – 36.0 <sup>a</sup>	29.3 <sup>a</sup>	Shepherd and Wyn-Jones 1996
		25.3 – 36.0 <sup>b</sup>	30.4 <sup>b</sup>	
1.2	30.8 – 52.2 <sup>b</sup>	42.1 (5.9) <sup>b</sup>	Falk et al. 1998	
Mixed-cellulose ester (cellulose acetate – cellulose nitrate) membrane filter	3.0	6 – 29 <sup>a</sup>	14.7 (7.6) <sup>a</sup>	Wohlsen et al. 2004
Versapore	1.2	10.2 – 36.0 <sup>a</sup>	22.5 <sup>a</sup>	Shepherd and Wyn-Jones 1996
		29.3 – 41.3 <sup>b</sup>	33.6 <sup>b</sup>	
	3.0	17.3 – 28.0 <sup>a</sup>	20.8 <sup>a</sup>	Shepherd and Wyn-Jones 1996
		18.6 – 26.7 <sup>b</sup>	22.4 <sup>b</sup>	
Polyethylsulfone	0.8	21.3 – 26.7 <sup>a</sup>	24.0 <sup>a</sup>	Shepherd and Wyn-Jones 1996
		18.7 – 25.3 <sup>b</sup>	21.8 <sup>b</sup>	
Acrylic copolymer Membrane (Gelman Versapore)	1.2	19.9 – 36.6	25.5 (4.7) <sup>a</sup>	Dawson et al. 1993
Capsule filter		4 – 44	15 (12)	Simmons et al. 2001
		37 – 43 <sup>c</sup>		DiGiorgio et al. 2002
		36 – 75 <sup>c</sup>		
		9 – 22.9	14.4 (7.5) <sup>a</sup>	Feng et al. 2003
Flitra Max foam filter	1.0	76.7 – 106.7 <sup>a</sup>	90.4 <sup>a</sup>	Sartory et al. 1998
			28.2 (8.0)	Wohlsen et al. 2004

<sup>a</sup> Tap water <sup>b</sup>Distilled water <sup>c</sup> Raw water

Falk et al. (1998) concluded that the initial concentration of *Cryptosporidium* in the sample did not significantly change the recovery efficiency of filtration as a concentration process. The use of membrane filters allowed higher recoveries and thus lower detection limits than cartridge filters regardless of the types of water sample (Nieminski et al. 1995; Hsu et al. 2001b), but was restricted by the low volume of sample that could be filtered. The use of cartridge filters allows the sampling of large volumes and highly turbid water, whereas the membrane filtration method is suitable for small volumes of less turbid and

high quality water. Any increase in turbidity resulted in a significant decrease in oocyst recovery efficiency (Nieminski et al. 1995; Hsu et al. 2001b). Nieminski et al. (1995) reported that the standard deviation varied from 1 – 90% with the sample water turbidity changing from 0.5 to 20 NTU. The presence of algae decreased recovery efficiencies more than the increase in turbidity caused by inorganic contaminants.

Wohlsen et al. (2004) assessed the efficiency of five commercially available filters, including Pall Life Science Envirochek filters (EC), Pall Life Science EC-high-volume filters (EC - HV), Millipore flatbed membrane filters (MMF), Sartorius flatbed membrane filters (SMF), and Filta-Max depth filters (FM), to recover *Cryptosporidium parvum* oocysts using distilled and surface water spiked samples ( $10 \text{ oocysts L}^{-1}$ ). Among all the filters evaluated, FM depth filter showed the highest recovery ( $28.2 \pm 3.8\%$ ) with the least variability and the lowest recovery was achieved with EC standard filter of  $0.2 \pm 0.2\%$ . The FM depth filters were susceptible to filter clogging when sampling surface water and showed a lower mean recovery ( $19.4 \pm 2.2\%$ ). An improvement over the mean recovery was achieved using 5-s backwash during filtration and the EC-HV filters operated with back wash showed the highest recovery of  $51.1 \pm 4\%$  ( $53 \pm 6.9\%$  for distilled water spiked sample). During the same study, Wohlsen et al. (2004) also evaluated all the filters with respect to time and complexity of operation of the filtration processes. The time for completion of the filtration processes did not differ significantly among the filters. Flat bed membranes were more susceptible to filter clogging than the rest and required a maximum 2 hours time of operation. Difficulty in operation varied from filter to filter. They concluded that EC-HV filter was the least cumbersome and labor-intensive.

Ultra-filtration is a pressure-driven, selective permeability-based separation process and is used for a wide range of applications from biological macromolecule processing to wastewater treatment. Recently, UF showed promise over current USEPA 1622 method

using appropriate molecular weight cutoffs (MWCOs) to concentrate *Cryptosporidium* spp. oocysts in the retentate while allowing water to pass through the pores as permeate or filtrate. To assess the compatibility of UF (~80 kDa MWCOs) as a primary concentration step to the subsequent processing steps of method USEPA 1622, Simmons et al. (2001) reported  $42 \pm 27\%$  recovery of *C. parvum* from a wide range of surface water quality. Sample turbidity ranged from 2.5 to 45 NTU, with an average of 14.9 NTU, the total dissolved solid ranged from 32.2 to 294 mg L<sup>-1</sup> and averaged 108.5 mg L<sup>-1</sup>. Kuhn and Oshima (2001;2002) reported an optimized hollow fiber ultra-filtration (~50 kDa MWCOs) method by using 5% fetal bovine serum (FBS) to block the filter and 5 min recirculation at the end of the filtration to achieve the oocyst-recovery efficiencies of 64.8 – 81.0 % and  $55.3 \pm 25.7\%$  for 2 L and 10 L surface-, well- and tap-water samples, respectively. Morales-Morales et al. (2003) reported the same recovery efficiency ( $54 \pm 1.5\%$ ) for 100 oocysts in 10 L of surface water by blocking hollow fiber ultra-filters (~50 kDa MWCOs) with 5% calf serum and using PBS and Tween 80 (0.1% v/v) as sample amendments, and 0.05 M glycine to elute the organisms from filters. Hill et al. (2005) used 0.1% sodium polyphosphate (NaPP) as filter pretreatment (“block”), a surfactant solution (sample amendment) and various combination of back flushing (0.01% NaPP; 0.01 Tween 80 plus 0.01% Tween 20; 0.5 – 1% Tween 80), and showed that an ultrafilter having MWCO of 15 to 20 kDa was capable of recovering 83 – 98 % oocysts in 10 L tap water. Later, Hill et al. (2007) reported high-seed recoveries of  $88 \pm 10\%$  for 100 L tap water samples using polysulphone dialysis filters with a MWCO of ~ 30 kDa using the same UF protocol.

Lindquist et al. (2007) used a hemoconcentrator (polysulfone membrane of 56 kDa MWCO), and was able to recover  $46 \pm 21\%$  of seeded oocysts in 100 L tap water samples. They evaluated various protocols to improve the recovery performance and

concluded that a filter back flushing ( $67 \pm 7\%$ ) with a surfactant solution resulted in higher recovery than forward flushing ( $50 \pm 7\%$ ) and no flushing ( $21 \pm 7\%$ ). Similar results in performance improvement of UF were reported by Polaczyk et al. (2008) using filter elution or back flushing. In a recent comparative study by Hill et al. (2009) between hollow fiber UF and USEPA Method 1623 for recovery of pathogens in 100 L dechlorinated seeded (average low seeded 150 oocysts per 100L and average high seeded  $10^5$  oocysts per 100 L) tap water samples, a significantly higher recovery of oocysts ( $51 \pm 18\%$  and  $83 \pm 11\%$  mean recovery for low and high seeded experiment, respectively) for UF than that of USEPA Method 1623 was reported. Ferguson et al. (2004) also compared *Cryptosporidium* oocyst recovery efficiency of flatbed membrane filter, FM filter, EC - HV capsules, and hemoflow UF, from raw water samples, they found that hemoflow UF showed significantly higher recovery than that of FM filter, EC - HV capsules. The processing time for EC - HV and flatbed membrane filters (approximately 30 minutes per sample) was shorter than that of FM filter and hemoflow UF (approximately 60 minutes per sample).

Filtration (especially, ultra-filtration) possesses promise for the concentration of a high percentage (up to 98%) of oocysts from large volumes of various types of water samples with the optimization of operating protocol of operation. Processing time (30 – 60 minutes) and complexity of operation for different filters do not differ greatly. This technique is subject to filter fouling in cases of highly turbid source water. Excessive manual operation during filtration operation and subsequent elution are required which increase the potential risk of cross contamination.

### 2.1.3 Continuous flow centrifugation

Another method of decreasing the time required for the concentration of *Cryptosporidium* is centrifugation. Concentration using continuous flow centrifugation (CFC) can be performed continuously and is effective with a wide variety of water matrices. Currently, USEPA method 1622/1623 has been validated using portable continuous flow centrifugation (PCFC) for *Cryptosporidium* in 50 L sample volume (USEPA 2005a; 2005b).

The preliminary applications of continuous separation centrifuges used by different researchers (Zuckerman et al. 1999; Borchardt and Spencer 2002; Higgins et al. 2003; Zuckerman and Tzipori 2006) were in pathology labs as blood cell separators. This equipment is large, not easily movable, and operates at a very low flow rate. Therefore, it is not suitable as a practical method for routine monitoring of *Cryptosporidium* in large volumes of water. Zuckerman et al. (1999) modified the standard components of a blood cell separator to a portable device usable in the field. With this modified system, they conducted an optimized recovery experiment collecting 45 L of sample at a flow rate of 1.41 L min<sup>-1</sup> and seed density of 2.6 × 10<sup>4</sup> oocysts L<sup>-1</sup>. The average recovery efficiencies of *Cryptosporidium* using spiked tap and river water were 55.3 ± 2.1% and 26.8 ± 4.0%, respectively. Using a basket centrifuge Swales and Wright (2000) reported that the average recovery efficiency of oocysts seeded into 100 L filtered tap water at densities of 100, 50, 14, 5 oocysts L<sup>-1</sup> were 70.3, 51.0, 37.8, 28.6%, respectively. The optimized operating condition was 2900 x g with a flow rate of 0.75 L min<sup>-1</sup> without further processing after concentration. Borchardt and Spencer (2002) operated blood cell separators as simple continuous centrifuges to evaluate the recovery efficiency of continuous separation channel centrifugation on different water matrices (sterile PBS, tap

water, and local pond water) of 2 – 100 L using a range seed density of 5 – 1000 oocysts L<sup>-1</sup> and achieved mean recovery ranges from 69 – 104%.

Using two different blood cell separator centrifuges, Borchardt and Spencer (2002) demonstrated that oocyst recovery reduced substantially at flow rates less than 0.5 L min<sup>-1</sup> and oocyst recovery did not vary significantly with turbidity levels between 1 – 45 NTU. Using a spiking dose of 100 oocysts in 10 L source water sample, Higgins et al. (2003) reported a mean recovery of  $4.4 \pm 2.27\%$  when the CFC runs used a flow rate of 0.2 L min<sup>-1</sup> at 4200 x g. This result is comparable to the recovery efficiency reported by Swales and Wright (2000) i.e.  $14.8 \pm 1.66\%$  and  $13.0 \pm 3.87\%$  for low seed (10 oocysts L<sup>-1</sup>), low turbidity (1 NTU) and high turbidity (5 NTU) water samples, respectively. Both groups of researchers used a protocol of purification steps (Percoll discontinuous gradients or Immunomagnetic separation) followed by the CFC concentration. Zuckerman et al. (1999) recovered *Cryptosporidium parvum* spiked at around 10 and 30 oocysts L<sup>-1</sup> from 50 L tap water sample at a flow rate of 0.75 L min<sup>-1</sup> and 3000 x g. Recovery ranged between 37.4% and 84% (average 66.85%) whereas 11 to 72% with a mean of  $35.4 \pm 23\%$  was achieved using a low number of oocysts ( $90 \pm 57.5\%$ ) at the same flow rate and centrifugal force. During the Tier 2: USEPA method 1623 validation of PCEC by the same group of researchers, the mean percent recovery was reported to  $43.3 \pm 17.9\%$  and  $48.33 \pm 12.53\%$  for 50 L reagent water and source water sample, respectively (Zuckerman and Tzipori 2006).

The low flow rate used during sample processing make this process time-consuming (approximately 1 hour for sampling 40 L of water) for the use in routine analysis of environmental samples. But, CFC is less susceptible to the adverse effects of clogging and breakthrough of filter matrices as well as the interference of eluent with the chosen detection method (Zuckerman et al. 1999; Borchardt and Spencer 2002; Higgins et al.

2003; Zuckerman and Tzipori 2006). None of the concentration techniques discussed above achieved complete recovery *Cryptosporidium* spp. However, UF and CFC achieved significantly high recovery (greater than 90%). All the techniques show limitation in recovery efficiency for high turbidity, presence of organic matters and non-specific interactions.

## **2.2 Re-concentration and purification**

During the sampling and concentration step, various other particles will also accumulate because they are the same size, have similar properties, or are larger than the pore size of the sampling apparatus. These foreign particles will interfere in the detection of oocysts and also affect the sensitivity of detection. In addition, the elution of samples from various filters or redissolution of pellets results in larger volumes of samples, thus making the detection phase more difficult. Therefore, after sampling and elution, a re-concentration and purification step, for example density gradient separation or immunomagnetic separation (IMS), is needed to minimize the effect of the foreign particles and to further decrease sample volume for the detection stage.

### **2.2.1 Density gradient separation**

Density gradient separation is used for the purification of cellular and subcellular materials. Particles of interest are separated based on the difference in density with respect to their surroundings. In its simplest form, a concentrated sample is mixed with or overlaid on a solution of appropriate specific gravity and centrifuged. After centrifugation, the intended particle is separated from the rest leaving the heavier debris behind. Stanfield et al. (2000) compared recovery efficiency of flotation and centrifugation and reported around four fold improvements in recovery using flotation step over concentration by centrifugation (1500 x g for 10 minutes). A number of

solutions have been used as flotation solutions for parasite purification such as sucrose, formaldehyde, sodium chloride, zinc sulphate, sodium nitrate, mercury (II) iodide, potassium iodide, magnesium sulphate, sodium thiosulphate, zinc chloride, cesium chloride, potassium bromide, and percoll (Cringoli et al. 2004; Zarlenga and Trout 2004). A large variability in *Cryptosporidium* oocyst recovery using flotation was reported in the literature. When a large number of seeded oocysts ( $>10^4$ ) was used, the recovery efficiency using sucrose flotation was reported to range from 24 – 65% depending on the number of oocysts seeded and their viability (Bukhari and Smith 1995). Moreover, Shepherd and Wyn-Jones (1996) claimed that the sucrose flotation step significantly diminished the recoveries when used as purification steps. Similar results were obtained by Skerrett and Holland (2000) in a study using calcium carbonate flocculation followed by sucrose gradient and calcium carbonate flocculation. They documented that a greater decrease in recovery was observed in lake water samples than in distilled water.

Nieminski et al. (1995) compared Percoll-Sucrose gradient (specific gravity, 1.10) separation and Percoll-Percoll step gradient (specific gravity, 1.09 was overlaid with a layer of specific gravity of 1.05) separation using seeded experiments and reported an average recovery of  $27 \pm 9\%$  and  $69 \pm 25\%$ , respectively. LeChevallier et al. (1995) evaluated the effectiveness of Percoll-Sucrose solutions of different specific gravity for the recovery of oocysts with respect to different pellet sizes and ages of oocysts. Their results indicated that with an increase in the specific gravity of Percoll-Sucrose gradient, the recovery efficiency also increased until a maximum value (1.3) was reached when it did not allow sample clarification and interfered with microscopic examination. They reported an increase in recovery from 32% to 67% when the specific gravity was changed from 1.0 to 1.15. In contrast, Stanfield et al. (2000) studied Percoll-sucrose of different specific gravities (1.09, 1.13, and 1.15), and there was no significant improvement in

recoveries except that using a specific gravity of 1.09 produced the least variation in final recovery. They also compared recovery efficiencies of Percoll-Sucrose (s.g.1.15), Sucrose (s.g. 1.15), Sheather (s.g. 1.15), and Percoll-Percoll (s.g. 1.09/1.05) in untreated and treated water samples and very little difference was reported. Sucrose ( $29.1 \pm 11.1\%$ ) was the most and Percoll-Percoll ( $15.7 \pm 5.8\%$ ) the least efficient. In a similar comparative study, Chesnot and Schwartzbrod (2004) reported  $11.7 \pm 0.5\%$  oocyst recovery in seeded surface water concentrate using Percoll-Sucrose flotation. The highest recovery ( $63.3 \pm 4.5\%$ ) was achieved using a Percoll gradient. Their results were in agreement with those reported by Hsu et al. (2001a; 2001b).

In brief, purification by density gradient separation and flotation exhibited a wide range of variability in oocysts recovery depending on the type of water and its composition, separation solution used and its specific gravity, and procedure followed. The time for processing was not longer than 30 minutes. This procedure was not able to differentiate non specific materials of the same specific gravity. Therefore, it was not a highly sensitive and efficient method of *Cryptosporidium* spp. purification from environmental samples.

#### 2.2.2 Immunomagnetic separation (IMS)

IMS is used to purify oocysts from debris that accumulates in the earlier sampling and concentration steps (filtration, elution, and centrifugation), and to re-concentrate the sample to a smaller volume for subsequent detection through microscopic examination. It has also been used for rapid and selective isolation and concentration of many eukaryotic and prokaryotic cells, macromolecules from blood, food, stool, and environmental samples (Olsvik et al. 1994). The IMS technique relies on the use of super-paramagnetic microspheres, or beads coated with ligand molecules, specific to surface exposed epitopes

on the outer wall of target cell. Commercially available *Cryptosporidium*-IMS kits use a monoclonal antibody (mAb) that is raised against *Cryptosporidium* species oocysts as the ligand molecule. This anti-*Cryptosporidium* antibody is covalently attached to the magnetic beads of predefined size (0.8 – 4.5µm). Dynabeads® anti-*Cryptosporidium* IMS kit, which is a USEPA approved IMS kit for sample re-concentration and purification for *Cryptosporidium* detection, consists of beads conjugated with an Immunoglobulin-M (IgM) monoclonal antibody (mAb), and another commercially available IMS kit [Cryptoscan IMS kit (Immucell)] utilizes magnetic beads conjugated with Immunoglobulin-G (IgG) mAb. An aliquot of conjugated beads is mixed in the buffered sample of interest for an optimal time period to capture the target organism. The bead conjugate-organism complex is then separated from the rest of the sample using a magnetic field. The magnetically separated bead conjugate-organism complex is then acidified using 0.1 N HCL for dissociation of the bead conjugate and captured target pathogen. A neutralization step is used to facilitate pH dependent mAb reactive detection or enumeration.

Different research groups compared different commercially available IMS kits and concluded that there was variability in recovery using various kits and within a kit (lot-to-lot) (Bukhari et al. 1998; Rochelle et al. 1999). The recovery variations were attributed to the level of turbidity, bead size and conjugated antibody type etc. Campbell and Smith (1997) reported a wide range of *Cryptosporidium* recovery (4.8 – 147.4 %) using Dynabeads in samples of three different turbidity levels (clean or non-turbid water, 40-60 NTU, and ~ 600 NTU) and concluded that in low turbidity samples, IMS consistently showed the highest recoveries and least number of negative results irrespective of sample volume. Ochiai et al. (2005) compared recovery efficiency of IMS confirmed by direct immunofluorescence assay (IFA) at two different turbidity levels (200 NTU and 1000

NTU) and obtained 87 – 91% and 52 – 71%, respectively. Feng et al. (2003) assessed IMS- direct IFA recovery efficiency using seeded tap water and achieved a level of recovery ranging from 92.4 – 99% ( $95.1 \pm 3.4\%$ ). During an optimization and standardization study for the determination of waterborne *Cryptosporidium*, Stanfield et al. (2000) evaluated four different commercially available IMS kits. The results showed a wide range of recoveries (30.5 – 96.1%). Their study revealed that the IMS Combo kit designed for *Giardia* cysts and *Cryptosporidium* oocysts was less efficient in performance than the kit designed for *Cryptosporidium* only. Simmons et al. (2001) also reported similar recovery ranges (31 – 117%) with an average recovery of  $83 \pm 21\%$ . Hsu and Huang (2001) studied the IMS recovery efficiency in a seeding experiment with oocyst concentrations ranging from  $32 \text{ mL}^{-1}$  to  $2.0 \times 10^5 \text{ mL}^{-1}$  deionized water and confirmed a 70.6 – 92.2% range in recovery averaging  $82.6\% \pm 18.2\%$ .

In a validation study of Dynabeads® GC-Combo IMS kit, McCuin et al. (2001) reported 62.2% ( $\pm 6.5\%$ ) average recovery efficiency with a range 54.7 – 67.0% and no significant decrease in recovery was observed in solutions with turbidity up to 5000 NTU. In contrast, Campbell and Smith (1997) found that with an increase in turbidity level above 600 NTU, efficiency of the IMS procedure was significantly reduced. Using MACS microbeads (50 nm diameter biodegradable beads coated with either mouse anti-FITC mAb or goat anti-rabbit IgG antibody), Deng et al. (2000) reported 95 – 104% recovery efficiency from oocyst positive samples in comparison to 0.04 – 0.8% for negative samples. In a recent study, Greinert et al. (2004) reported an oocyst recovery of efficiency of  $51.3 \pm 2.1\%$  using 1 L distilled water sample.

Di Giovanni et al. (1999) found that IMS- direct IFA was more efficient in seeded raw water concentrates (mean recovery  $26.1 \pm 16.5\%$ ) than in the seeded filter backwash water concentrates (mean recovery  $9.1 \pm 6.9\%$ ) because of the interference of large

amount of debris in the filter backwash water. For both water sample types, IMS-direct IFA offered significantly better recovery efficiency than Percole-Sucrose- direct IFA assay ( $16.6 \pm 3.0\%$  and  $5.8 \pm 3.7\%$ , respectively). Their hypothesis was also supported by the conclusion of Campbell and Smith (1997) that the type of materials that contribute to turbidity may play an important role in IMS recovery. Several researchers showed that the IMS protocol did not affect the viability of the recovered oocysts, which allows detection and determination of the significance of environmentally isolated oocysts using viability/infectivity assays such as polymerase chain reaction (PCR) (Di Giovanni et al. 1999; Rochelle et al. 1999; Deng et al. 2000; Hallier-Soulier and Guillot 2000; Lowery et al. 2000; Sturbaum et al. 2002; Straub et al. 2005).

In an optimization experiment for *Cryptosporidium* recovery, Pezzana et al. (2000) reported an average recovery of  $68.8 \pm 13.7\%$ . They concluded that the beads/sample ratio significantly affected oocyst recovery. Di Giovanni et al. (1999) reported a significantly higher oocyst recovery for 0.1 N HCl as IMS dissociation solution over AHBSS-1% trypsin using deionized water, raw water, and filter backwash water samples. Ware et al. (2003) found that heat dissociation (10 min incubation at 80°C) instead of 0.1 N HCl, significantly improved oocysts recovery efficiency for both seeded reagent water and river water samples. The age of oocysts did not affect IMS-FA recovery of *Cryptosporidium* oocysts significantly (Bukhari et al. 1998; Yakub and Stadterman-Knauer 2000; McCuin et al. 2001). Yakub and Stadterman-Knauer (2000) evaluated IMS recovery efficiency of *Cryptosporidium parvum* from high iron matrices and concluded that the level of recovery decreased significantly with dissolved iron concentration greater than  $4 \text{ mg L}^{-1}$ .

In conclusion, the IMS procedure had a high specificity and was an effective means of sample purification. IMS was not efficient at the high levels of turbidity encountered in

environmental water samples and was not capable of recovering 100% or close to 100% of spiked oocysts. The average time of sample purification using IMS was about 1.5 hours. Efforts should be made to develop new purification techniques, which will provide specifically high recoveries of *Cryptosporidium* oocysts.

### **2.3 Detection**

The detection of oocysts from the concentrated and purified sample includes microscopic examination using epifluorescent microscopy after immunofluorescent staining of oocysts to define size and shape. Further steps include the use of the nuclear fluorochrome 4', 6-diamidino-2-phenylindole (DAPI) to stain nuclei of oocyst sporozites, and differential interface contrast (DIC) microscopy determines internal morphology. The use of DAPI and DIC microscopy in conjunction with IFA reduces false positive and false negative results from raw water samples and final water samples (Grimason et al. 1994; Smith et al. 2002). The flow cytometry (FC) method is also promising for routine monitoring of oocysts from environmental samples. Molecular technologies, mainly based on polymerase chain reaction (PCR) or fluorescent in situ hybridization (FISH) are also being developed but are not mature enough for their application in routine analysis and field conditions. Thus, molecular techniques are not included in this literature review.

#### **2.3.1 Immunofluorescent assay**

During the detection stage, oocysts can be recognized from the background and enumerated by immunofluorescent staining. For direct IFA, fluorescein isothiocyanate (FITC) conjugated monoclonal antibody (mAb) specific to *Cryptosporidium* oocysts is used. Indirect IFA uses a primary antibody specific to *Cryptosporidium* followed by a FITC-conjugated secondary antibody. Using a spike dose of  $2010 \pm 111.1$  oocysts  $10 \mu\text{l}^{-1}$ , a range of 96 – 100% averaging  $98.3 \pm 2.1\%$  recovery was reported by Feng et al. (2003)

using direct IFA. Nieminski et al. (1995) compared the detection efficiency of two different IFA staining procedures. In their seeding experiment using Hydrofluor Combo kit, they used the ASTM method and reported average recoveries of 56%. In a seeding experiment in environmental water sample of low turbidity levels (less than 9 NTU) IMS-direct IFA was able to detect as low as 5 oocysts mL<sup>-1</sup> (Sturbaum et al. 2002).

Table 2.4 summarizes commercially available antibodies specific to *Cryptosporidium* investigated by different groups along with their characteristics. The term “avidity” defines the strength of the antibody-antigen complex. Hoffman et al. (1999) expressed “avidity” as the percent reduction in fluorescent intensity of antibody-antigen complexes following exposure to 8M urea for 3 minutes, while Weir et al. (2000) defined avidity in terms of the affinity constant,  $K_a$ , as reciprocal to the concentration at which 50% maximal binding to the oocysts was obtained. There was variability in the avidity and specificity between the different antibody kits and lot-to-lot antibodies of the same kit (Hoffman et al. 1999).

**Table 2.4: Commercially available *Cryptosporidium* specific antibodies**

Commercial Name	Class	Avidity		Lot to Lot variation (1-5, 5 being the least variable)	Cross Reactivity					Specificity (1-5, 5 being the highest specificity)
		% susceptibility to stress [(1-5, 5 being the highest avidity)]	Affinity Constant, $k_a$ , ( $\text{mol}^{-1}$ )		Algal Species and minerals	<i>C. baileyi</i>	<i>C. muris</i>	<i>C. wrairi</i>	<i>C. serpentis</i>	
Hydrofluor Combo	IgM	59.1-61.3%		4	2; 2 <sup>c</sup>	0; 0 <sup>a</sup>	0; 1 <sup>a</sup>	1 <sup>a</sup>	1 <sup>a</sup>	3
Merifluor	IgM	73.3-93.3%		5	2; 3 <sup>c</sup>	0;	0; 1 <sup>a</sup>	1 <sup>a</sup>	1 <sup>a</sup>	
Crypto/Giardia Cel		93.6-95.1%		2	4	0 <sup>b</sup>	1			
AquaGlo/Crypto-a-Cry 104	IgM	14.8-23.9%		3	3	1	1			1
Cry 104	IgG1		$7 \times 10^8$							5
Cry 26	IgM		$3 \times 10^7$		5 <sup>c</sup>					2
Immucell	IgG		$6 \times 10^7$							3
Cry 212	IgM									4
Crypto-Cell	IgM				5 <sup>c</sup>					3
Source		Hoffman et al. 1999	Weir et al. 2000	Hoffman et al. 1999	Rose et al. 1989; Graczyk et al. 1996; Vesey et al. 1997b; Hoffman et al. 1999					Ferrari et al. 1999

Source: <sup>a</sup> Graczyk et al., 1996; <sup>b</sup> Rose et al., 1989; <sup>c</sup> Vesey et al., 1997b

Using IFA with the Hydrofluor™ Combo immunofluorescence kit (Meridian Diagnostics, Cincinnati, Ohio), Rodgers and Flanigan (1995) analyzed 54 species of algae for cross reaction and of them 24 species showed positive results with some degree of green fluorescence. Vesey et al. (1997a; 1997b) also reported the autofluorescence of algae and mineral particles and also non-specific binding of different mAbs. Detection of fluorescent-mAb labeled *Cryptosporidium* oocysts in water concentrates using epifluorescent microscopy or flow cytometry is hindered by autofluorescence and non-specific binding. However, direct IFA showed less non-specific binding than indirect IFA (Vesey et al. 1997b). Background staining due to non-specific mAb binding could be reduced significantly by the optimization of the staining procedure such as incubation temperature, use of blocking agent (Rodgers and Flanigan 1995; Vesey et al. 1997b). Vesey et al. (1997a) argued that use of different colored fluors such as fluorochrom CY3, phycoerythrin (PE), and tetramethylrhodamine B thioisocyanate (TRITC) which are all red eliminates much of the autofluorescence which is usually green.

Ferrari et al. (1999) compared commercially available mAbs of IgG<sub>1</sub>, IgG<sub>3</sub>, and IgM subclasses for the non-specific binding using flow cytometry. They evaluated seven antibodies (six of them were FA and one was IFA) specific to *Cryptosporidium* in composite untreated water samples. A large variation in number of fluorescent particles was detected after staining with different mAbs. IgG<sub>1</sub> produced less non-specific binding than IgM and IgG<sub>3</sub> mAbs. Weir et al. (2000) produced an IgG<sub>1</sub> (Cry 104) mAb that showed higher avidity and specificity to oocysts in water concentrates than other commercial antibodies examined [Cry26 and Immucell (Immucell, Portland, Oreg.)]. The time required for the completion of detection using IFA depends on the expertise of operators, but typical time of slide preparation and analysis is 2.5 hours.

### 2.3.2 Flow cytometry

Flow cytometry uses the optical characteristics of light that is directed at in a fluid stream to measure various physical or chemical characteristics such as size, complexity, phenotype, and health (with appropriate staining). In general, cells of interest should be labeled with different fluorescent molecules. In addition to various cell properties measurements, flow cytometers are capable of sorting fluorescently stained cells. Vesey et al. (1991) first described the potency of flow cytometry to detect *Cryptosporidium* in water samples. Later, they proposed a protocol consisting of sample concentration using flocculation, purification and sorting by means of flow cytometry with fluorescent activated cell sorting, followed by the epifluorescent microscopy for the routine monitoring of *Cryptosporidium* in water samples (Vesey et al. 1993b; Vesey et al. 1994). They analyzed 325 river, reservoir and drinking water samples with flow cytometry and direct epifluorescence microscopy and concluded that purification using flow cytometry and cell sorting before epifluorescence microscopy could increase the sensitivity, ease of operation, and reduce the time of completion of examination (Vesey et al. 1993b). Following this protocol, more than 95% of recovery efficiency was accomplished from river and reservoir water samples (Vesey et al. 1994).

Hsu et al. (2005) assessed the staining efficiency of three commercial antibodies, FA (Meridian Diagnostics, Inc., Cincinnati, Ohio), Crypt-a-Glo™ (Waterborne™, Inc., New Orleans, LA, U.S.A.), and Hydrofluor™ Combo-IFA (Strategic Diagnostics Inc., Newark, DE, U.S.A.), using flow cytometry to quantify *Cryptosporidium* oocysts in seeded water. Their study showed that the use of primary mAb significantly separated oocysts from other particles. Their conclusion was supported by the results from other researchers that FA exhibits less non-specific binding than IFA (Vesey et al. 1997b; Ferrari et al. 1999). In a recent study, Barbosa et al. (2007) optimized a flow cytometry

protocol for the detection of *Cryptosporidium* oocysts resulting in a detection limit of  $2 \times 10^3 \text{ mL}^{-1}$ . They reported the optimal antibody concentration of  $3.0 \mu\text{g mL}^{-1}$  for *Cryptosporidium* specific mAb conjugated with R-phycoerythrin (RPE, phycoerythrin isolated from Rhodophyta) (Crypt-a-Glo, RPE, 20X concentrate Waterborne™ Inc.), above this value no improvement in intensity of fluorescence in labeled oocysts was observed. Their findings were similar to that of other researchers that uses of higher concentrations of antibody conjugates than an optimal value do not produce brighter oocysts (Valdez et al. 1997; Vesey et al. 1997a). This optimal mAb concentration varies with antibody type, their specificity and labeling dye in use.

Montemayor et al. (2007) compared the detection efficiency of two laser scanning cytometers and epifluorescent microscopy using spiked surface water samples and no significant difference was observed. The time required for detection using flow cytometry (1.5 hours) was less than that of IFA and also independent of operators' expertise. In essence, the effectiveness of both methods to obtain accurate and reproducible results depends on the quality (specificity) of reagents, standardization and the validation protocol. However, with recent advances in design and potential, flow cytometry is a good candidate for automated detection of oocysts.

Current methods are time-consuming, labor-intensive, insensitive, expensive, and require well-trained personnel and highly equipped lab facilities, therefore are a challenge to implement for routine (daily) monitoring. In a hypothetical scenario with an environmental sample contaminated with *Cryptosporidium* oocysts, and concentration, purification, and detection phases are optimized, the maximum recoveries attainable are 85%, 95%, and 99%, respectively. Therefore, a maximum of 80% oocysts can be detected through the whole system. Typical recovery ranges are much less than the maximum values reported. So, the typical "whole system" recovery would be much less than 80%.

The errors in percent recovery magnify with the addition of each step in the sample concentration to detection phase. Additionally, the concentration techniques are very sensitive to interferences due to extreme water quality parameters such as pH, turbidity. The current purification methods are subject to a lack of specificity to *Cryptosporidium*, while detection techniques show variability with respect to operators. There is still a need for improved detection methods that would provide a tool for rapid, robust, sensitive, specific, accurate, and reproducible detection of *Cryptosporidium* spp. for frequent analysis of environmental samples.

#### **2.4 Antibody chemistry**

Antibodies (immunoglobulins, Ig) are molecules produced by biological systems in response to a contaminating agent (antigen). They were chosen as the capture molecule for this research because they can be quite specific. Five primary types (isotypes) of antibody are generated for different immunoresponses: IgG, IgA, IgG, IgE, and IgD. Different types of antibody molecules have different heavy chain. In this research only IgG and IgM are considered because of their commercial availability.

IgG (~ 150 KDa) is found intravascular and extra-vascular and is the secondary response antibody isotype and the most abundant in the blood serum (around 75% of total serum immunoglobulin). This complex globular glycoprotein is made of two pairs of polypeptide chains linked together by disulphide bond (Figure 2.1). Each pair of polypeptide is composed one heavy chain (gamma,  $\gamma$ ) and one light chain (Kappa,  $\kappa$  or lambda,  $\lambda$ ) also connected by disulphide bonds. Each light chain is composed of two domains: constant domain ( $C_L$ ) and variable domain ( $V_L$ ). The heavy chain has three constant domains ( $C_{H1}$ ,  $C_{H2}$ , and  $C_{H3}$ ) and one variable domain ( $V_H$ ). The variable regions of the heavy chain and the light chain are the region of antigen interaction.

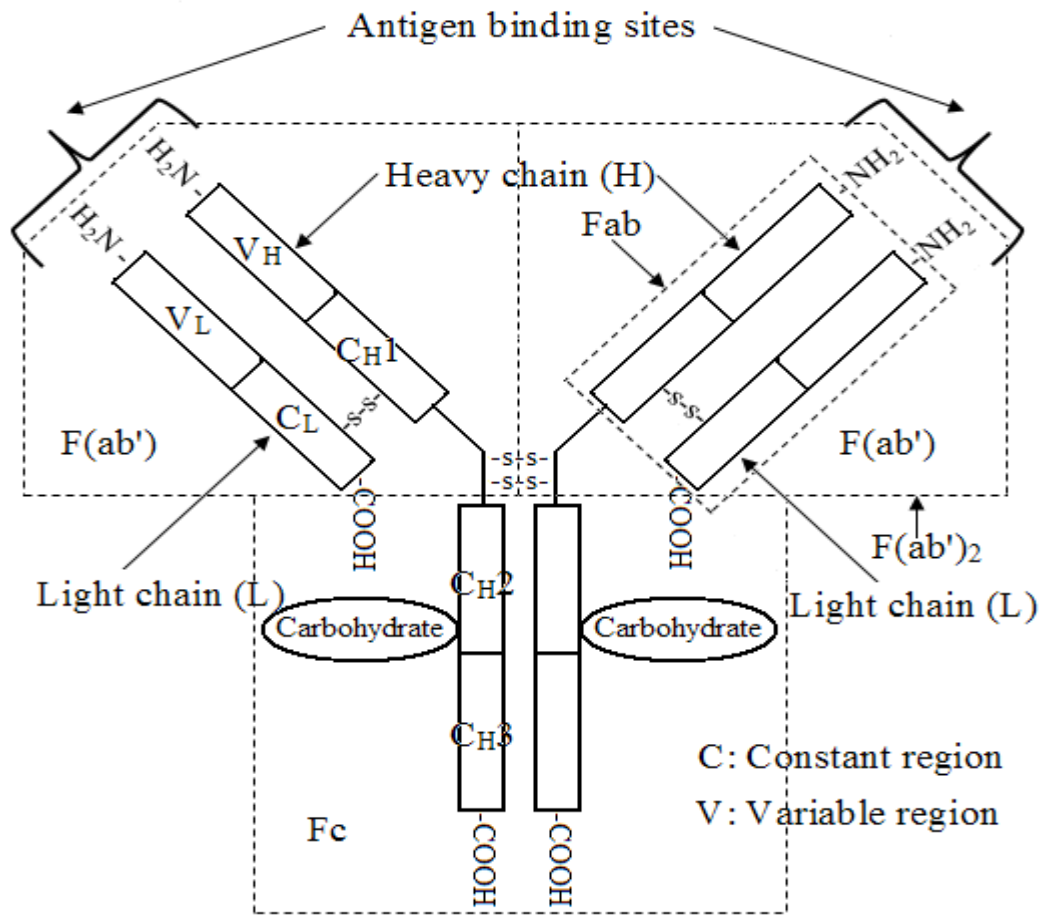


**Figure 2.1: Schematic diagram of IgG and its fragments**

The IgG molecule can be divided into  $F(ab')_2$  and  $F_c$  fragments. The  $F_c$  (fragment crystallization) fragment does not have binding properties. It contains the antibody effector functions, such as complement activation, cell membrane receptor interaction and transplacental transfer.  $F(ab')_2$  consists of two identical  $F(ab')$  [fragment antigen binding] held together by disulphide bond at the hinge region. Each  $Fab'$  fragment has one light chain ( $V_L$  and  $C_L$ ) and two domains of heavy chain ( $V_H$  and  $C_{H1}$ ). The carbohydrate moieties are located at the constant heavy chain domain  $C_{H2}$ .  $Fab$  fragment is the fragment that does not have any hinge region with the thiol group but does have other domains like  $Fab'$ .

IgM is mainly intravascular and is primary response antibody. Its percentage in the blood serum is the third highest (~ 6%). It usually exists in two forms: monomeric (in the membrane) and polymeric (a secreted form). The structure of secretory IgM varies

between species. Figure 2.2 presents the structure of mouse IgM. In general, monomeric IgM (~180 KDa) is joined together by disulfide and the J chain (~ 15 KDa: an acidic peptide rich in carbohydrate and cysteine, arginine and lysine residues) in polymeric IgM. IgM monomers also have two pairs of light chain [kappa ( $\kappa$ ) or lambda ( $\lambda$ )] and heavy chain, mu ( $\mu$ ). Each  $\mu$  chain has one variable domain ( $V_H$ ) and four constant domains ( $C_{\mu 1}$ ,  $C_{\mu 2}$ ,  $C_{\mu 3}$ , and  $C_{\mu 4}$ ). The carbohydrate moieties are located in the  $C_{\mu 2}$  region. IgM lacks a hinge region, the hinge region is replaced by an actual domain ( $C_{\mu 2}$ ).

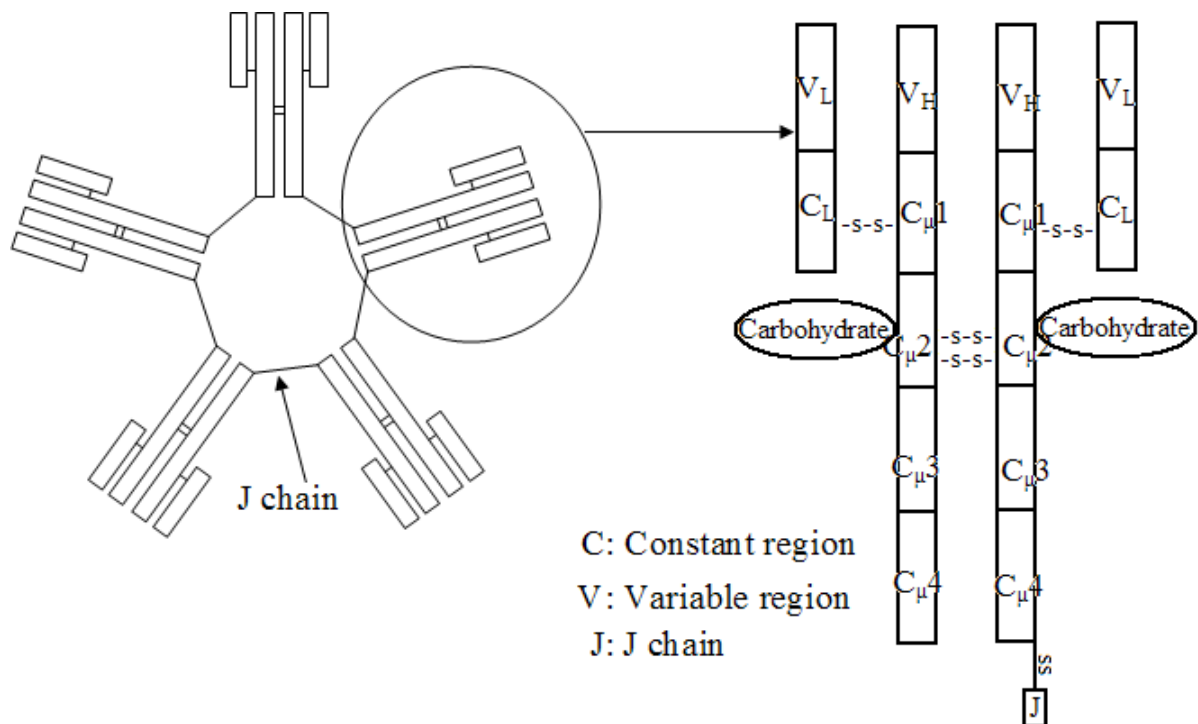


**Figure 2.2: Schematic representation of mouse IgM**

### 2.5 Immobilization of antibodies onto solid surfaces

Antibodies immobilized onto solid surfaces have been used for a number of applications such as immunosensors, immunoaffinity chromatography, diagnostic immunoassays, industrial applications and environmental monitoring because of the high specificity and sensitivity of the antibody-antigen interaction (Wiseman 1993; Lu et al. 1996; Rao et al. 1998). The easiest immobilization strategy involves non-covalent adsorption of antibody onto solid surfaces especially plastic, poly-lysine-coated glass, and other surfaces. This

immobilization technique results in randomly oriented antibodies, therefore causes a subsequent decrease in antigen-binding activity (Catt and Tregear 1967; Catt et al. 1970; Fell et al. 1972; Bernath and Haberman 1974). Various molecules such as as N-hydroxysuccinimide, periodate, gluteraldehyde, or isothiocyanate have been used as intermediates that develop covalent bonds with the surface amino group of lysine of the antibody. But, due to the randomly distributed lysine residues of the antibody, thus multiple binding sites, these strategies also produce random antibody orientation (Domen et al. 1990).

Random immobilization of whole antibodies shows a greater decrease in specific activity, which is defined as the molar ratio of bound antigen to immobilized antibody, in response to a large antigen due to the close proximity of the support surface (due to size and/or charge repulsion), high protein loading, surface crowding and improper orientation than site specifically immobilized F(ab') fragment (Spitznagel and Clark 1993). Most of these problems can be minimized to an acceptable limit by oriented immobilization of antibodies. Different strategies for site specific orientation of whole antibody or antibody fragments are summarized in Table 2.5.

**Table 2.5: Site specific antibody immobilization strategies**

<b>Surface</b>	<b>Support treatment</b>	<b>Antibody treatment</b>	<b>Reactive residue</b>	<b>Source</b>
Silica	Lipid: N-( $\epsilon$ -maleimidocaproyl)-dipalmitoylphosphatidyl-ethanolamine	Fragmentation of whole IgG to Fab'	Sulfhydryl of cysteine (-SH)	Vikholm et al., 1998
Silica	Pyridyl disulfide	Fragmentation of whole IgG to Fab'	Sulfhydryl of cysteine (-SH)	Lu et al., 1995
Gold	No support treatment	Fragmentation of whole IgG to Fab'	Sulfhydryl of cysteine (-SH)	Karyakin et al., 2000; O'Brien et al., 2000; Brogan et al., 2003; Vikholm, 2005a; Kim et al., 2007;
Gold	Streptavidin activation	Biotinylation of whole IgG or Fab'	Sulfhydryl of cysteine (-SH) of Fab' or Carbohydrate moiety in the CH <sub>2</sub> domain whole IgG	Peluso et al., 2003
Borosilicate glass	Silanization using aminopropyltrimethoxysilane	1-Ethyl-3-(3-dimethylaminopropyl)-carbodiimide (EDC) and Protein A	Fc region of Antibody	Danczyk et al., 2003

Surface	Support treatment	Antibody treatment	Reactive residue	Source
Borosilicate glass	Silanization using 3-mercaptopropyltrimethoxysilane	N-[γ-Maleimidobutyryloxy] succinimide ester (GMBS) and Protein A	Fc region of Antibody	Danczyk et al., 2003
Gold	No surface treatment; lysine residues in the protein G molecule were converted to thiol groups using 2-iminothiolane.	No antibody treatment	Fc region of Antibody	Fowler et al., 2007
Gold	No surface treatment; Genetically engineered cysteine-fused <i>Streptococcus</i> protein G at the N-terminus.	No antibody treatment	Fc region of Antibody	Lee et al., 2007
Gold	Tri(ethylene glycol) and maleimide-terminated alkanethiolates; Triazacyclononane (aza); NiSO <sub>4</sub> , and recombinant hexahistidine protein A/G	No antibody treatment	Fc region of Antibody	Patrie and Mrksich, 2007
Carboxyl modified magnetic particle	Acipic dihydrazide and EDC (1-ethyl-3-(3-dimethylamino-	Oxidation of the carbohydrate moiety using sodium <i>m</i> -periodate	Carbohydrate moiety in the CH <sub>2</sub> domain	Kang et al., 2007

Surface	Support treatment	Antibody treatment	Reactive residue	Source
	propyl)carbodiimide)			
Carboxyl modified magnetic particle	Streptavidin hydrazide and EDC	Oxidation of the carbohydrate moiety using sodium <i>m</i> -periodate and biotinylation using biotin hydrazide	Carbohydrate moiety in the CH <sub>2</sub> domain	Kang et al., 2007
Silica	N,N'-Disuccinimidyl carbonate (DSC); Streptavidin	Oxidation of the carbohydrate moiety using sodium <i>m</i> -periodate and biotinylation using biocytinhydrazide	Carbohydrate moiety in the CH <sub>2</sub> domain	Franco et al., 2006
Silica	DSC; 6-aminocaproic acid and adipic acid dihydrazide	Oxidation of the carbohydrate moiety using sodium <i>m</i> -periodate	Carbohydrate moiety in the CH <sub>2</sub> domain	Franco et al., 2006
Silica	DSC and recombinant protein A/G	No antibody treatment	Fc region of Antibody	Franco et al., 2006
Silica	N,N'-Disuccinimidyl carbonate (DSC); Streptavidin	Biotinylation of antibody at the carboxy-termini using biocytinamide and lyophilized carboxypeptidase Y (CPD-Y)	C-terminus carboxyl group	Franco et al., 2006
Gold	Complimentary ssDNA and oligo(ethylene glycol) (OEG – terminated thiol	Sulfosuccinimidyl 4-( <i>p</i> -maleimidophenyl) butyrate (sulfo-SMPB) ; thiolated ssDNA	C-terminus carboxyl group	Boozer et al., 2004, 2006.

Several linkage chemistries have been used to immobilize antibodies in an oriented manner. One of them uses Fc receptors such as protein A, protein G or recombinant protein A/G to bind the Fc portion of whole antibodies which in turn leave the antigen specific sites free. To reduce nonspecific protein interaction, Brogan et al. (2004) assessed the effectiveness of different nonionic and zwitterionic surfactants and antibody immobilization strategies. Using enzyme-linked immunosorbent assay, surface plasmon resonance, and atomic force microscopy, they concluded that oriented immobilization of whole IgG via protein A resulted in higher antigen binding specificity than randomly immobilized IgG via glutaraldehyde. They also summarized that when used as blocking agent, nonionic surfactants zwitterionic such as, Tween 20, Tween 80, and Triton X-100 at a concentration equal to or slightly higher than the critical micelle concentration reduced the influence of nonspecific interaction significantly.

The oxidation of a carbohydrate moiety in the C<sub>H</sub>2 domain of the Fc portion of antibodies to aldehyde groups followed by the formation of covalent hydrazone bonds with a hydrazide activated support also lead to an oriented antibody immobilized surface in such way that its antibody binding sites remain available for specific antibody-antigen interaction (O'Shannessy and Hoffman 1987). Another popular strategy for preparing site-specific oriented immunosurfaces involves the utilization of the sulfhydryl group on univalent antibody fragments (Fab') fabricated by enzymatic fragmentation of Immunoglobulin G (IgG). To obtain univalent fragment, antibodies (IgG or IgM) need to be cleaved by digestion using a protease for example, papain, pepsin or ficin. Papain digestion of IgG produces three fragments: two Fab fragments and one Fc fragment, whereas pepsin splits IgG to one bivalent F(ab')<sub>2</sub> and several pieces of Fc fragments. SH-protease, for example ficin, is required for the digestion of isotype IgG<sub>1</sub> to bivalent fragment F(ab')<sub>2</sub> and is quite effective in terms of yield, immunoreactivity, and stability.

This is because the mouse  $\gamma 1$  chain sequence lacks the residue corresponding to the pepsin digestion site (Burton 1985; Mariani et al. 1991).

Bivalent  $F(ab')_2$  is then transformed into univalent Fab' by selective reduction using dithiothreitol (DTT), 2-mercaptoethanol, 2-mercaptoethylamine·HCl (2-MEA·HCl), or Cysteine·HCl. Lu et al. (1995) found that selective reduction of  $F(ab')_2$  of rabbit IgG using DTT produced monomers containing 0.91 sulfhydryl groups on average, whereas theoretical value of sulfhydryl group in Fab' is 1. DeSilva and Wilson (1995) reported an average of 3.2 (theoretical value is 1) and 4.7 (theoretical value is 3) sulfhydryl groups with 2-mercaptoethylamine reduction from goat and mouse IgG respectively. These Fab'-SH fragments that can be immobilized by a disulfide exchange reaction on several surfaces including liposome, monolayer vesicles, and thiolated supports.

Lu et al. (1995) also compared antibody binding activities of random (silanized silica surface by glutaraldehyde coupling reaction) and oriented immobilization of Fab' on derivatized silica surfaces containing pyridyl disulfide group and concluded that the antibody binding activity of Fab' in the oriented form was 2.7 times greater than that in random form. Peluso et al. (2003) compared random and oriented immobilization of biotinylated full size antibodies and Fab' fragments to streptavidin-coated surfaces and concluded that the site specific orientation of full antibody (or fragments) increased the binding capacity up to 10 fold than that of random orientation. Brogan et al. (2003) and Lee et al. (2006) have successfully immobilized IgG fragments onto bare gold surface through the native thiol group (without any linking layer). O'Brien et al. (2000) determined that directly immobilized Fab' fragments on gold surfaces are useful for preparing antigenic surfaces with enhanced epitope densities relative to surfaces modified with non-specifically adsorbed whole molecule IgG.

To compare different immobilization strategies for direct coupling of F(ab')<sub>2</sub> (random immobilization) and Fab' (oriented immobilization) onto gold, Vikholm (2005a;b) analyzed the changes in surface plasma resonance intensity upon attachment. He concluded that direct coupling of Fab' onto gold surfaces followed by blocking of the remaining free space using nonionic hydrophilic polymer of *N*-[tris (hydroxy-methyl) methyl]-acrylamide between the antibody to suppress nonspecific binding showed the highest response to antigen. The Fab' layer showed about four-folds greater binding capacity than that of F(ab')<sub>2</sub>. Kang et al. (2007) compared immunobinding efficiency of oriented anti-mouse IgG antibody using the oxidation of carbohydrate moiety in C<sub>H</sub>2 domain of Fc portion and biotin-streptavidin system onto hydrazine-coated magnetic particle to that of conventional random immobilization using the amino-coupling. Both the oriented immobilization techniques resulted in identical efficiency and were about 2 times greater than that of random immobilization. Several immobilization conditions such as the procedure for cleaning the gold surface i.e. cleanliness and hydrophilic nature of gold surface, procedure for reductive splitting of the F(ab')<sub>2</sub> - fragments, use of freshly split Fab'- fragments affect the antigen binding properties (Albers et al. 2009). So, care and attention to immobilization details is important.

In summary, to obtain a highly specific antigenic surface, orientation of immobilized antibody is a critical consideration. Site directed immobilization of Fab' through the native thiol appears to be the most promising among various strategies because of simplicity in preparation and reduction of whole IgG to Fab' results in a higher degree of immobilization of well oriented and active antibody per surface area.

## Chapter 3: Materials and Methods

### 3.1 Source of *Cryptosporidium* oocysts and antibodies

*Cryptosporidium parvum* (Iowa isolate) oocysts were purchased from Waterborne™, Inc. Waterborne™, Inc. extracted the oocysts from feces of experimentally infected calves with diethyl ether and further purified them by the Percoll-Sucrose density gradient centrifugation. They used gamma irradiation or heat inactivation (70 °C water bath for 8 minutes) to produce non-viable oocysts. Oocysts were stored at 2 – 6 °C.

*Cryptosporidium parvum* specific mouse monoclonal antibody of isotype IgG<sub>1</sub> (6D3-UN) of subclass IgG and of subclass IgM (A400UN 2C9) were also obtained from Waterborne™, Inc. Isotype IgG<sub>1</sub> was purified by Waterborne™, Inc. using precipitation from mouse ascites fluid using 45% ammonium sulfate, followed by dialysis versus 0.01 M tris buffer, and ion exchange chromatography on diethylaminoethyl cellulose-sephacel gel. Antibody IgM was purified by precipitation from mouse ascites fluid using 2% boric acid, followed by dialysis versus phosphate-buffered saline (PBS)/0.02% sodium azide, and extraction from fatty material using 1,1,2-trichlorotrifluoroethene.

### 3.2 Preparation of antibody fragments

#### 3.2.1 Preparation of IgG<sub>1</sub>-Fab' antibody fragments

Pierce® Mouse IgG<sub>1</sub> Fab and F(ab')<sub>2</sub> preparation kits (Thermo Scientific) were used for the fragmentation of IgG<sub>1</sub> to F(ab')<sub>2</sub> following the manufacturer's instructions. Figure 3.1 shows the schematic of the fragmentation procedure. In brief, 0.5 mL of 1 mg/mL IgG<sub>1</sub> was prepared for digestion by removing salts and other smaller molecules using a Zeba™ Desalt spin column (7 K MWCO). The prepared IgG<sub>1</sub> sample was incubated at 37°C for 24 hours in an end-over-end mixer in the presence of protease ficin and 4 mM

cysteine-HCl. The resulting  $F(ab')_2$  was purified from Fc and undigested  $IgG_1$  using a Protein A column.  $F(ab')_2$  fragments were subjected to centrifugal concentration (4500 x g, 20 minutes) in a spin column with a nominal molecular weight limit (NMWL) of 30kDa. Final concentrations were determined via absorbance at 280 nm ( $\epsilon = 1.48$  L/cm/g).  $Fab'$  was prepared by selective reduction of  $F(ab')_2$  in reaction buffer [PBS containing EDTA (PBS-EDTA): 20-100 mM sodium phosphate, 150 mM NaCl, 1-10 mM EDTA, pH 7.2] using a mild reducing agent [2 MEA-HCL (50mM)] at 37 °C for 90 minutes.  $Fab'$  fragments were subjected to centrifugal concentration using the spin column as described above to obtain the desired concentration.

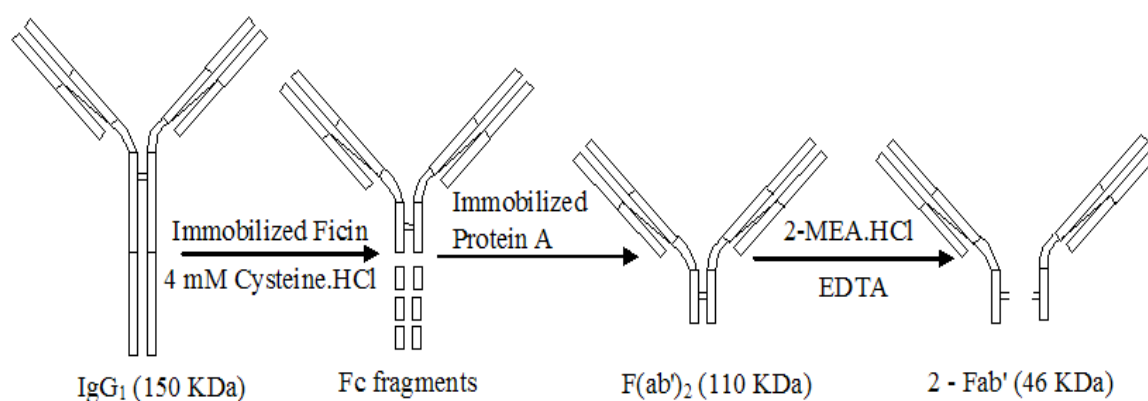


**Figure 3.1: Fragmentation of  $IgG_1$  to  $Fab'$**

### 3.2.2 Preparation of $IgG_1$ -Fab antibody fragments

$IgG_1$  was fragmented to Fab using the same Pierce® Mouse  $IgG_1$  Fab and  $F(ab')_2$  preparation kit as described in section 3.2.1 except as follows: after preparation of 0.5 mL  $IgG_1$  by a Zeba™ Desalt spin column (7K MWCO),  $IgG_1$  sample was incubated at 37 °C for 5 hours in an end-over-end mixer in presence of protease ficin and 25 mM cysteine-HCl. Final concentrations were determined via absorbance at 280 nm ( $\epsilon = 1.25$  L/cm/g).

### 3.2.3 Preparation of IgM-Fab' antibody fragments

The Pierce® IgM fragmentation kit was used to cleave IgM to F(ab')<sub>2</sub> following the manufacturer's instructions. Samples of 1mL of 1 mg/mL IgM were prepared by performing a buffer exchange using a Dextran Desalting column or centrifugal concentrator (NMWL ~ 30kDa). Prepared IgM was then added to an immobilized Pepsin column for digestion and incubated at 37 °C for 1.5 hours. Digested IgM was transferred to a C30 Concentrator and centrifuged at 4,500 × g for 30 minutes to remove the smaller molecular fragments. IgM-Fab' was prepared by cleaving F(ab')<sub>2</sub> with the selective reduction of mild reducing agent 2 MEA-HCL (50 mM) during incubation at 37 °C for 90 minutes. Fab' fragments were further concentrated using centrifugal concentration (4500 x g, 20 minutes) with a NMWL of 30kDa. Final concentrations were determined via absorbance at 280 nm ( $\epsilon = 1.25 \text{ L/cm/g}$ ).

### 3.3 Gold coated slide preparation

Gold coated slides (50 Å Cr, 1000 Å Au) from EMF, Dynasil Corporation, were dipped into a 3:7 solution of 30% H<sub>2</sub>O<sub>2</sub> and pure H<sub>2</sub>SO<sub>4</sub> (Piranha Solution) for 40 minutes to remove the organic materials. Slides were then rinsed with PBS buffer followed by Type 1 (18.2 Ωm) water. Cleaned slides were dried using a stream of ultrapure N<sub>2</sub> (Air Liquide).

### 3.4 Antibody fragment immobilization

For the preliminary capture tests, an aliquot of 20 μL of fragmented antibody (Fab' and Fab) from 0.5 mL of 1 mg/mL IgG<sub>1</sub>/IgM was placed in the center (4 x 4 mm<sup>2</sup>) of clean gold coated slides and was incubated at 4 °C overnight followed by a gentle rinsing with PBS and Type 1 water. To determine the optimum antibody concentration i.e. to evaluate the changes in capture efficiency with respect to antibody concentration, fragmented Fab' from five different dilutions (1:30, 1:8, 1:4, 1:2, and 1:1.5) of the original antibody

concentration (0.5 mL of 1 mg/mL IgG<sub>1</sub>) were used to activate the whole slide (6.8 cm x 1 cm) using the same procedure as described above.

### **3.5 Preparation of *Cryptosporidium parvum* oocysts**

To confirm the concentration of *Cryptosporidium* in the stock suspension, oocysts were enumerated using a Petroff-Hausser counting chamber (Hausser Scientific). The cell counting chamber was loaded with an aliquot of vortexed stock suspension ( $\approx 1 \times 10^6$  oocysts/mL). Then the chamber was placed on the microscope stage and oocysts were allowed to settle for 2 minutes. Using 400X magnification and phase contrast microscopy, the actual number of oocysts per mL of stock suspension was enumerated.

The spiking suspension was prepared by mixing the tube containing enumerated stock suspension with vortex for a minimum of 2 minutes. An aliquot containing around 20,000 oocysts was stained with 1:1 ratio (v/v) of 0.1 mg/mL 4',6-diamidino-2-phenylindole (DAPI) for 1 hour at 37 °C in a micro-centrifuge tube. The DAPI stained spiking suspension was added to a 250 mL erlenmeyer flask containing a stir bar and 0.01% Tween®20 or 0.01 % Na<sub>4</sub>HPO<sub>4</sub>. The diluted suspension in the flask was mixed for a minimum of 30 minutes before beginning the tests. The glass funnel and beakers were coated with Sigmacote®. A cellulose nitrate membrane filter (0.2 µm, 25 mm-diameter) from Fisher Scientific was wetted by dipping it into 0.01% Tween 20®/0.1 % Na<sub>4</sub>HPO<sub>4</sub> and placed onto clean filter holder base fitted in a vacuum flask, before 5 mL of 0.01% Tween 20®/0.1 % Na<sub>4</sub>HPO<sub>4</sub> was added to the filtration unit and allowed to stand.

A volume of 5 mL spiking suspension was removed while the stir bar was still spinning and added into Tween® 20 (5 mL of 0.01%) standing in the filtration unit. A vacuum was applied to allow liquid to drain to the meniscus. Type 1 water (10 mL) was added into the funnel and drained to the meniscus twice. The membrane filter was peeled off the filter base and placed on the microscopic stage for enumeration (200 X magnification using

DAPI excitation). The number of *Cryptosporidium* in 10 microscopic fields was determined and averaged. The total number of *Cryptosporidium* was calculated by multiplying the average density by the area of filtration. After examination of 5 filters, the mean, standard deviation, and RSD (relative standard deviation) of the 5 replicates were calculated. From the mean value, the volume of diluted suspension for 200 oocysts was calculated. The diluted suspension was used within 24 hours of enumeration.

### **3.6 Design of shear test**

Antibody coated slides with *Cryptosporidium* oocysts (DAPI stained) attached were prepared then assembled into the GlycoTech rectangular flow chamber (Product no. 31-010). A 50 mL syringe pump (KD Scientific: Model series 200 series) was then used to pump water through the flow cell, and the outlet water was captured in a beaker. Figure 3.2 presents the experimental setup of the shear test. The test duration and rate were limited by the syringe pump, as it could only operate a maximum flow of 81 mL/min. To achieve higher flow rate, the flow cell was connected to an in house water supply system. Microscopic images were taken at selected and random locations on the slide before the test. Following the test, images were captured on the same locations. Both sets of images were analyzed using a Matlab program which calculated the total number of non-black and white pixels. The percent difference between the number of pixels before and after the shear test was calculated to determine the percentage of oocyst removed due to shear flow and the shear stress which will not shear off *Cryptosporidium*.

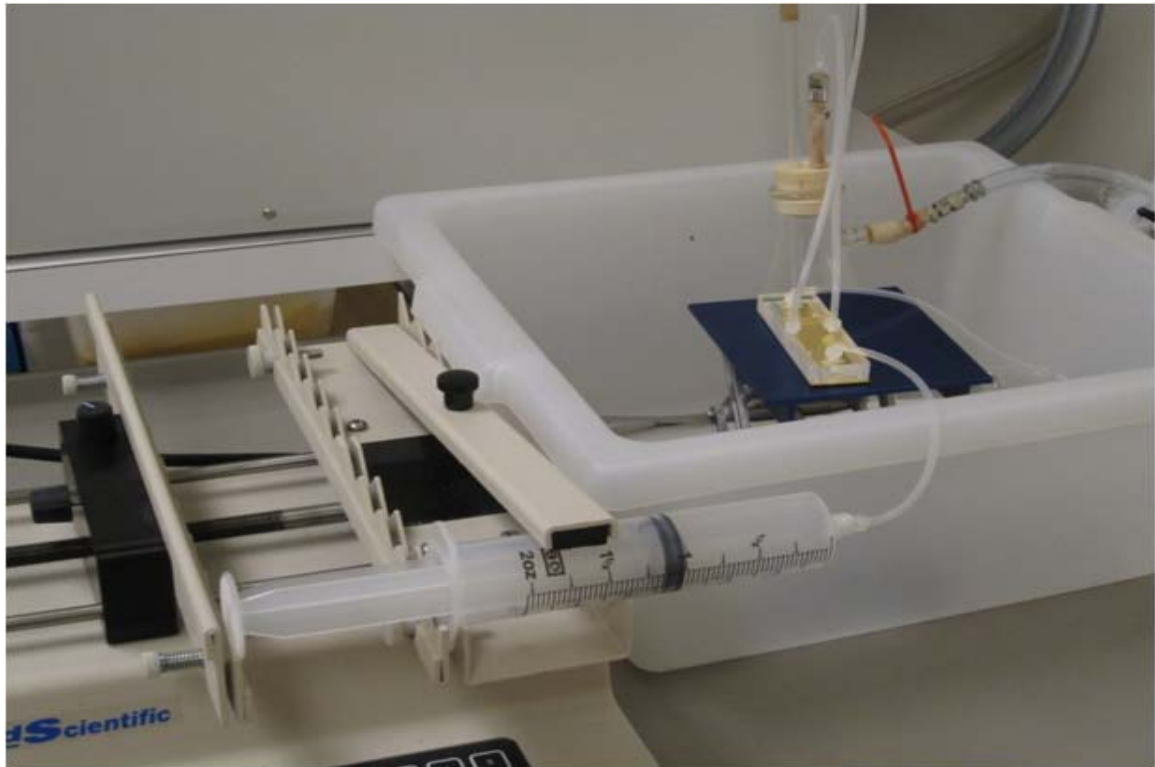


**Figure 3.2: Shear test and capture test setup**

### **3.7 Design of capture tests**

The syringe pump from KD Scientific and a medium flow peristaltic pump (Model 3386: Control Company) were used to maintain the predetermined flow rates (42, 28, and 14 mL/min). A volume of 50 mL Type1 water spiked with 200 DAPI stained *Cryptosporidium parvum* oocysts was pumped over the immobilized antibody onto gold slides through a the rectangular flow chamber with two different gasket depths (125  $\mu\text{m}$  and 250  $\mu\text{m}$ ).

The total number of oocysts captured was counted by direct enumeration of DAPI stained oocysts at randomly selected microscopic fields in the activated area (4x4 mm<sup>2</sup> area) under the microscope using fluorescence excitation/emission filters. For each experiment, nine measurements were made to cover the entire activated area and averaged. The number of total captured cells was calculated by multiplying average cell density by the total area of activation. During antibody optimization experiments, the entire slide was thoroughly observed by one microscopic field at a time to determine the number of

captured *Cryptosporidium*. The capture efficiency was calculated by dividing the number of cells captured by the total number of cells in the volume tested.

In order to validate the efficiency of the capture surface to concentrate oocysts from the suspension, the effluent liquid was collected from the outlet of the device during each experiment and filtered using a 0.22  $\mu\text{m}$  membrane filter. Again, the number of *Cryptosporidium* in 10 microscopic fields was determined and averaged (200 X magnification using DAPI excitation). The total number of *Cryptosporidium* was calculated by multiplying the average density by the area of filtration. The syringe, tubing, flow cell, beakers, and gaskets were cleaned by rinsing with deionized water and air dried between each experiment. Each experiment was performed in triplicate. Capture tests were performed using 5 different test conditions (Table 3.1). Wall shear stress ( $\tau_w$ ) in the flow chamber was calculated using the following equation assuming two-dimensional, steady, fully developed flow between two infinite parallel plates (Chung et al., 2003; Bacabac et al., 2005):

$$\tau_w = \frac{6\mu Q}{a^2 b} \quad \text{Equation 3.1}$$

Where,  $\mu$  is the dynamic viscosity of the flow ( $1 \times 10^3 \text{ Kg}/(\text{m}\cdot\text{s})$  for water),  $Q$  is the volumetric flow rate ( $\text{mL}/\text{s}$ ) in the flow cell,  $a$  is the depth of cell ( $\text{cm}$ ) and  $b$  is the flow path width ( $1 \text{ cm}$ ). The Reynolds number ( $\text{Re}$ ) in the test chamber was calculated as:

$$\text{Re} = \frac{\rho v L}{\mu} \quad \text{Equation 3.2}$$

Where,  $\rho = 1000 \text{ kg}/\text{m}^3$  is the density of flow (water),  $v$  is the characteristic velocity (for example, mean velocity at the inlet),  $L$  is the characteristic length (the height of the channel) and  $\mu$  is the dynamic viscosity of the flow ( $1 \times 10^3 \text{ Kg}/(\text{m}\cdot\text{s})$  for water).

**Table 3.1: Hydrodynamic experimental variables of capture tests**

Flow rate (mL/min)	Depth of cell $\mu\text{m}$	Shear Stress (dyne/cm <sup>2</sup> )	Reynolds number	Sampling time Hours*
14	125	87	15	48
28	125	174	29	24
28	250	44	59	24
42	125	261	44	16
42	250	65	88	16

\* Amount of time required to sample 40 L of water at the particular flow condition

To investigate the effect of antibody type on the capture efficiency, capture surfaces were activated with two different types of monoclonal antibody specific to *Cryptosporidium*, IgG<sub>1</sub> and IgM. To evaluate the effect of antibody orientation on the capture efficiency, two different antibody fragments, Fab and Fab', were used for capture surface preparation. For IgG-Fab' and IgG-Fab, capture test was performed at all the five test conditions described above, but IgG-Fab ' was tested for capture efficiency at two test shear stresses ( 87 and 174 dyne/cm<sup>2</sup>).

### 3.8 Implementation of retroreflectors

The corner cube micro retroreflectors (cc $\mu$ RR) have three sides that are coated with gold and underneath one of these gold layers is a magnetic material (nickel). This nickel layer was utilized to separate them out of solution under the action of a magnetic field. The gold layers were used to activate the cubes with antibody fragments using the gold-thiol chemistry described previously.

#### 3.8.1 Retroreflector cube release

Cc $\mu$ RR were fabricated on wafer pieces in Dr. Paul Ruchhoeft's lab at the University of Houston [Kemper, 2008]. Cubes were released by placing the wafer into a 2.3% solution of tetra methyl ammonium hydroxide (TMAH), and water, in an ultrasonic bath for about 30 minutes. If all the cubes were not released, an additional 30 minutes sonication was

performed. The released cubes were collected on the bottom of a beaker by allowing them to settle in a beaker placed on a rare earth magnet [McMaster-Carr] for 1 hour, and the solution was then exchanged with EDTA buffer.

### 3.8.2 Retroreflector activation

Activation of cc $\mu$ RR with Fab' fragments was performed by overnight incubation in an end-over-end mixer. FITC conjugated affinity purified IgG goat anti-mouse IgG-F(ab')<sub>2</sub> fragment specific (MP Biomedicals, LLC.; catalog no. 55518) and Texas Red<sup>®</sup> conjugated affinity purified F(ab')<sub>2</sub> fragment goat anti-mouse IgG-F(ab')<sub>2</sub> fragment specific (Jackson ImmunoResearch laboratory, Inc.; code no. 115-076-006) were used to test the activation of cc $\mu$ RR with Fab'. A sample of 1 mL activated suspended cc $\mu$ RR was incubated with FITC and Texas Red conjugated anti-mouse IgG-F(ab')<sub>2</sub> to Fab' for 1 hr at 37°C. Images were taken using phase contrast microscopy, a sensitive black/white camera used for fluorescent detection and color camera at 40x magnification with DAPI, FITC and Texas Red excitation.

## 3.9 Detector system

The system to detect cc $\mu$ RR was developed in the lab with the assistance of Ms. Deanna Erickson and Mr. Danny Trommelen and is comprised of a light source (laser beam), an iris diaphragm, a 50R/50T beamsplitter, a Y-Z axis stage, a beam dump, and a CCD array. Figure 3.3 shows the image of the detector system. Figure 3.4 shows a schematic of the detector system. A light source (laser beam) was directed to the beamsplitter, through the iris diaphragm. The beamsplitter (50R/50T) splits the incident light to different fractions. The refracted light that passes through the beamsplitter illuminates the capture surface. The retroreflectors, if present, then reflect the light back to the beamsplitter. The light that is reflected from the retroreflector returns to the beamsplitter and is reflected down to the CCD array to give a signal to identify the presence of *Cryptosporidium*. The

capture surface was placed at an angle that allows the background noise to reflect off the surface.

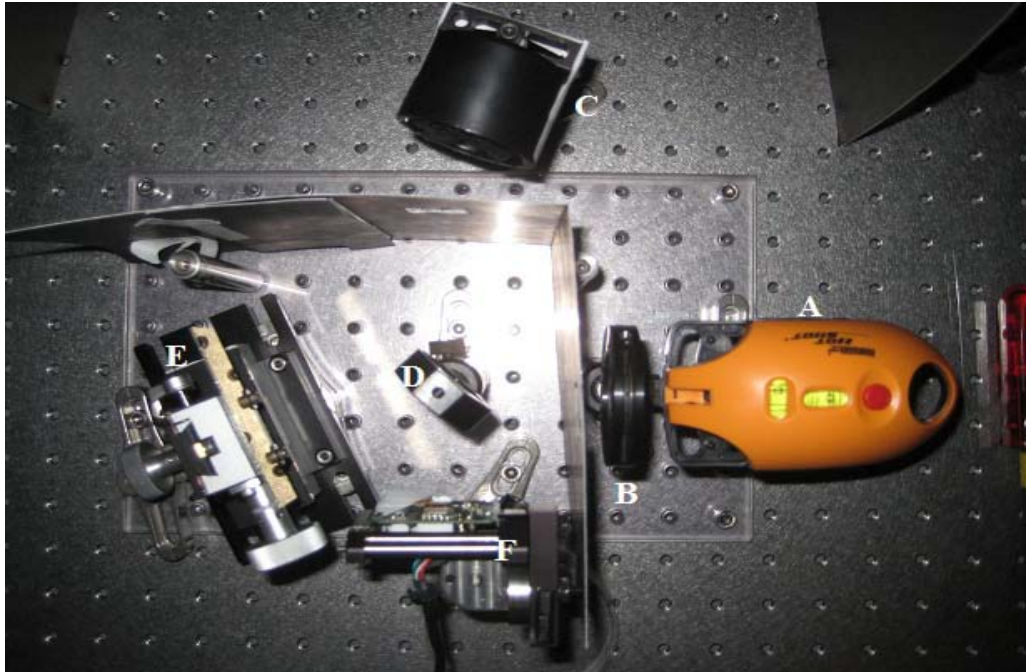


Figure 3.3: Detector system

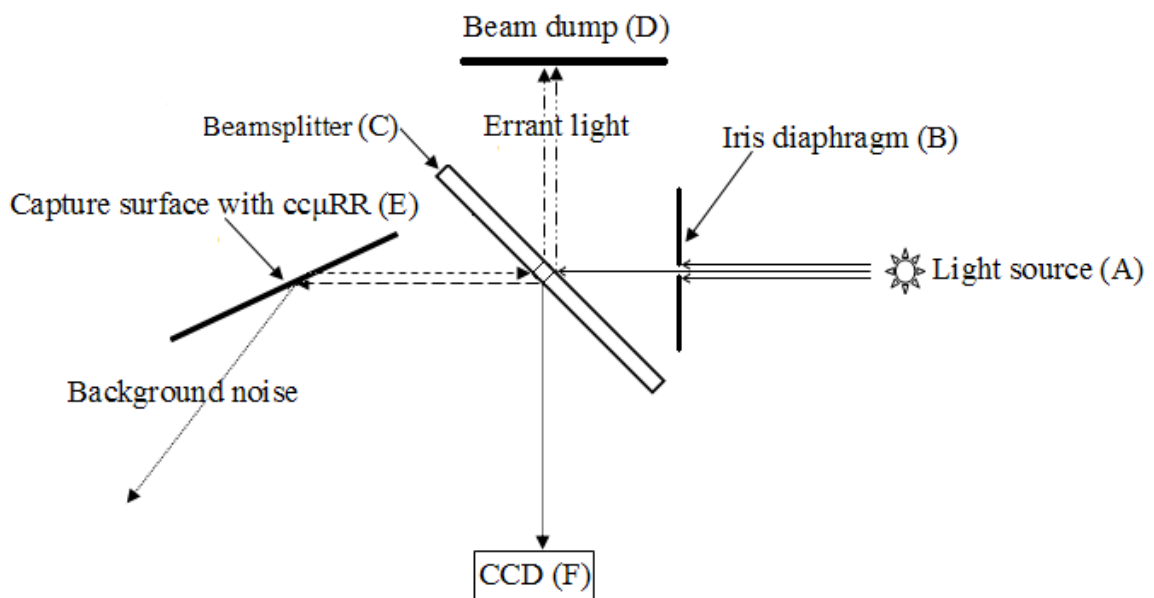


Figure 3.4: Schematic of detector system configuration

### **3.10 Statistical analysis**

All data were expressed as the mean  $\pm$  SD of the mean values unless otherwise specified.

Results were analyzed by analysis of variance (ANOVA). A paired t-test was used for the comparison of the capture efficiencies between different treatments and antibody types.

The level of significance was accepted at  $P < 0.05$ .

## Chapter 4: Results and Discussion

### 4.1 Shear test results

A shear test was performed to determine the wall shear stress that the antibody-*Cryptosporidium* oocyst bond can withstand without any significant bond dissociation. This threshold value was then used to design the capture test. Images of 10 random locations on the slide before and after 81 mL/min flow rate were analyzed through a Matlab program (Appendix A) which output an image intensity histogram and the total number of non-black and white pixels. The number of white pixels in the image was correlated to the number of *Cryptosporidium* oocysts. Figure 4.1 and Figure 4.2 present a captured microscopic image and the corresponding histogram generated by the Matlab program, respectively. A comparison of the pixel count (Table B.1 in Appendix B) at different random locations before and after the shear test is illustrated in Figure 4.3.

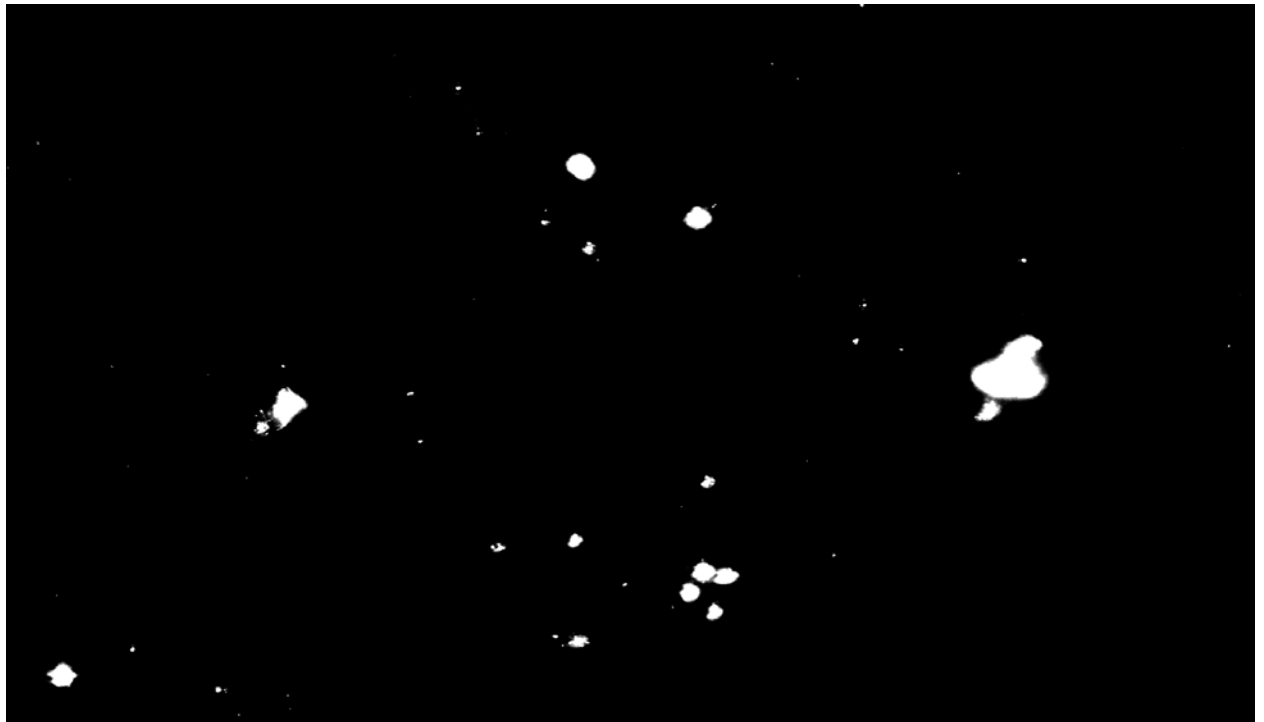
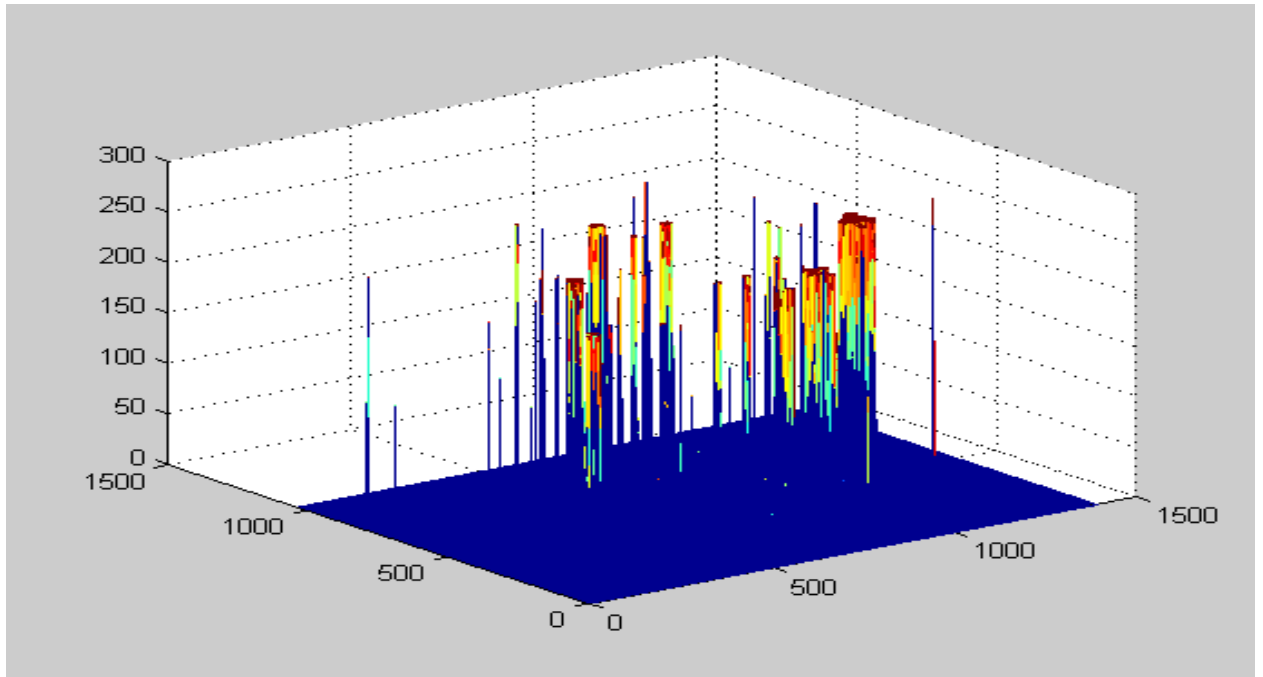
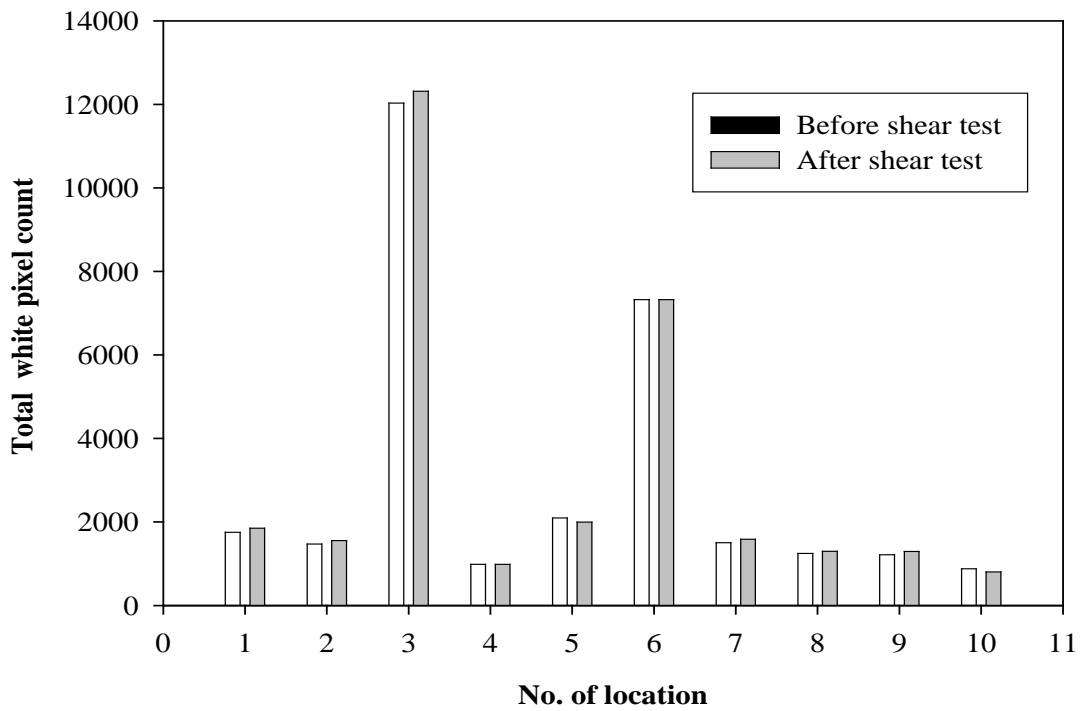


Figure 4.1: Microscopic image used for Matlab analysis



**Figure 4.2: Matlab output (Histogram)**



**Figure 4.3: Example of total while pixel count before and after the shear experiment at 81 mL/min flow rate and 250  $\mu$ m cell depth**

The total white pixel count of images for certain locations before the shear test were less than that of after the shear test. This could be due to the fact that it is extremely difficult to take the after picture in the exact same location as the before picture. A slight variation in any direction could result in a change in the number of pixels on that image. A statistical analysis of 10 images at 81 mL/min flow rate and 250  $\mu\text{m}$  cell depth showed that there was no significant loss ( $p = 0.87$ ; paired t-test) of captured oocysts for a shear stress of up to 126  $\text{dyne/cm}^2$  (corresponding to 250  $\mu\text{m}$  deep flow cell and 81 mL/min flow rate). The results obtained beyond this value were not reproducible because the flow cell could not repeatedly withstand the pressure generated, but showed that a shear stress of 280  $\text{dyne/cm}^2$  caused the removal of oocysts from the system.

#### **4.2 Capture test results**

The purpose of the capture test was to compare the capture efficiency of surfaces activated with different antibody fragments and hence optimize the operating conditions. Two techniques were used to determine the capture efficiency. The filtration technique measured the number of *Cryptosporidium* that made it through the system, while direct microscopic observation of the actual activated surface measured *Cryptosporidium* directly on the slide. The capture efficiency measured with direct microscopic observation was preferred because it counted the captured oocysts directly on the slides, whereas, the filtration technique also counted oocysts that could have been lost in the tubing, beaker and filtration apparatus. The recovery efficiencies using different antibody fragments for different flow conditions and cell depths are summarized in Table 4.1. Figure 4.4 summarizes the capture efficiencies for three different antibody fragments with respect to the different treatments.

**Table 4.1: Summary of capture test results (direct microscopic observation)**

Flow Rate (mL/min)	Depth of cell ( $\mu\text{m}$ )	Wall Shear Stress (Dyne/cm <sup>2</sup> )	% Recovery* (RSD)		
			IgG-Fab'	IgG-Fab	IgM-Fab'
14	125	87	8.7 <sup>a</sup> (18)	3.9 <sup>a</sup> (40)	2.9 <sup>a</sup> (16)
28	125	174	12 <sup>a</sup> (28)	2.9 <sup>a</sup> (31)	2.4 <sup>b</sup> (0)
28	250	44	8.4 <sup>a</sup> (14)		3.4 <sup>a</sup> (13)
42	125	261	7.4 <sup>a</sup> (44)		3.7 <sup>a</sup> (12)
42	250	65	1.3 <sup>b</sup> (35)		1.8 <sup>c</sup> (25)

\*Different superscripts with in a column denote a statistical difference ( $P < 0.05$ )

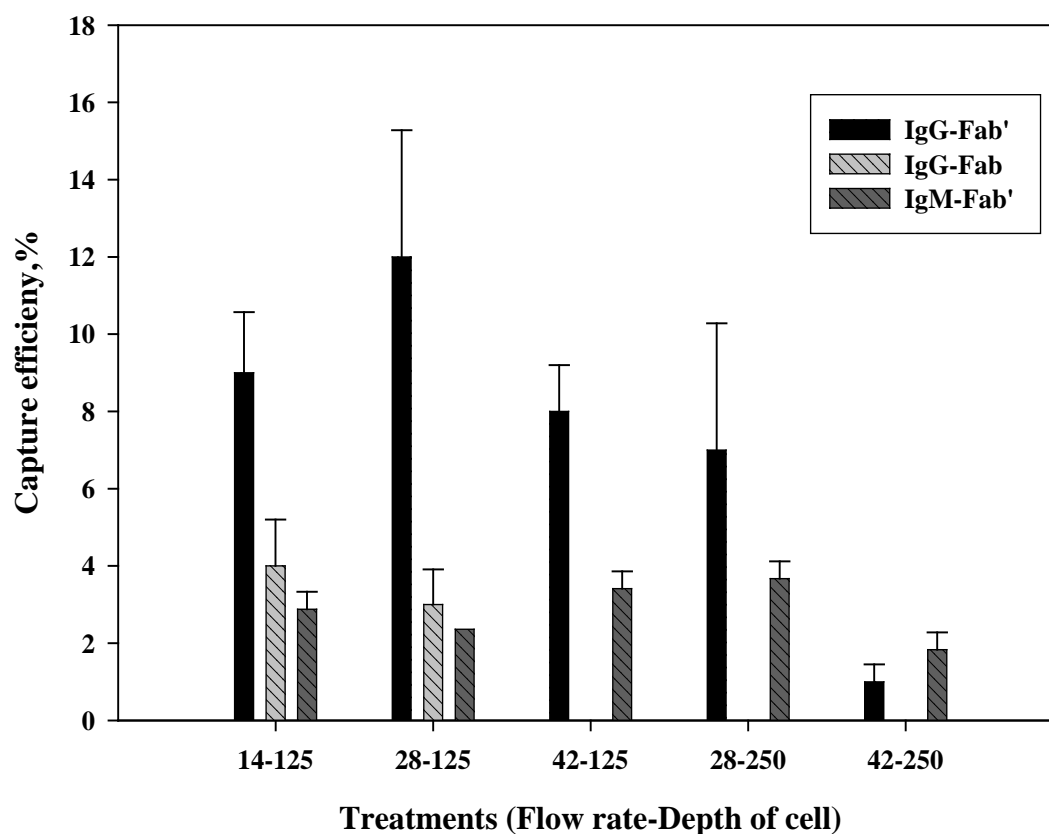


**Figure 4.4: Capture efficiency of different antibody fragments under different treatment conditions**

#### 4.2.1 IgG-Fab'

The average percent capture efficiency measured using direct microscopic enumeration of slides varied from 1.3 to 14.2 for the different treatments (Table B.2 in Appendix B). The maximum average efficiency (11.5%) was obtained with flow rate of 28 mL/min and cell depth of 125  $\mu\text{m}$  (28 – 125), and 42 mL/min flow rate - 250  $\mu\text{m}$  cell depth (42 – 250) resulted in the minimum (1.3%) efficiency.

The capture efficiency measured using filtration of the effluent was higher than that of direct microscopic examination of the capture slides in all cases. This is because of the variability in measurement of concentration of spiked oocysts and in the technique of measurement itself. A one way ANOVA analysis revealed that the differences in mean capture efficiencies among the different flow conditions were greater than would be expected by chance ( $P = 0.003$ ). A pair wise comparison using Student Newman-Keuls (SNK) method between the treatments showed that there were no significant differences for different treatments except that the use of treatment 42 – 250 resulted in significantly lower recovery efficiency. Trends in the change of oocyst recovery efficiency with respect to flow rate, depth of cell and shear stress are shown in Figure 4.5, Figure 4.6, and Figure 4.7, respectively. Although the data are not significantly different, from Figure 4.5, it can be implied that increasing the flow rate from 14 to 28 mL/min optimized the capture efficiency. The capture efficiency decreased slightly with an increase in the depth of the cell (Figure 4.6). Figure 4.7 illustrates that there might be a window of shear stress (150 – 200  $\text{dyne/cm}^2$ ) that optimized the capture efficiency.

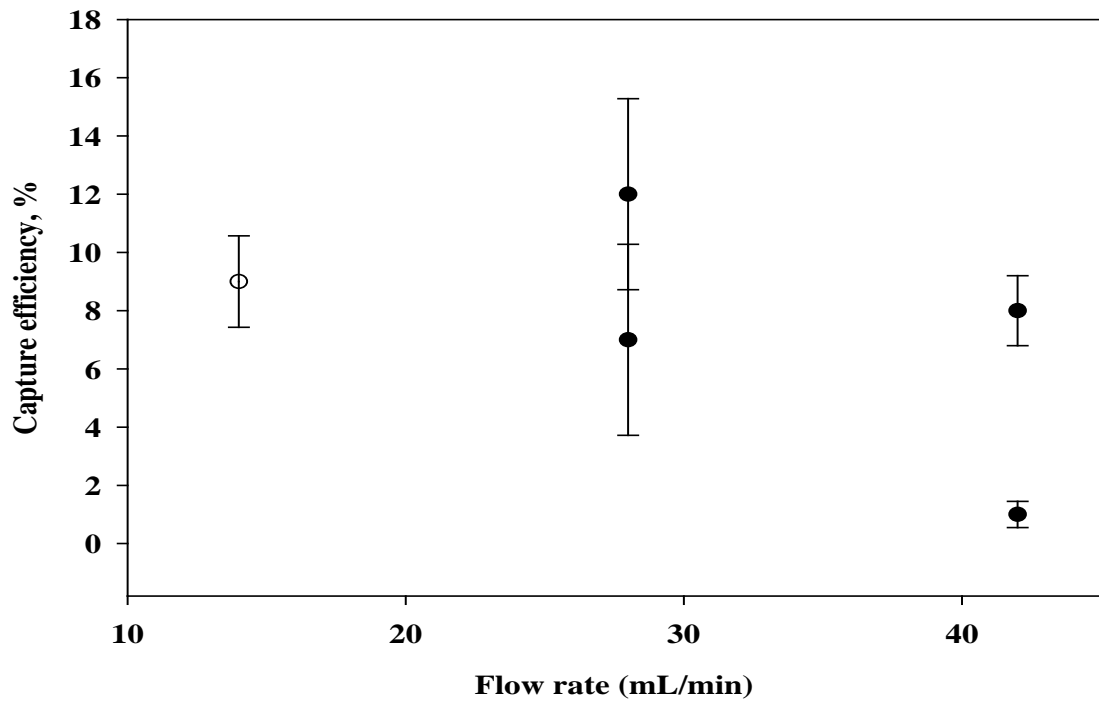


Figure 4.5: *Cryptosporidium* recovery with respect to the flow rate (IgG-Fab')

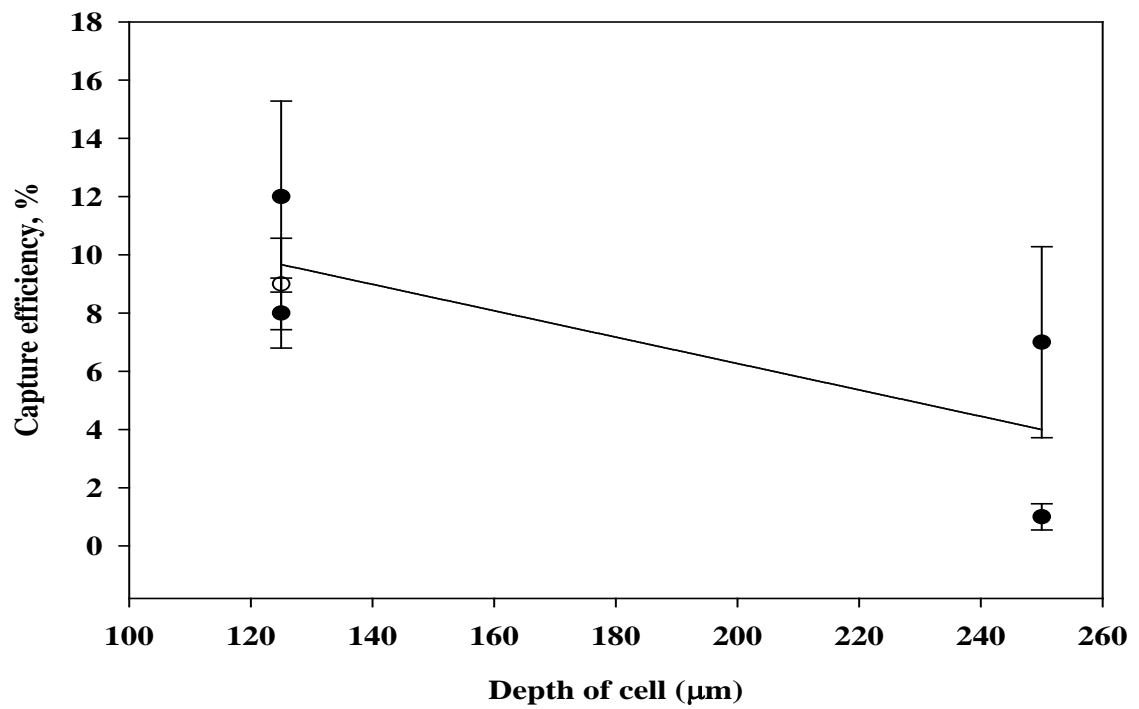
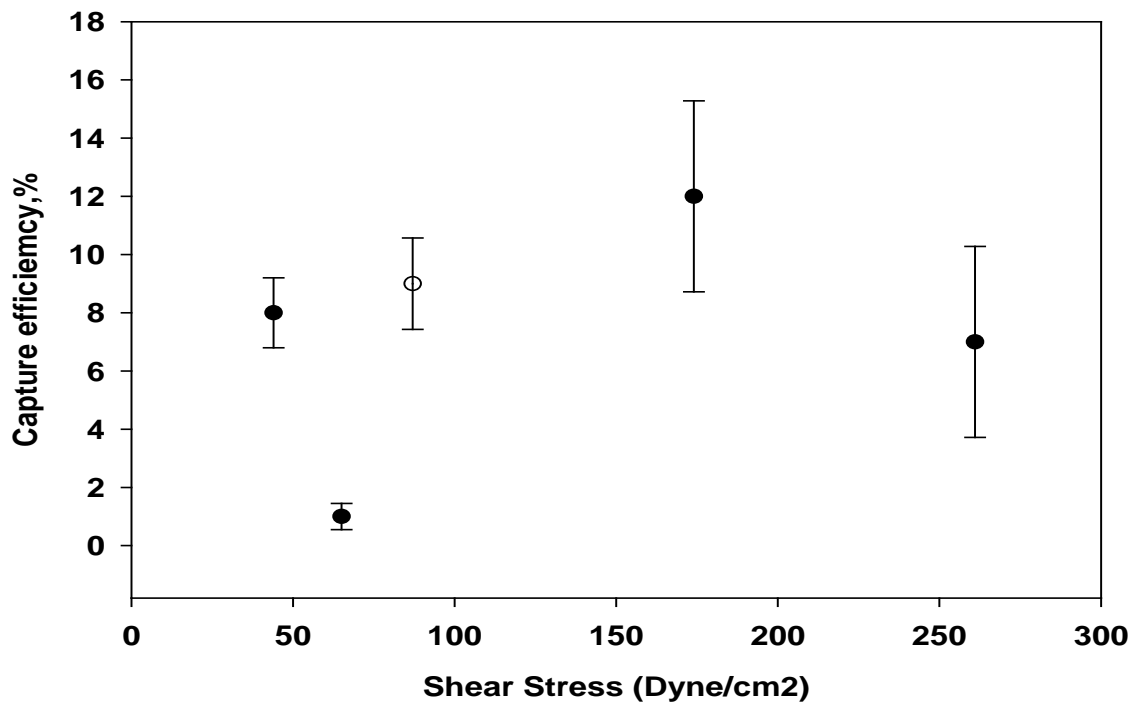


Figure 4.6: *Cryptosporidium* recovery with respect to the depth of flow cell (IgG-Fab')



**Figure 4.7: *Cryptosporidium* recovery with respect to the shear stress (IgG-Fab')**

#### 4.2.2 IgM-Fab'

The capture efficiency for IgM-Fab' immobilized on the surfaces ranged from 1.6 to 3.9% (Table B.3 in Appendix B). A flow rate of 42 mL/min and cell depth of 125  $\mu\text{m}$  produced the maximum average efficiency (3.7%), and as with IgG-Fab', the minimum (1.8%) capture efficiency was obtained with the treatment 42 – 250. The capture efficiency measured through the effluent filtration was again higher than that measured through microscopic examination. A statistical analysis showed that different treatments significantly changed the average capture efficiency (one way ANOVA;  $P = 0.001$ ) using direct microscopic counts. There was no significant difference in the capture efficiency for treatments 28 – 125 and 42 – 250. Treatment 42 – 250 showed significantly less capture efficiency than treatments 14 – 125, 42 – 125, and 28 – 250. However, average capture efficiency of treatments 14 – 125, 42 – 125, and 28 – 250 were not significantly different. The optimal window (14 – 28 mL/min) of flow rate was not as obvious as that

of IgG-Fab' (Figure 4.8). There was no clear trend in change of capture efficiency with cell depth and shear stress (Figure 4.9 and Figure 4.10).

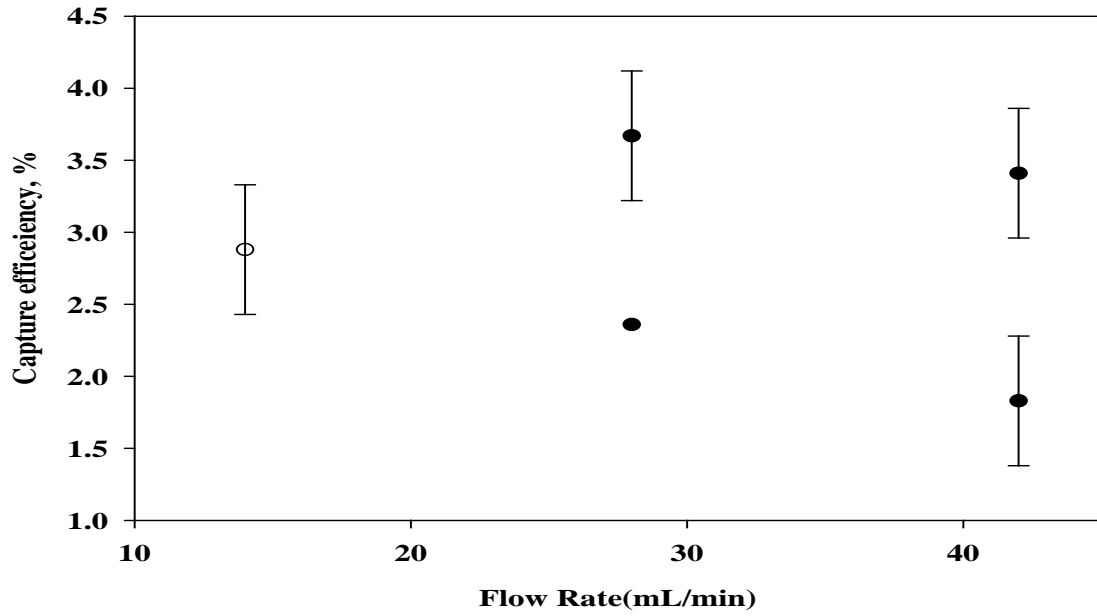


Figure 4.8: *Cryptosporidium* recovery with respect to the flow rate (IgM-Fab')

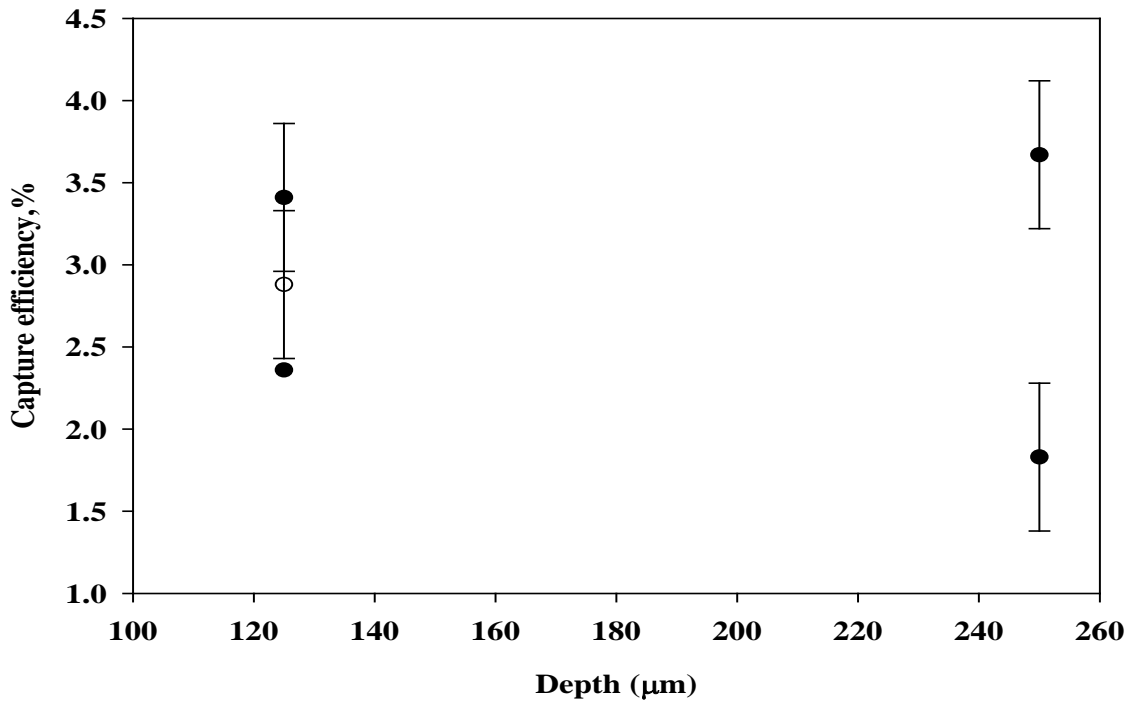
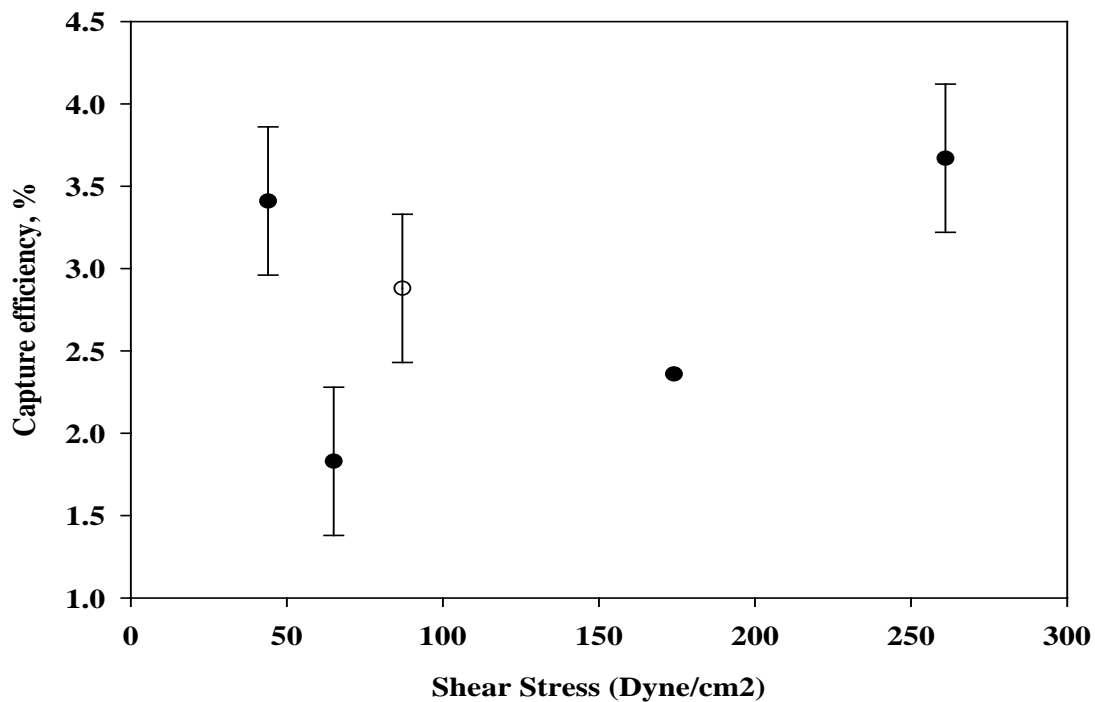


Figure 4.9: *Cryptosporidium* recovery with respect to the depth of flow cell (IgM-Fab')



**Figure 4.10: *Cryptosporidium* recovery with respect to the shear stress (IgM-Fab')**

#### 4.2.3 IgG-Fab

The capture tests using IgG-Fab activated slides were performed only at treatments 14 – 125 and 28 – 125. It is well established from the literature that random immobilization of antibody fragments was not as efficient as the site specific oriented immobilization. So, only the two best operating conditions from sections 4.2.1 and 4.2.2 were used to evaluate the effect of antibody orientation on capture efficiency. A range of 2.4 to 5.5% capture efficiency was obtained (detailed data are presented in Table B.4 in Appendix B). There was not a statistically significant difference between the two treatments ( $P = 0.374$ ).

#### 4.2.4 Effect of antibody type

The average capture efficiency of IgG-Fab' activated slides was higher than that of IgM-Fab'. Using the conditions 42 – 125 and 42 – 250, mean capture efficiencies of IgG-Fab' and IgM-Fab' were not significantly different ( $P = 0.127$  and  $P = 0.23$ , respectively). However, IgG-Fab' resulted in significantly higher capture efficiencies for the three other

different treatments (14 – 125, 28 – 125, and 28 – 250). A non-parametric Mann-Whitney Rank Sum test was performed to compare all the recovery efficiencies of IgG-Fab' and IgM-Fab' because the data are not normally distributed ( $P = 0.003$ ). The statistics implied that the difference in the median values between the two groups was greater than would be expected by chance ( $P = 0.004$ ). A linear best subsets regression analysis was performed to predict the trends in the capture efficiency. There was no significant correlation between the capture efficiencies and flow rate and depth of cell for the slides activated with IgG-Fab' and IgM-Fab'. The R squared value for the best combination was 0.432 and 0.053, respectively.

#### 4.2.5 Effect of antibody fragments

The average capture efficiency for IgG-Fab' at 14 – 125 was about twice that of IgG-Fab, and for 28 – 125, it was about four times as large as IgG-Fab. For both treatments, the difference in the mean capture efficiencies of IgG-Fab' and IgG-Fab is statistically significant ( $P = 0.021$  and  $P = 0.012$ , respectively).

#### 4.2.6 Effect of antibody loading

The initial capture tests were performed using capture surfaces activated with Fab' fragments prepared from 500  $\mu\text{g}$  of IgG<sub>1</sub> and the efficiencies were low because of the small reactive area ( $4 \times 4 \text{ mm}^2$ ). From the results of IgG-Fab', a 125  $\mu\text{m}$  cell depth and 28 mL/min flow rate resulted in the maximum capture efficiency (section 4.2.1), therefore, this particular treatment was selected as the operating condition in full scale capture test experiments to optimize the antibody concentration to be used. Four different dilutions of the original IgG-Fab' concentration were used to evaluate the effect of antibody concentration on capture efficiency. Sample raw data of microscopic counts of full scale test at 1:8 dilutions are presented in Table B.5 in Appendix B. The capture was influenced by the vacuum applied to create the seal for the flow cell. The results of the antibody

optimization test for different dilutions are summarized in Table 4.2. Figure 4.11 presents the effect of antibody concentration on the capture efficiency. There was no significant difference in the capture efficiencies within this dilution range ( $P = 0.073$ ). The maximum capture efficiency was obtained at 1:4 of the original dilution, though the variability (RSD = 48%) was also the highest at this concentration.

**Table 4.2: Capture test results with different antibody concentration**

Flow rate (mL/min)	Depth of cell ( $\mu\text{m}$ )	Dilution	% Captured	Average (%)	RSD (%)
28	125	1:8	16.0	15.17	32
			19.5		
			10.0		
		1:4 (without BSA)	57.5	37.50	48
			32.0		
			23.0		
		1:4 (with BSA)	12.5	11.5	9
			10.5		
			11.5		
		1:2	25.0	24.17	26
			30.0		
			17.5		
		1:1.5	14.0	14.83	26
			19.0		
			11.5		

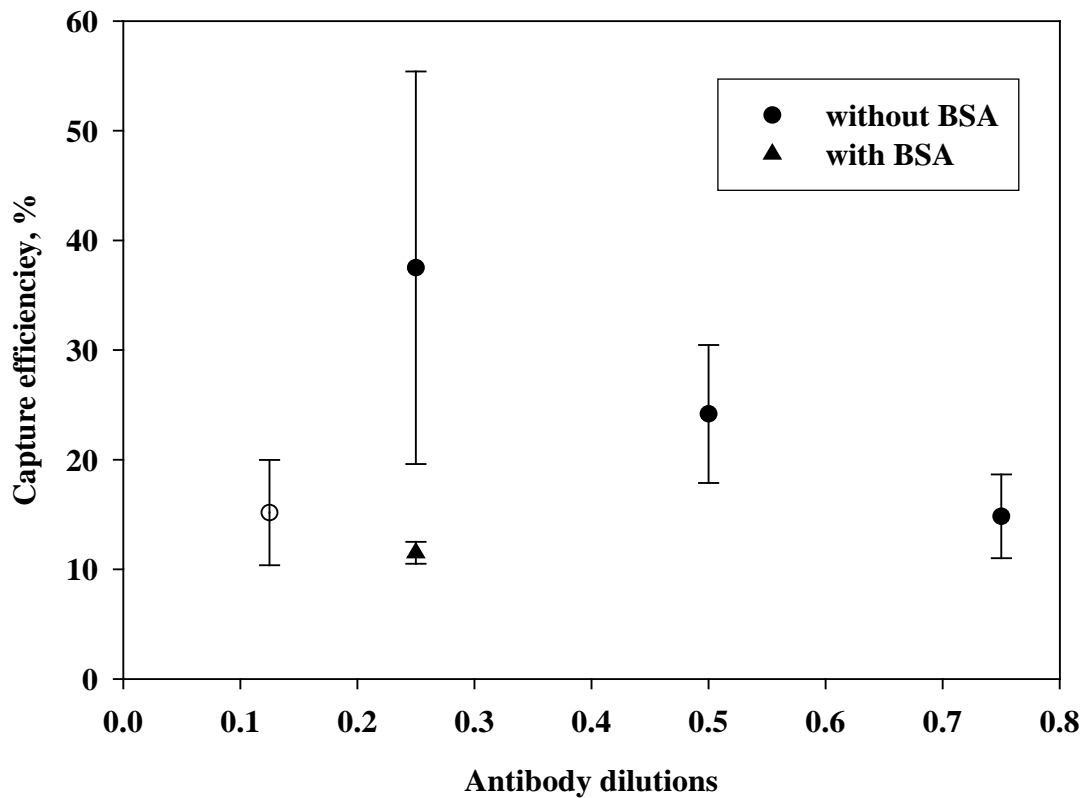


**Figure 4.11: Optimization of antibody concentration**

### 4.3 Blocking using BSA

There was an increase in the capture efficiency using full slides activated with different antibody dilutions, but precision of the results was not achieved. This variability may be attributed to the variability in preparing spike suspension and also the conformational change of immobilized antibody fragments under high wall shear stress. The relative standard deviation (RSD) of the spike solution in 0.01% Tween 20® varied from 20 to 46 %. Tween 20® was used to prepare the spike suspension because it is recommended for the use in the USEPA method 1622/1623 for *Cryptosporidium* detection. This variation in number of *Cryptosporidium* spiked was due to an inadequate mixing of suspension. The mixing of the spike suspension (with 0.01% Tween20®) at a rate more than 500 rpm produced foam. To reduce the variability in spike enumeration and reduce foam production, sodium pyrophosphate ( $\text{Na}_4\text{P}_2\text{O}_7$ ) was used instead of Tween 20®. The use of

0.1%  $\text{Na}_4\text{P}_2\text{O}_7$  consistently resulted in lower RSD [8 to 24%] than that of Tween 20®. There was no change in shape while mixing a higher rate [1200 rpm] and no foam development.

An attempt was made to cover the empty spaces in the slides after the antibody fragment immobilization with a blocking agent and to reduce the conformational change under the action of wall shear stress. A capture test was performed with Bovine serum albumin (BSA: 1 mg/mL) as blocking agent and 1:4 dilutions of the original concentration (Table 4.2 and Figure 4.11). The average capture efficiency ( $11.5 \pm 1\%$ ) was highly reproducible, but not significantly different than that of 1:4 dilutions obtained previously ( $P = 0.066$ ).

#### **4.4 Implementation of retroreflectors**

Corner cube micro-retroreflectors were successfully released by placing the wafer, supplied by University of Houston (Figure 4.12), into a 2.3% solution of TMAH in an ultrasonic bath for about 30 minutes. To obtain maximum recovery, an additional 30 minutes sonication was performed. The released cubes were collected on the bottom of a beaker by allowing them to settle in a beaker placed on a rare earth magnet for 1 hour, and the released retroreflectors were then re-suspended into EDTA buffer. Figure 4.13 shows the wafer after retroreflectors were released.

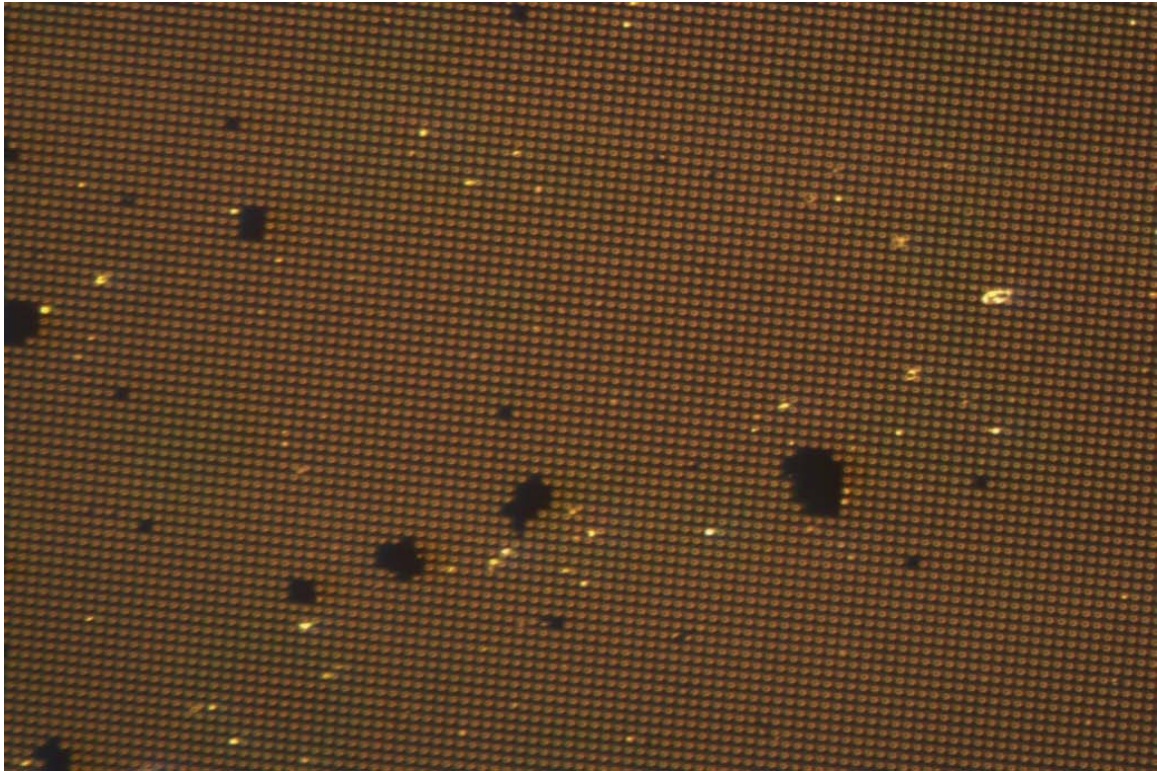


**Figure 4.12: Unreleased retroreflector on wafer (8X magnification)**

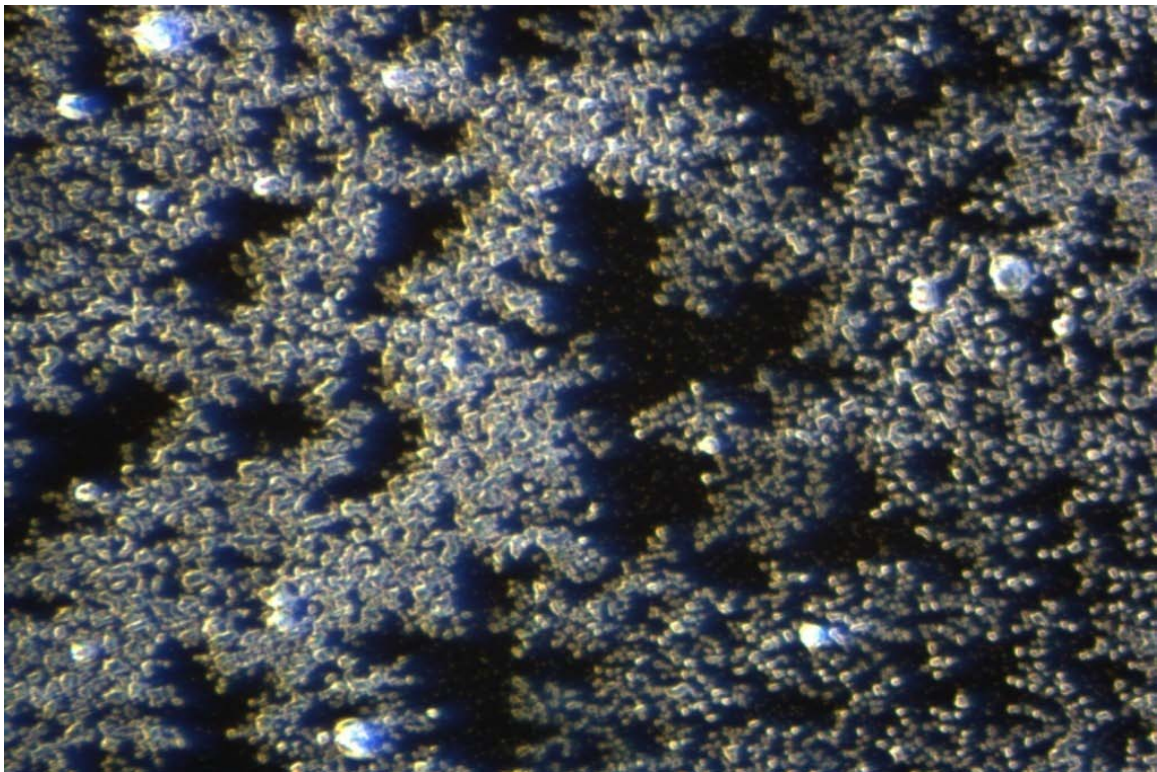


**Figure 4.13: Wafer after retroreflector was released (8X magnification)**

Suspended ccμRR were conjugated with Fab' fragments as described in the methods section. Attempts to visualize the success of antibody immobilization on the gold surface of the ccμRR involved the use of FITC conjugated IgG goat anti-mouse IgG-F(ab')<sub>2</sub> fragment specific. Excitation using DAPI, FITC, and Texas Red of the activated ccμRR conjugated with the FITC conjugated F(ab')<sub>2</sub> showed that ccμRR were autofluorescent with DAPI and FITC excitation but not with Texas Red. Therefore, Texas Red<sup>®</sup> conjugated F(ab')<sub>2</sub> goat anti-mouse IgG-F(ab')<sub>2</sub> fragment specific was used in the conformation experiments. Again, ccμRR were autofluorescent with the Texas Red excitation. Thus anti-F(ab')<sub>2</sub> could not distinguish conjugation of Fab' to retroreflector.

#### 4.5 Detection system

The detection system should be able to detect every single *Cryptosporidium* that is captured in the sampling device. In our lab, a detection system was developed that is very simple to use and inexpensive compared to the conventional detection systems that utilize fluorochromes and a microscope. The retroreflectors have a property such that they redirect the incident light to its source (Figure 4.14).

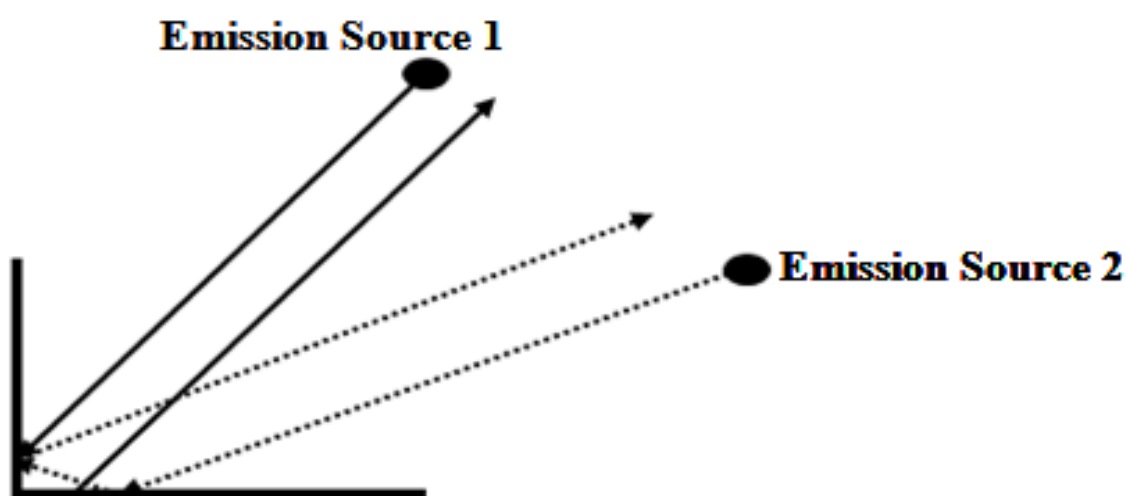
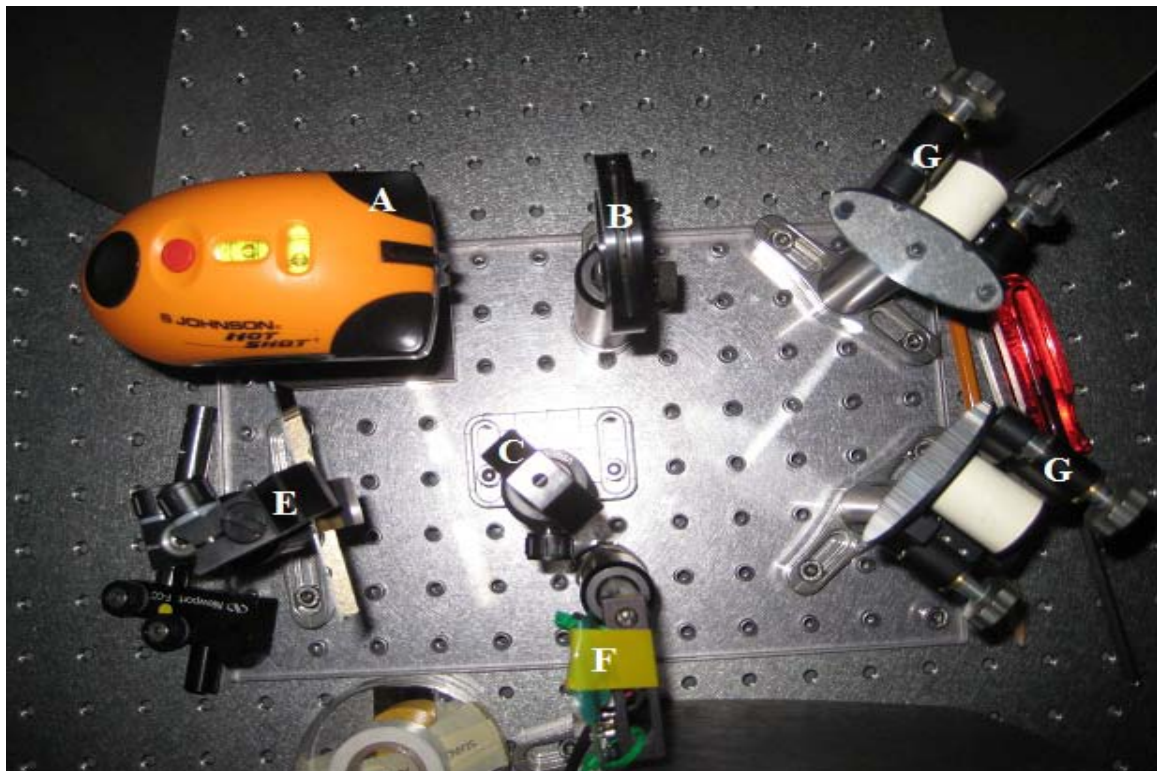


Figure 4.14: Property of retroreflector

A detector system was built by trial and errors eliminating different challenges that were encountered throughout the process. The preliminary design of the optical setup to detect cc $\mu$ RR consisted of a laser beam as light source (A), two mirrors (G), an iris diaphragm (B) and a beamsplitter [C] (Figure 4.15). The camera used was a CCD array from a 1.3 MP digital webcam. The light source was a laser beam without any polarizing lens. The laser beam passed through the iris diaphragm to the mirrors. The use of an iris diaphragm provided control over any minor adjustments of illumination by controlling the size of the laser beam. A 50R/50T beamsplitter split the light beam into transmitted and reflected fragments and thus, redirected the light from the light source to the retro-reflectors (E) and then to the CCD camera (F).



**Figure 4.15: Preliminary Signal detection configuration**

There were some difficulties with the system described above due to the quality of mirrors. The mirrors created a duplicate beam after each reflection; therefore a total of three light beams were reaching the beamsplitter and the gold slide with cc $\mu$ RR. These replicate beams were reflected onto the camera from the cc $\mu$ RR and duplicated the results

of the retro reflectors' presence on the gold slide. In addition, it was difficult to position the gold slide exactly where it was needed and to quickly compare two different areas of a gold slide at the same angle.

In the second iteration, a modified set up was created to identify and overcome the limitations of the first system. A digital camera (7.1 MP Canon Camera with 4x Zoom) was used instead of the CCD array to aid in determining light sources that were being redirected towards the camera. A lot of noise from the different light sources was hitting the beamsplitter and the redirected light from the initial beam to the background were noticed. This created too much light sensed by the CCD camera causing too much signal. Therefore, the determination of the difference between the light from the retro reflectors and the background noise was difficult. Another concern was the zoom and focusing of the camera lens. The camera would focus on a distance past the beam splitter. Also the zoom of the camera was not good enough to zoom into a small enough area of the beam splitter (4x).

Third system (Figure 4.16) developed overcame the drawbacks that were found from the first two systems. Changes made include the removal of mirrors, i.e. the laser beam from the iris diaphragm directly hit the beamsplitter. Secondly, a Y-Z axis stage was added to the system to allow more control over the movement of the gold slide. This also allowed the gold slide to be positioned at 90° from the horizontal. Thirdly, a beam dump (D) was made with corduroy material and a stand. The beam dump reduced the amount of light that appeared in the background behind the beamsplitter and helped to reduce the background noise. A stand was made to hold the gold slide closer to the beamsplitter while still allowing room for access to the Y-Z stage turning pins. By positioning the slide closer to the beamsplitter, there was less room for the slide reflection to escape. The images produced from this setup with the slide closer to the beamsplitter were clearer

than when it was farther away. With the current setup, differentiation between the presence and absence of the retroreflector to the gold slide was possible (Figure 4.17 and Figure 4.18). The air-polyimide interface of cc $\mu$ RR might create an environment with a specific angle of incidence so that the light cannot escape the cube. This phenomenon is known as total internal reflection. This can be minimized by using a water (not air) ambient environment around the retroreflectors or by using spherical  $\mu$ RR. The measurement of retroreflection from rotated angle of incidence may improve the directionality of the current setup and also improve the resolution of the images of cc $\mu$ RR.

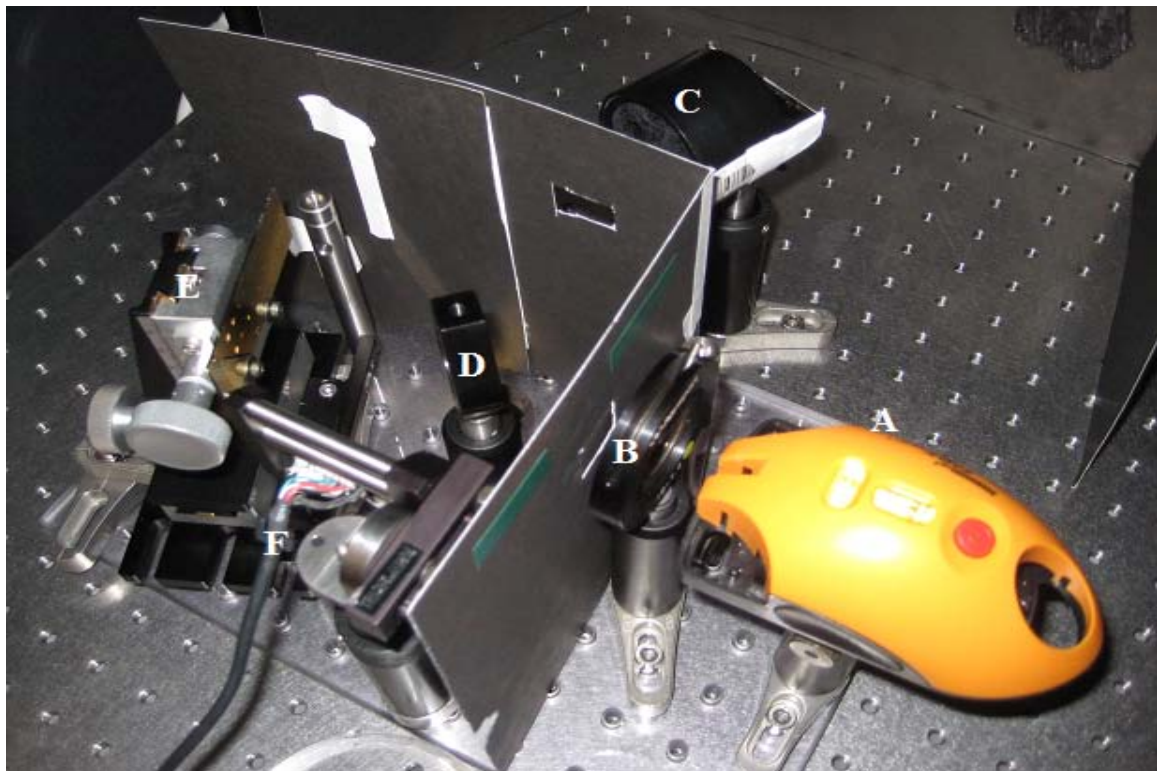


**Figure 4.16: Modified setup of the signal detector system**



**Figure 4.17: Image of slide with retroreflectors while laser was off**

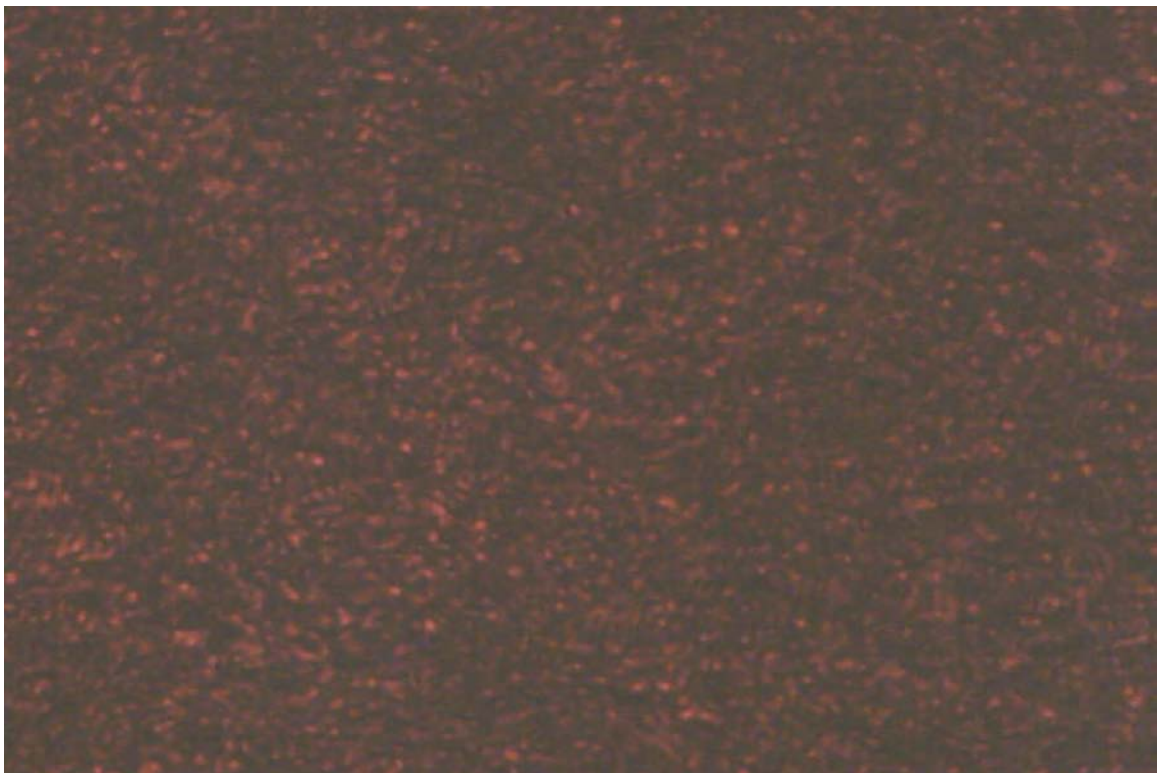


**Figure 4.18: Image of retroreflectors with clear edge**

#### 4.6 Discussion

The challenge that had to be addressed in the development of the sampling device is the low ratio of target cell to sample volume of various waterborne pathogens. The clinical application of cell affinity chromatography (CAC) for selective cell enrichment is quite common. CAC uses antibody activated solid surfaces to separate target cells from a high target to sample volume ratio in a microfluidic environment. In this research, efforts were made to concentrate the target cell from a low ratio of target cell to sample volume using the same principle as CAC i.e. an antibody activated solid surface. A rectangular parallel plate flow chamber was used to prove the concept that antibody modified solid surfaces can be effectively used to concentrate different water borne pathogens. *Cryptosporidium* was used as a model organism because it is well documented in the literature and the commercial availability of *Cryptosporidium* specific antibodies.

The total volumetric flow rate through the device varied from 14 to 42 mL/min and two flow chamber depths, 125 and 250  $\mu\text{m}$ , were used for the capture tests. The values of  $Re$  in the test chambers were always low (less than 90) in the chamber. This implies that the flow was always laminar and the velocity profile would be uniform throughout the channel cross section except a very small no-slip boundary near the channel wall. Shear stresses that prevailed in the flow chamber varied between 44 to 261  $\text{dyne/cm}^2$  and for a specific flow condition the shear stress would also be uniform throughout the device.

Two *Cryptosporidium* specific antibodies, IgG<sub>1</sub> and IgM were used to prepare the capture surface. Antibody selection is important in terms of high specificity and avidity that affect capture efficiency. Anti *Cryptosporidium* IgM is used in the purification phase of USEPA method 1622. An IgG<sub>1</sub> type of antibody was proven to be more specific to *Cryptosporidium* and showed higher avidity than IgM type of antibody (Ferrari et al., 1999; Weir et al. 2000).

In addition to the antibody type, the antibody fragments that are used to prepare the capture surface are also important. Two different antibody fragments, Fab' and Fab, were used in the preparation of the active surfaces. Fab' was used to prepare surfaces with site specific oriented immobilization and Fab resulted in random immobilization. Thiol groups of Fab' develop a covalent bond with gold giving an immobilization that keeps antigen-antibody binding moiety free for binding. The reduction of full length IgG to Fab' resulted in a higher degree of immobilization of well oriented and active antibody per surface area (Brogan et al., 2003; O'Brien et al., 2000). Fab fragments do not have free thiol group and therefore absorb nonspecifically to the gold side.

The capture test results showed that capture efficiency of slides coated with Fab' were better than the capture efficiency slides coated with Fab. The capture efficiency of IgG-Fab' modified surfaces was better than that of IgM-Fab'. Fragmentation of whole IgM to IgM-Fab' is not well documented in the literature. Thus, the difference in the capture efficiencies between the two antibody types may be attributed to the difference in specificity, avidity, and uncertainty of the fragmentation procedure.

Another factor that affects the capture efficiency is the antibody surface density which is influenced by the antibody concentration. A greater number of active sites will increase the capture efficiency. But, after a certain surface mass density the capture efficiency does not increase significantly. A range of dilutions (1:8 to 1:1.5) of the original concentration was used to prepare the reactive surfaces. There was no significant difference within the range of dilutions tested.

If a 60% fragmentation efficiency of IgG<sub>1</sub> to Fab' (Mariani et al., 1991) was assumed, 1:8 and 1:4 dilutions of the original concentration, respectively, would result in a concentration of ~ 38 and ~77 µg/mL, which brackets commonly used concentration (~ 50 µg/mL reported in literature) range for the preparation of self assembled monolayers.

Based on 7 nm x 5 nm x 4 nm dimension and 46 KDa weight of F(ab'), a closely packed surface of Fab' has a mass density of 220 ~ 440 ng/cm<sup>2</sup> (Buijs et al., 1995). Brogan et al. (2003) applied 50 µg/mL of F(ab') and obtained a surface density of 134 ± 75 ng/cm<sup>2</sup>. This implies that the initial two dilutions would develop near closely packed self assembled monolayer providing approximately 10<sup>12</sup>/cm<sup>2</sup> epitopes available for antigen interaction. Considering that the average diameter of oocysts is 4 µm, ~ 65 active epitopes would be available for interaction to a single oocyst.

BSA is commonly used as a blocking agent to suppress the nonspecific binding and also to limit the conformational change of the immobilized antibody. The use of BSA reduced the variability (increased the reproducibility) but also decreased the capture efficiency. Murthy et al. (2004) also reported the improvement in the reproducibility in cell adhesion using poly(ethylene glycol) chains as blocking agent along with the antibodies. Therefore, more diluted antibody fragments than current range with different blocking agents could be investigated to prepare the capture surface for the improvement in the capture efficiency accuracy and precision.

The antibody fragments that are site specifically attached to the flow cell are expected to be able to capture some oocysts directly from suspension. After initial capture three phenomena take place: cell rolling, cell tethering, and transient re-suspension before re-capture. These three phases will continue to occur before final entrapment. The cell capture and re-suspension happen because of transient adhesion between the antibody-antigen that dissociate readily under mechanical loading exerted by the fluid flow system (Chang et al., 2005; Radisic et al., 2006; Lyczkowski et al., 2009). This dissociation rate controls the optimum operating condition (shear stress) for each antibody-antigen pair because of the difference in avidity in antibody-antigen pairs (Du et al., 2007; Murthy et al., 2004; Plouffe et al., 2007; Plouffe et al., 2008).

An increase in shear stress increases the dissociation of the once captured antigen and decreases the antigen-antibody interaction time. At high shear stress cell deformation happens which will increase the probability of adhesion by increasing the available area for antibody-antigen interaction (Zhang et al., 2008). For the Fab' reactive surface, the optimization window was 150 – 200 dyne/cm<sup>2</sup> provided that excess antigen binding sites were present. This range of shear stress or flow rate might provide the allowable kinetic energy for cell activation; therefore it offers the favorable condition for optimum cell attachment. The tangential drag force acting on an oocyst is around 2350 pN for 200 dyne/cm<sup>2</sup> shear stress. The critical bond force for single antigen-antibody (IgG) interaction ranges from 40 to 260 pN (Dammer et al., 1996; Stuart and Hladly, 1995; Hinterdorfer et al., 1996). Assuming that the critical bond strength is around 200 pN, around 12 bonds are required at the interface to keep the cell attached on the surface. The presence of ~ 65 active sites for interaction (calculated previously) implies the possible stability of the captured oocyst in the optimum shear window.

An increase in the cell retention time in the flow cell increases the probability of antigen-antibody interaction. The capture efficiency also increases with the increase in antigen-antibody interaction under favorable operating conditions. Therefore, an increase in channel length, which also increases the cell retention time, will increase the capture efficiency in a straight channel device (Green et al., 2009). A decrease cell depth from 250 μm to 125 μm increased the capture efficiencies for IgG-Fab' activated surfaces. So, it can also be hypothesized that probability of antigen-antibody interaction is negatively correlated with the depth of cell.

## Chapter 5: Conclusions and Recommendations

### 5.1 General

The goal of the present research was to prove that antibody activated solid surfaces can successfully be utilized to concentrate different water borne pathogens from water. *Cryptosporidium* oocysts were used as the model organism. Antibodies specific to *Cryptosporidium* (IgG<sub>1</sub> and IgM) were used to prepare the reactive surfaces. Shear and capture tests were designed and performed to determine the best antibody fragments to be used for surface activation, to determine the optimum concentration of antibody, and the optimum operating conditions. Corner cube micro retroreflectors (ccμRR) were released and activated with antibody fragments to use as a signal molecule to detect the captured oocysts. A detection system was designed to detect the captured oocysts using the ccμRR.

The results of various experiments lead to the following conclusions:

- There was no significant dissociation of antibody-antigen bonds up to a shear stress of 126 dyne/cm<sup>2</sup>.
- Capture surfaces prepared with the IgG-Fab' fragments showed better capture efficiencies than that of IgM-Fab'. Surfaces activated with oriented IgG-Fab' were better in capturing the suspended oocysts than that of random immobilization using IgG-Fab.
- Capture efficiencies did not differ significantly with the experimental range of flow rate (14 to 42 mL/min) and shear stress.
- A decrease in cell depth from 250 μm to 125 μm improved the oocyst capture efficiency.
- There was no significant improvement in capture efficiencies in the dilution (1:8, 1:4, 1:2, and 1:1.5 of 500 μg IgG<sub>1</sub>) range used to prepare the capture surfaces.

- The precision of the capture test results showed improvement with the use of BSA as a blocking agent, but there was no significant improvement in the capture efficiencies.
- Cc $\mu$ RR were successfully released in solution, but activation using Fab' was not confirmed because of the autofluorescent properties under DAPI, FITC, and Texas Red excitation.
- A detection system was developed with the use of a laser beam, beamsplitter and a CCD array that can successfully detect presence and absence of large number of cc $\mu$ RR on a slide.

## **5.2 Limitations of the study**

The present study is limited by the following factors:

- The higher flow rates that can be used for shear test were limited by the capacity of the flow cell. Therefore, threshold values of the shear stress of the antibody-antigen interaction could not be determined.
- The image analysis program was not validated with the actual oocyst count.
- Initial capture test results should be interpreted carefully, because only a small area of the exposed surfaces was activated with antibody.
- The change in capture efficiencies with respect to cell depth was evaluated at a depth of 125  $\mu$ m and 250  $\mu$ m, because of the availability of the gaskets at these two depths.
- Full scale capture test results were limited by the influence of vacuum used to seal the flow cell.
- The final detection system was not fine tuned enough with respect to the directionality of cc $\mu$ RR detection.

### 5.3 Future recommendations

There is some future research that should be undertaken to improve the current assay. The following are the recommendations that could direct upcoming research:

- For commercialization, the fragmentation of IgG<sub>1</sub> to F(ab')<sub>2</sub> should be optimized with respect to time (24 – 30 hours) and temperature (37°C) of reaction and selective reduction of F(ab')<sub>2</sub> to F(ab') using 2 - MEA also needs to be optimized with respect to concentration of sample to be used for fragmentation, time (1.5 hours) and temperature (37°C) of incubation. To develop SAM, and to determine the number of thiol groups per mole titration should be done as a confirmatory test.
- The rinsing of gold coated surface to make the surface as hydrophilic as possible with some solution is necessary for gold-thiol chemistry. Piranha solution was used for this study to clean organic contaminant from the gold coated surfaces. Piranha solution is a very strong oxidant and extremely hazardous. Various other solutions, for example a boiling solution of hydrogen peroxide (4.3%) and ammonium hydroxide (4.3%), can also be used. A comparative study should be done to obtain an effective solution.
- To alleviate nonspecific interaction and improve the reproducibility a matrix of non-ionic hydrophilic polymers, pTHMAA should be used instead of BSA.
- The regeneration time (storage) and solution of regeneration of antibody activated surfaces need to be determined.
- A limitation of this current assay is the scarcity of highly selective and high-affinity antibodies or ligands for the different target cells. DNA-aptamers and phage peptide array can be examined to overcome this situation.

- To reduce reflection of the gold coating during detection, other oriented immobilization techniques on glass surfaces could be used.
- Effect of various disinfectants, such as chlorine on the capture efficiencies should be evaluated.
- The beamsplitter should be thick (more than 6 mm). The greater the thickness, the easier it will be to control the ghost images created. A thin beam splitter will cause an overlap of the image reflected by the retro reflectors. One of the possible ways to get rid of the ghost image is to use a thicker beamsplitter to separate the ghost image from the real image. The use of an anti-reflection coating on one side of the beamsplitter can also reduce the effect of ghost image.
- The directionality of ccμRR detection can be improved by measuring the retroreflection from rotated angles of incidence and/or using spherical retroreflector.

## References

- Albers, W.M., Auer, S., Helle, H., Munter, T. & Vikholm-Lundin, I. 2009, "Functional characterisation of Fab -fragments self-assembled onto hydrophilic gold surfaces", *Colloids and Surfaces B: Biointerfaces*, vol. 68, no. 2, pp. 193-199.
- Bacabac, R.G., Smit, T.H., Cowin, S.C., Van Loon, J.J.W.A., Nieuwstadt, F.T.M., Heethaar, R. & Klein-Nulend, J. 2005, "Dynamic shear stress in parallel-plate flow chambers", *Journal of Biomechanics*, vol. 38, no. 1, pp. 159-167.
- Barbosa, J.M.M., Costa-de-Oliveira, S., Rodrigues, A.G., Hanscheid, H., Shapiro, H. & Pina-Vaz, C. 2007, "A flow cytometric protocol for detection of *Cryptosporidium* spp.", *Cytometry Part A*, vol. 73A, no. 1, pp. 44-47.
- Bernath, S. & Haberman, E. 1974, "Solid-Phase Radioimmunoassay in Antibody-Coated Tubes for Quantitative-Determination of Tetanus Antibodies", *Medical microbiology and immunology*, vol. 160, no. 1, pp. 47-51.
- Boozer, C., Ladd, J., Chen, S. & Jiang, S. 2006, "DNA-Directed Protein Immobilization for Simultaneous Detection of Multiple Analytes by Surface Plasmon Resonance Biosensor", *Analytical Chemistry*, vol. 78, no. 5, pp. 1515-1519.
- Boozer, C., Ladd, J., Chen, S., Yu, Q., Homola, J. & Jiang, S. 2004, "DNA Directed Protein Immobilization on Mixed ssDNA/Oligo(ethylene glycol) Self-Assembled Monolayers for Sensitive Biosensors", *Analytical Chemistry*, vol. 76, no. 23, pp. 6967-6972.
- Borchardt, M.A. & Spencer, S.K. 2002, "Concentration of *Cryptosporidium*, *microsporidia* and other water-borne pathogens by continuous separation channel centrifugation", *Journal of applied microbiology*, vol. 92, no. 4, pp. 649-656.
- Brogan, K.L., Shin, J.H. & Schoenfish, M.H. 2004, "Influence of Surfactants and Antibody Immobilization Strategy on Reducing Nonspecific Protein Interactions for Molecular Recognition Force Microscopy", *Langmuir*, vol. 20, no. 22, pp. 9729-9735.
- Brogan, K.L., Wolfe, K.N., Jones, P.A. & Schoenfish, M.H. 2003, "Direct oriented immobilization of F(ab') antibody fragments on gold", *Analytica Chimica Acta*, vol. 496, no. 1-2, pp. 73-80.
- Buijs, J., Lichtenbelt, J.W.T., Norde, W. & Lyklema, J. 1995, "Adsorption of monoclonal IgGs and their F(ab')<sub>2</sub> fragments onto polymeric surfaces", *Colloids and Surfaces B: Biointerfaces*, vol. 5, no. 1-2, pp. 11-23.
- Bukhari, Z., McCuin, R.M., Fricker, C.R. & Clancy, J.L. 1998, "Immunomagnetic Separation of *Cryptosporidium parvum* from Source Water Samples of Various

- Turbidities", *Applied and Environmental Microbiology*, vol. 64, no. 11, pp. 4495-4499.
- Bukhari, Z. & Smith, H. 1995, "Effect of three concentration techniques on viability of *Cryptosporidium parvum* oocysts recovered from bovine feces", *Journal of clinical microbiology*, vol. 33, no. 10, pp. 2592-2595.
- Burton, D.R. 1985, "Immunoglobulin G: Functional sites", *Molecular immunology*, vol. 22, no. 3, pp. 161-206.
- Campbell, A.T., Robertson, L.J. & Smith, J.J. and Girdwood, R.W.A. 1994, "Viability of *Cryptosporidium parvum* oocysts concentrated by calcium carbonate flocculation.", *The journal of applied bacteriology*, vol. 76, no. 6, pp. 638-639.
- Campbell, A. & Smith, H. 1997, "Immunomagnetic separation of *Cryptosporidium* oocysts from water samples: Round robin comparison of techniques", *Water Science and Technology*, vol. 35, no. 11-12, pp. 397-401.
- Catt, K., Tregear, G.W. & Burger, H.G. and Skermer, G. 1970, "Antibody-coated tube method for radioimmunoassay of human growth hormone", *Clinica Chimica Acta*, vol. 27, pp. 267-279.
- Catt, K. & Tregear, G.W. 1967, "Solid-Phase Radioimmunoassay in Antibody-Coated Tubes", *Science*, vol. 158, no. 3808, pp. 1570-&.
- Chang, W.C., Lee, L.P. & Liepmann, D. 2005, "Biomimetic technique for adhesion-based collection and separation of cells in a microfluidic channel", *Lab on a Chip*, vol. 5, no. 1, pp. 64-73.
- Chesnot, T. & Schwartzbrod, J. 2004, "Quantitative and qualitative comparison of density-based purification methods for detection of *Cryptosporidium* oocysts in turbid environmental matrices", *Journal of Microbiological Methods*, vol. 58, no. 3, pp. 375-386.
- Chung, B.J., Robertson, A.M. & Peters, D.G. 2003, "The numerical design of a parallel plate flow chamber for investigation of endothelial cell response to shear stress", *Computers & Structures*, vol. 81, no. 8-11, pp. 535-546.
- Corso, P.S., Kramer, M.H., Blair, K.A., Addiss, D.G., Davis, J.P. & Haddix, A.C. 2003, "Cost of illness in the 1993 waterborne *Cryptosporidium* outbreak, Milwaukee, Wisconsin", *Emerging Infectious Diseases*, vol. 9, no. 4, pp. 426-431.
- Cringoli, G., Rinaldi, L., Veneziano, V., Capelli, G. & Scala, A. 2004, "The influence of flotation solution, sample dilution and the choice of McMaster slide area (volume) on the reliability of the McMaster technique in estimating the faecal egg counts of gastrointestinal strongyles and *Dicrocoelium dendriticum* in sheep", *Veterinary parasitology*, vol. 123, no. 1-2, pp. 121-131.

- Dammer, U., Hegner, M., Anselmetti, D., Wagner, P., Dreier, M., Huber, W. & Güntherodt, H.J. 1996, "Specific antigen/antibody interactions measured by force microscopy", *Biophysical journal*, vol. 70, no. 5, pp. 2437-2441.
- Danczyk, R., Krieder, B., North, A., Webster, T., HogenEsch, H. & Rundell, A. 2003, "Comparison of antibody functionality using different immobilization methods", *Biotechnology and bioengineering*, vol. 84, no. 2, pp. 215-223.
- Dawson, D.J., Maddocks, M., Roberts, J. & Vidler, J.S. 1993, "Evaluation of Recovery of *Cryptosporidium-Parvum* Oocysts using Membrane Filtration", *Letters in applied microbiology*, vol. 17, no. 6, pp. 276-279.
- Deng, M.Q., Lam, K.M. & Cliver, D.O. 2000, "Immunomagnetic separation of *Cryptosporidium parvum* oocysts using MACS MicroBeads and high gradient separation columns", *Journal of microbiological methods*, vol. 40, no. 1, pp. 11-17.
- DeSilva, B.S. & Wilson, G.S. 1995, "Solid phase synthesis of bifunctional antibodies", *Journal of immunological methods*, vol. 188, no. 1, pp. 9-19.
- Di Giovanni, G.D., Hashemi, F.H., Shaw, N.J., Abrams, F.A., LeChevallier, M.W. & Abbaszadegan, M. 1999, "Detection of Infectious *Cryptosporidium parvum* Oocysts in Surface and Filter Backwash Water Samples by Immunomagnetic Separation and Integrated Cell Culture-PCR", *Applied and Environmental Microbiology*, vol. 65, no. 8, pp. 3427-3432.
- DiGiorgio, C.L., Gonzalez, D.A. & Huitt, C.C. 2002, "*Cryptosporidium* and *Giardia* Recoveries in Natural Waters by Using Environmental Protection Agency Method 1623", *Applied and Environmental Microbiology*, vol. 68, no. 12, pp. 5952-5955.
- Domen, P.L., Nevens, J.R., Mallia, A.K., Hermanson, G.T. & Klenk, D.C. 1990, "Site-directed immobilization of proteins", *Journal of Chromatography A*, vol. 510, pp. 293-302.
- Du, Z., Cheng, K.H., Vaughn, M.W., Collie, N.L. & Gollahon, L.S. 2007, "Recognition and capture of breast cancer cells using an antibody-based platform in a microelectromechanical systems device", *Biomedical Microdevices*, vol. 9, no. 1, pp. 35-42.
- Dupont, H.L., Chappell, C.L., Sterling, C.R., Okhuysen, P.C., Rose, J.B. & Jakubowski, W. 1995, "The Infectivity of *Cryptosporidium-Parvum* in Healthy-Volunteers", *New England Journal of Medicine*, vol. 332, no. 13, pp. 855-859.
- Falk, C.C., Karanis, P., Schoenen, D. & Seitz, H.M. 1998, "Bench scale experiments for the evaluation of a membrane filtration method for the recovery efficiency of giardia and *Cryptosporidium* from water", *Water Research*, vol. 32, no. 3, pp. 565-568.
- Fell, L.R., Brown, J.M., Catt, K.J., Beck, C., Cumming, I.A. & Goding, J.R. 1972, "Solid-Phase Radioimmunoassay of Ovine Prolactin in Antibody-Coated Tubes - Prolactin Secretion during Estradiol Treatment, at Parturition, and during Milking", *Endocrinology*, vol. 91, no. 5, pp. 1329-&.

- Feng, Y.Y., Ong, S.L., Hu, J.Y., Song, L.F., Tan, X.L. & Ng, W.J. 2003, "Effect of Particles on the Recovery of *Cryptosporidium* Oocysts from Source Water Samples of Various Turbidities", *Applied and Environmental Microbiology*, vol. 69, no. 4, pp. 1898-1903.
- Ferguson, C., Kaucner, C., Krogh, M. & Deere, D. and Warnecke, M. 2004, "Comparison of methods for the concentration of *Cryptosporidium* oocysts and *Giardia* cysts from raw waters", *Canadian journal of microbiology*, vol. 50, no. 9, pp. 675-682.
- Ferrari, B.C., Vesey, G., Weir, C., Williams, K.L. & Veal, D.A. 1999, "Comparison of *Cryptosporidium*-specific and *Giardia*-specific monoclonal antibodies for monitoring water samples", *Water Research*, vol. 33, no. 7, pp. 1611-1617.
- Fowler, J.M., Stuart, M.C. & Wong, D.K.Y. 2007, "Self-assembled layer of thiolated protein G as an immunosensor scaffold", *Analytical Chemistry*, vol. 79, no. 1, pp. 350-354.
- Franco, E.J., Hofstetter, H. & Hofstetter, O. 2006, "A comparative evaluation of random and site-specific immobilization techniques for the preparation of antibody-based chiral stationary phases", *Journal of Separation Science*, vol. 29, no. 10, pp. 1458-1469.
- Goldstein, S.T., Juranek, D.D., Ravenholt, O., Hightower, A.W., Martin, D.G., Mesnik, J.L., Griffiths, S.D., Bryant, A.J., Reich, R.R. & Herwaldt, B.L. 1996, "Cryptosporidiosis: An outbreak associated with drinking water despite state-of-the-art water treatment", *Annals of Internal Medicine*, vol. 124, no. 5, pp. 459-&.
- Graczyk, T.K., Cranfield, M.R. & Fayer, R. 1996, "Evaluation of commercial enzyme immunoassay (EIA) and immunofluorescent antibody (IFA) test kits for detection of *Cryptosporidium* oocysts of species other than *Cryptosporidium parvum*", *American Journal of Tropical Medicine and Hygiene*, vol. 54, no. 3, pp. 274-279.
- Green, J.V., Kniazeva, T., Abedi, M., Sokhey, D.S., Taslim, M.E. & Murthy, S.K. 2009, "Effect of channel geometry on cell adhesion in microfluidic devices", *Lab on a Chip*, vol. 9, no. 5, pp. 677-685.
- Greinert, J.A., Furtado, D.N., Smith, J.J., Monte Barardi, C. R. & Simões, C.M.O. 2004, "Detection of *Cryptosporidium* oocysts and *Giardia* cysts in swimming pool filter backwash water concentrates by flocculation and immunomagnetic separation.", *International Journal of Environmental Health Research*, vol. 14, no. 6, pp. 395-404.
- Grimason, A.M., Smith, H.V., Parker, J.F.W., Bukhari, Z., Campbell, A.T. & Robertson, L.J. 1994, "Application of DAPI and immunofluorescence for enhanced identification of *Cryptosporidium* spp oocysts in water samples", *Water research*, vol. 28, no. 3, pp. 733-736.
- Hallier-Soulier, S. & Guillot, E. 2000, "Detection of cryptosporidia and *Cryptosporidium parvum* oocysts in environmental water samples by immunomagnetic separation-polymerase chain reaction.", *Journal Of Applied Microbiology*, vol. 89, no. 1, pp. 5-10.

- Hansen, J.S. & Ongerth, J.E. 1991, "Effects of time and watershed characteristics on the concentration of *Cryptosporidium* oocysts in river water.", *Applied and Environmental Microbiology*, vol. 57, no. 10, pp. 2790-2795.
- Higgins, J.A., Trout, J.M., Fayer, R., Shelton, D. & Jenkins, M.C. 2003, "Recovery and detection of *Cryptosporidium parvum* oocysts from water samples using continuous flow centrifugation", *Water Research*, vol. 37, no. 15, pp. 3551-3560.
- Hill, V.R., Kahler, A.M., Jothikumar, N., Johnson, T.B., Hahn, D. & Cromeans, T.L. 2007, "Multistate Evaluation of an Ultrafiltration-Based Procedure for Simultaneous Recovery of Enteric Microbes in 100-Liter Tap Water Samples", *Applied and Environmental Microbiology*, vol. 73, no. 13, pp. 4218-4225.
- Hill, V.R., Polaczyk, A.L., Hahn, D., Narayanan, J., Cromeans, T.L., Roberts, J.M. & Amburgey, J.E. 2005, "Development of a Rapid Method for Simultaneous Recovery of Diverse Microbes in Drinking Water by Ultrafiltration with Sodium Polyphosphate and Surfactants", *Applied and Environmental Microbiology*, vol. 71, no. 11, pp. 6878-6884.
- Hill, V.R., Polaczyk, A.L., Kahler, A.M., Cromeans, T.L., Hahn, D. & Amburgey, J.E. 2009, "Comparison of Hollow-Fiber Ultrafiltration to the USEPA VIRADEL Technique and USEPA Method 1623", *Journal of environmental quality*, vol. 38, no. 2, pp. 822-825.
- Hinterdorfer, P., Baumgartner, W., Gruber, H.J., Schilcher, K. & Schindler, H. "Detection and localization of individual antibody-antigen recognition events by atomic force microscopy", *Proceedings of the National Academy of Sciences of the United States of America*, vol. 93, no. 8, pp. 3477-3481.
- Hoffman, R., Chauret, C. & Standridge, J. and Peterson, L. 1999, "Evaluation of four commercial antibodies", *Journal American Water Works Association*, vol. 91, no. 9, pp. 69-78.
- Hsu, B.M., Huang, C.P. & Hsu, C.L.L. 2001a, "Analysis for Giardia cysts and *Cryptosporidium* oocysts in water samples from small water systems in Taiwan", *Parasitology research*, vol. 87, no. 2, pp. 163-168.
- Hsu, B. & Huang, C. 2001, "Performances of the Immunomagnetic Separation Method for *Cryptosporidium* in Water under Various Operation Conditions", *Biotechnology progress*, vol. 17, no. 6, pp. 1114-1118.
- Hsu, B., Huang, C., Hsu, Y., Jiang, G. & Hsu, C.L.L. 2001b, "Evaluation of two concentration methods for detecting Giardia and *Cryptosporidium* in water", *Water Research*, vol. 35, no. 2, pp. 419-424.
- Hsu, B., Huang, C. & Pan, J.R. 2001c, "Filtration behaviors of giardia and *Cryptosporidium*—ionic strength and pH effects", *Water Research*, vol. 35, no. 16, pp. 3777-3782.

- Hsu, B., Wu, N., Jang, H., Shih, F. & Wan, M.a.K.,Chien-Min 2005, "Using the flowcytometry to quantify *Giardia* cysts and *Cryptosporidium* oocysts in water sample", *Environmental Monitoring and Assessment*, vol. 104, no. 1-3, pp. 155-162.
- Kang, J.H., Choi, H.J., Hwang, S.Y., Han, S.H., Jeon, J.Y. & Lee, E.K. 2007, "Improving immunobinding using oriented immobilization of an oxidized antibody", *Journal of Chromatography A*, vol. 1161, no. 1-2, pp. 9-14.
- Karanis, P. & Kimura, A. 2002, "Evaluation of three flocculation methods for the purification of *Cryptosporidium parvum* oocysts from water samples", *Letters in applied microbiology*, vol. 34, no. 6, pp. 444-449.
- Karanis, P., Kourenti, C. & Smith, H. 2007, "Waterborne transmission of protozoan parasites: A worldwide review of outbreaks and lessons learnt.", *Journal of Water & Health*, vol. 5, no. 1, pp. 1-38.
- Karyakin, A.A., Presnova, G.V., Rubtsova, M.Y. & Egorov, A.M. 2000, "Oriented immobilization of antibodies onto the gold surfaces via their native thiol groups", *Analytical Chemistry*, vol. 72, no. 16, pp. 3805-3811.
- Kemper, S.M. 2008, *Immunoassays Based Upon Micro-Fabricated Retroreflectors*, University of Houston.
- Kim, B.Y., Swearingen, C.B., Ho, J.A., Romanova, E.V., Bohn, P.W. & Sweedler, J.V. 2007, "Direct Immobilization of Fab' in Nanocapillaries for Manipulating Mass-Limited Samples", *Journal of the American Chemical Society*, vol. 129, no. 24, pp. 7620-7626.
- Korich, D.G., Mead, J.R., Madore, M.S., Sinclair, N.A. & Sterling, C.R. 1990, "Effects of ozone, chlorine dioxide, chlorine, and monochloramine on *Cryptosporidium parvum* oocyst viability.", *Applied and Environmental Microbiology*, vol. 56, no. 5, pp. 1423-1428.
- Kuhn, R.C. & Oshima, K.H. 2002, "Hollow-fiber ultrafiltration of *Cryptosporidium parvum* oocysts from a wide variety of 10-L surface water samples.", *Canadian Journal Of Microbiology*, vol. 48, no. 6, pp. 542-549.
- Kuhn, R.C. & Oshima, K.H. 2001, "Evaluation and optimization of a reusable hollow fiber ultrafilter as a first step in concentrating *Cryptosporidium parvum* oocysts from water", *Water research*, vol. 35, no. 11, pp. 2779-2783.
- LeChevallier, M., Norton, W., Siegel, J. & Abbaszadegan, M. 1995, "Evaluation of the immunofluorescence procedure for detection of *Giardia* cysts and *Cryptosporidium* oocysts in water", *Applied and Environmental Microbiology*, vol. 61, no. 2, pp. 690-697.
- Lee, J.M., Park, H.K., Jung, Y., Kim, J.K. & Jung, S. O. and Chung, B.H. 2007, "Direct Immobilization of Protein G Variants with Various Numbers of Cysteine Residues on a Gold Surface", *Analytical Chemistry*, vol. 79, no. 7, pp. 2680-2687.

- Lee, N.Y., Yang, Y., Kim, Y.S. & Park, S. 2006, "Microfluidic immunoassay platform using antibody-immobilized glass beads and its application for detection of *Escherichia coli* O157 : H7", *Bulletin of the Korean Chemical Society*, vol. 27, no. 4, pp. 479-483.
- Lindquist, H.D.A., Harris, S., Lucas, S., Hartzel, M., Riner, D., Rochele, P. & DeLeon, R. 2007, "Using ultrafiltration to concentrate and detect *Bacillus anthracis*, *Bacillus atrophaeus* subspecies *globigii*, and *Cryptosporidium parvum* in 100-liter water samples", *Journal of Microbiological Methods*, vol. 70, no. 3, pp. 484-492.
- Lowery, C.J., Moore, J.E., Millar, B.C., Burke, D.P., McCorry, K.A.J. & Crothers, E.a.D.,J.S. G. 2000, "Detection and speciation of *Cryptosporidium* spp. in environmental water samples by immunomagnetic separation, PCR and endonuclease restriction.", *Journal of medical microbiology*, vol. 49, no. 9, pp. 779-785.
- Lu, B., Xie, J., Lu, C., Wu, C., Xie, Y.W., Lu, C., Wu, C. & and Wei, Y. 1995, "Oriented Immobilization of Fab' Fragments on Silica Surfaces", *Analytical Chemistry*, vol. 67, no. 1, pp. 83-87.
- Lu, B., Smyth, M.R. & and O'Kennedy, R. 1996, "Tutorial review. Oriented immobilization of antibodies and its applications in immunoassays and immunosensors", *Analyst*, vol. 121, no. 3, pp. 29R-32R.
- Lyczkowski, R.W., Alevriadou, B.R., Horner, M., Panchal, C.B. & Shroff, S.G. 2009, "Application of Multiphase Computational Fluid Dynamics to Analyze Monocyte Adhesion", *Annals of Biomedical Engineering*, vol. 37, no. 8, pp. 1516-1533.
- Mackenzie, W.R., Hoxie, N.J., Proctor, M.E., Gradus, M.S., Blair, K.A., Peterson, D.E., Kazmierczak, J.J., Addiss, D.G., Fox, K.R., Rose, J.B. & Davis, J.P. 1994, "A Massive Outbreak in Milwaukee of *Cryptosporidium* Infection Transmitted through the Public Water-Supply", *New England Journal of Medicine*, vol. 331, no. 3, pp. 161-167.
- Mariani, M., Camagna, M., Tarditi, L. & Seccamani, E. 1991, "A new enzymatic method to obtain high-yield F(ab)<sub>2</sub> suitable for clinical use from mouse IgG1", *Molecular immunology*, vol. 28, no. 1-2, pp. 69-77.
- McCuin, R.M., Bukhari, Z., Sobrinho, J. & Clancy, J.L. 2001, "Recovery of *Cryptosporidium* oocysts and *Giardia* cysts from source water concentrates using immunomagnetic separation", *Journal of Microbiological Methods*, vol. 45, no. 2, pp. 69-76.
- Montemayor, M., Galofre, B. & Ribas, F. and Lucena, F. 2007, "Comparative study between two laser scanning cytometers and epifluorescence microscopy for the detection of *Cryptosporidium* oocysts in water", *Cytometry Part A*, vol. 71A, no. 3, pp. 163-169.
- Morales-Morales, H.A., Vidal, G., Olszewski, J., Rock, C.M., Dasgupta, D., Oshima, K.H. & Smith, G.B. 2003, "Optimization of a Reusable Hollow-Fiber Ultrafilter for

- Simultaneous Concentration of Enteric Bacteria, Protozoa, and Viruses from Water", *Applied and Environmental Microbiology*, vol. 69, no. 7, pp. 4098-4102.
- Murthy, S.K., Sin, A., Tompkins, R.G. & Toner, M. 2004, "Effect of Flow and Surface Conditions on Human Lymphocyte Isolation Using Microfluidic Chambers", *Langmuir*, vol. 20, no. 26, pp. 11649-11655.
- Nieminski, E. C., Bellamy, W.D., and Moss, L.R. 2000, "Using surrogates to improve the plant performance", *Journal American Water Works Association*, vol. 92, no. 3, pp. 67-78.
- Nieminski, E. C., Schaefer, F., 3rd & Ongerth, J. 1995, "Comparison of two methods for detection of *Giardia* cysts and *Cryptosporidium* oocysts in water", *Appl. Environ. Microbiol.*, vol. 61, no. 5, pp. 1714-1719.
- O'Brien, J.C., Jones, V.W., Mosher, M.D.P.L. & Henderson, E. 2000, "Immunosensing Platforms Using Spontaneously Adsorbed Antibody Fragments on Gold", *Analytical Chemistry*, vol. 72, no. 4, pp. 703-710.
- Ochiai, Y., Takada, C. & Hosaka, M. 2005, "Detection and Discrimination of *Cryptosporidium parvum* and *C. hominis* in Water Samples by Immunomagnetic Separation-PCR", *Applied and Environmental Microbiology*, vol. 71, no. 2, pp. 898-903.
- Olsvik, O., Popovic, T., Skjerve, E., Cudjoe, K.S., Hornes, E., Ugelstad, J. & Uhlen, M. 1994, "Magnetic separation techniques in diagnostic microbiology.", *Clinical microbiology reviews*, vol. 7, no. 1, pp. 43-54.
- Ongerth, J.E. & Stibbs, H.H. 1987, "Identification of *Cryptosporidium* oocysts in river water.", *Applied and Environmental Microbiology*, vol. 53, no. 4, pp. 672-676.
- O'Shannessy, D.J. & Hoffman, W.L. 1987, "Site-directed immobilization of glycoproteins on hydrazide-containing solid supports. ", *Biotechnology and applied Biochemistry*, vol. 9, no. 6, pp. 488-496.
- Patrie, S.M. & Mrksich, M. 2007, "Self-assembled monolayers for MALDI-TOF mass Spectrometry for Immunoassays of human protein antigens", *Analytical Chemistry*, vol. 79, no. 15, pp. 5878-5887.
- Peluso, P., Wilson, D.S., Do, D., Tran, H., Venkatasubbaiah, M., Quincy, D., Heidecker, B., Poindexter, K., Tolani, N., Phelan, M., Witte, K., Jung, L.S., Wagner, P. & Nock, S. 2003, "Optimizing antibody immobilization strategies for the construction of protein microarrays", *Analytical Biochemistry*, vol. 312, no. 2, pp. 113-124.
- Pezzana, A., Vilaginès, P., Bordet, F., Coquard, D. & Sarrette, B. and Vilaginès, R. 2000, "Optimization of the Envirochek capsule method and Immunomagnetic separation procedure for the detection of low levels of *Cryptosporidium* in large drinking water samples.", *Water science and technology*, vol. 41, no. 7, pp. 111-117.

- Plouffe, B.D., Njoka, D.N., Harris, J., Liao, J., Horick, N.K., Radisic, M. & Murthy, S.K. 2007, "Peptide-Mediated Selective Adhesion of Smooth Muscle and Endothelial Cells in Microfluidic Shear Flow", *Langmuir*, vol. 23, no. 9, pp. 5050-5055.
- Plouffe, B.D., Radisic, M. & Murthy, S.K. 2008, "Microfluidic depletion of endothelial cells, smooth muscle cells, and fibroblasts from heterogeneous suspensions", *Lab on a Chip*, vol. 8, no. 3, pp. 462-472.
- Polaczyk, A.L., Narayanan, J., Cromeans, T.L., Hahn, D., Roberts, J.M., Amburgey, J.E. & Hill, V.R. 2008, "Ultrafiltration-based techniques for rapid and simultaneous concentration of multiple microbe classes from 100-L tap water samples", *Journal of microbiological methods*, vol. 73, no. 2, pp. 92-99.
- Quintero-Betancourt, W., Peele, E.R. & Rose, J.B. 2002, "*Cryptosporidium parvum* and *Cyclospora cayetanensis*: a review of laboratory methods for detection of these waterborne parasites", *Journal of Microbiological Methods*, vol. 49, no. 3, pp. 209-224.
- Radisic, M., Iyer, R.K. & Murthy, S.K. 2006, "Micro- and nanotechnology in cell separation", *International Journal of Nanomedicine*, vol. 1, no. 1, pp. 3-14.
- Rao, S.V., Anderson, K.W. & Bachas, L.G. 1998, "Oriented immobilization of proteins", *Microchimica Acta*, vol. 128, no. 3-4, pp. 127-143.
- Robertson, L.J., Campbell, A.T. & Smith, H.V. 1992, "Survival of *Cryptosporidium-Parvum* Oocysts Under various Environmental Pressures", *Applied and Environmental Microbiology*, vol. 58, no. 11, pp. 3494-3500.
- Rochelle, P.A., De Leon, R., Johnson, A., Stewart, M.H. & Wolfe, R.L. 1999, "Evaluation of Immunomagnetic Separation for Recovery of Infectious *Cryptosporidium parvum* Oocysts from Environmental Samples", *Applied and Environmental Microbiology*, vol. 65, no. 2, pp. 841-845.
- Rodgers, M.R. & Flanigan, D.J.a.J.,W. 1995, "Identification of algae which interfere with the detection of *Giardia* cysts and *Cryptosporidium* oocysts and a method for alleviating this interference.", *Applied and Environmental Microbiology*, vol. 61, no. 10, pp. 3759-3763.
- Rose, J.B., Cifrino, A., Madore, M.S., Gerba, C.P. & Sterling, C.R. and Arrowood, M.J. 1986, "Detection of *Cryptosporidium* from wastewater and freshwater environments.", *Water science and technology*, vol. 18, no. 10, pp. 233-239.
- Rose, J.B., Landeen, L.K., Riley, K.R. & Gerba, C.P. 1989, "Evaluation of immunofluorescence techniques for detection of *Cryptosporidium* oocysts and *Giardia* cysts from environmental samples.", *Appl. Environ. Microbiol.*, vol. 55, no. 12, pp. 3189-3196.
- Sartory, D.P., Parton, A., Parton, A.C. & Roberts, J. and Bergmann, K. 1998, "Recovery of *Cryptosporidium* oocysts from small and large volume water samples using a

- compressed foam filter system", *Letters in applied microbiology*, vol. 27, no. 6, pp. 318-322.
- Shepherd, K.M. & Wyn-Jones, A.P. 1996, "An evaluation of methods for the simultaneous detection of *Cryptosporidium* oocysts and *Giardia* cysts from water.", *Applied and Environmental Microbiology*, vol. 62, no. 4, pp. 1317-1322.
- Shepherd, K.M. & Wyn-Jones, A.P. 1995, "Evaluation of Different Filtration Techniques for the Concentration of *Cryptosporidium* Oocysts from Water", *Water Science and Technology*, vol. 31, no. 5-6, pp. 425-429.
- Simmons, O.D., Sobsey, M.D., Heaney, C.D. & Schaefer, F.W. and Francy, D.S. 2001, "Concentration and detection of *Cryptosporidium* oocysts in surface water samples by method 1622 using ultrafiltration and capsule filtration", *Applied and Environmental Microbiology*, vol. 67, no. 3, pp. 1123-1127.
- Skerrett, H.E. & Holland, C.V. 2000, "The occurrence of *Cryptosporidium* in environmental waters in the greater Dublin area", *Water Research*, vol. 34, no. 15, pp. 3755-3760.
- Smith, H.V., Campbell, B.M., Paton, C.A. & Nichols, R.A.B. 2002, "Significance of Enhanced Morphological Detection of *Cryptosporidium* sp. Oocysts in Water Concentrates Determined by Using 4',6'-Diamidino-2-Phenylindole and Immunofluorescence Microscopy", *Applied and Environmental Microbiology*, vol. 68, no. 10, pp. 5198-5201.
- Spitznagel, T.M. & Clark, D.S. 1993, "Surface-Density and Orientation Effects on Immobilized Antibodies and Antibody Fragments", *Biotechnology*, vol. 11, pp. 825-829.
- Stanfield, G., Carrington, E., Albinet, F., Compagnon, B., Dumoutier, N., Hambsch, B., Lorthioy, A., Medema, G., Pezoldt, H., De Roubin, M.R., De Lohman, A. & Whitmore, T. 2000, "An optimization and standardised test to determine the presence of the protozoa *Cryptosporidium* and *Giardia* in water", *Water science and technology*, vol. 41, no. 7, pp. 103-110.
- Steiner, T.S., Thielman, N. M., and Guerrant, R. L. 1997, "PROTOZOAL AGENTS: What Are the Dangers for the Public Water Supply?", *Annual Review of Medicine*, vol. 48, pp. 329-340.
- Straub, T.M., Dockendorff, B.P., Quiñonez-Díaz, M.D., Valdez, C.O., Shutthanandan, J.I., Tarasevich, B.J., Grate, J.W. & Bruckner-Lea, C.J. 2005, "Automated methods for multiplexed pathogen detection", *Journal of Microbiological Methods*, vol. 62, no. 3, pp. 303-316.
- Stuart, J.K. & Hlady, V. 1995, "Effects of Discrete Protein-Surface Interactions in Scanning Force Microscopy Adhesion Force Measurements", *Langmuir*, vol. 11, no. 4, pp. 1368-1374.

- Sturbaum, G.D., Klonicki, P.T., Marshall, M.M., Jost, B.H., Clay, B.L. & Sterling, C.R. 2002, "Immunomagnetic Separation (IMS)-Fluorescent Antibody Detection and IMS-PCR Detection of Seeded *Cryptosporidium parvum* Oocysts in Natural Waters and Their Limitations", *Applied and Environmental Microbiology*, vol. 68, no. 6, pp. 2991-2996.
- Swales, C. & Wright, S. 2000, "Evaluation of a continuous flow centrifuge for recovery of *Cryptosporidium* oocysts from large volume water samples", *Water research*, vol. 34, no. 6, pp. 1962-1966.
- Thomas, R.J., Gardner, E.A., Barry, G.A., Chinivasagams, H.N., Green, P.E., Klieve, A.V., Blackall, P.J., Blight, G.W. & Blaney, B.J. 2000, "Indicator organism levels in effluent from Queensland coastal STP's.", *Water*, vol. 27, pp. 38-45.
- Tsushima, Y., Karanis, P., Kamada, T., Makala, L., Xuan, X.N., Tohya, Y. & Akashi, H. and Nagasawa, H. 2003, "Seasonal change in the number of *Cryptosporidium parvum* oocysts in water samples from the rivers in Hokkaido, Japan, detected by the ferric sulfate flocculation method", *The journal of veterinary medical science*, vol. 65, no. 1, pp. 121-123.
- Tsushima, Y., Karanis, P., Kamada, T., Nagasawa, H., Xuan, X., Igarashi, I., Fujisaki, K. & Takahashi, E. and Mikami, T. 2001, "Detection of *Cryptosporidium* Oocysts in Environmental Water in Hokkaido, Japan", *The journal of veterinary medical science*, vol. 63, no. 3, pp. 233-236.
- US Environmental Protection Agency (2005a). Method 1622: *Cryptosporidium* in water by filtration/IMS/FA. Publication EPA 815-R-05-001, Office of Water, Washington DC, USA.
- US Environmental Protection Agency (2005b). Method 1623: *Cryptosporidium* and *Giardia* in water by filtration/IMS/FA. Publication EPA 815-R-05-002, Office of Water, Washington DC, USA.
- Valdez, L., Dang, H., Okhuysen, P. & Chappell, C. 1997, "Flow cytometric detection of *Cryptosporidium* oocysts in human stool samples", *Journal of clinical microbiology*, vol. 35, no. 8, pp. 2013-2017.
- Vesey, G., Deere, D., Weir, C.J., Ashbolt, N. & Williams, K.L. and Veal, D.A. 1997b, "A simple method for evaluating *Cryptosporidium*-specific antibodies used in monitoring environmental water samples", *Letters in applied microbiology*, vol. 25, no. 5, pp. 316-320.
- Vesey, G., Hutton, P., Champion, A., Ashbolt, N., Williams, K.L., Warton, A. & Veal, D. 1994, "Application of flow cytometric methods for the routine detection of *Cryptosporidium* and *Giardia* in water.", *Cytometry*, vol. 16, no. 1, pp. 1-6.
- Vesey, G., Deere, D., Gauci, M.R., Griffiths, K.R., Williams, K.L. & Veal, D.A. 1997a, "Evaluation of fluorochromes and excitation sources for immunofluorescence in water samples", *Cytometry*, vol. 29, no. 2, pp. 147-154.

- Vesey, G., Slade, J.S., Byrne, M. & Shepherd, K. and Fricker, C.R. 1993a, "A new method for the concentration of *Cryptosporidium* oocysts from water", *Journal of applied microbiology*, vol. 75, no. 1, pp. 82-86.
- Vesey, G., Slade, J.S. & Fricker, C.R. 1991, "Taking the eye strain out of environmental *Cryptosporidium* analysis", *Letters in applied microbiology*, vol. 13, no. 2, pp. 62-65.
- Vesey, G., Slade, J.S., Byrne, M., Shepherd, K., Dennis, P.J. & Fricker, C.R. 1993b, "Routine Monitoring of *Cryptosporidium* Oocysts in Water using Flow-Cytometry", *Journal of Applied Bacteriology*, vol. 75, no. 1, pp. 87-90.
- Vikholm, I. 2005a, "Self-assembly of antibody fragments and polymers onto gold for immunosensing", *Sensors and Actuators B: Chemical*, vol. 106, no. 1, pp. 311-316.
- Vikholm-Lundin, I. 2005b, "Immunosensing Based on Site-Directed Immobilization of Antibody Fragments and Polymers that Reduce Nonspecific Binding", *Langmuir*, vol. 21, no. 14, pp. 6473-6477.
- Vikholm, I., Albers, W.M., Välimäki, H. & Helle, H. 1998, "In situ quartz crystal microbalance monitoring of Fab-fragment binding to linker lipids in a phosphatidylcholine monolayer matrix. Application to immunosensors", *Thin Solid Films*, vol. 327-329, pp. 643-646.
- Ware, M.W., Wymer, L., Lindquist, H.D.A. & Schaefer, F.W. 2003, "Evaluation of an alternative IMS dissociation procedure for use with Method 1622: detection of *Cryptosporidium* in water", *Journal of microbiological methods*, vol. 55, no. 3, pp. 575-583.
- Weir, C., Vesey, G., Slade, M., Ferrari, B., Veal, D.A. & Williams, K. 2000, "An Immunoglobulin G1 Monoclonal Antibody Highly Specific to the Wall of *Cryptosporidium* Oocysts", *Clinical and Diagnostic Laboratory Immunology*, vol. 7, no. 5, pp. 745-750.
- Wiseman, A. 1993, "Designer Enzyme and Cell Applications in Industry and in Environmental Monitoring", *Journal of Chemical Technology and Biotechnology*, vol. 56, no. 1, pp. 3-13.
- Wohlsen, T., Bates, J., Gray, B. & Katouli, M. 2004, "Evaluation of Five Membrane Filtration Methods for Recovery of *Cryptosporidium* and *Giardia* Isolates from Water Samples", *Applied and Environmental Microbiology*, vol. 70, no. 4, pp. 2318-2322.
- Wohlsen, T. & Katouli, M. 2008, "A review of the existing methods for detection, enumeration and inactivation of *Cryptosporidium* in surface waters", *Journal of Water Supply Research and Technology-Aqua*, vol. 57, no. 2, pp. 65-77.
- Yakub, G.P. & Stadterman-Knauer, K.L. 2000, "Evaluation of Immunomagnetic Separation for Recovery of *Cryptosporidium parvum* and *Giardia duodenalis* from High-Iron Matrices", *Applied and Environmental Microbiology*, vol. 66, no. 8, pp. 3628-3631.

- Zarlenga, D.S. & Trout, J.M. 2004, "Concentrating, purifying and detecting waterborne parasites", *Veterinary Parasitology*, vol. 126, no. 1-2, pp. 195-217.
- Zhang, L.T. 2008, "Shear stress and shear-induced particle residence in stenosed blood vessels", *International Journal for Multiscale Computational Engineering*, vol. 6, no. 2, pp. 141-152.
- Zuckerman, U., Armon, R., Tzipori, S. & Gold, D. 1999, "Evaluation of a portable differential continuous flow centrifuge for concentration of *Cryptosporidium* oocysts and *Giardia* cysts from water.", *Journal of Applied Microbiology*, vol. 86, no. 6, pp. 955-961.
- Zuckerman, U. & Tzipori, S. 2006, "Portable continuous flow centrifugation and method 1623 for monitoring of waterborne protozoa from large volumes of various water matrices.", *Journal of applied microbiology*, vol. 100, no. 6, pp. 1220-1227.

# Appendices

## Appendix A

### Matlab code for shear test:

```
clear
clc
%Input Image file to be analyzed
image=input('Image File Name: ','s');
%Read grayscale Image
I=imread(image);
%initialize z matrix
for j=1:size(I,1)
    for i=1:size(I,2)
        z(j,i)=0;
    end
end
%Read in z falues from I
dens_tot=0;
dens_white=0;
for j=1:size(I,1)
    for i=1:size(I,2)
        if(I(j,i)>0)
            z(size(I,1)-j+1,i)=I(j,i);
            dens_tot=dens_tot+1;
        end
        if I(j,i)==255
            dens_white=dens_white+1;
        end
    end
end
%Find density of white portions
total_size=size(I,1)*size(I,2);
Density_Total=dens_tot/total_size*100
Density_White=dens_white/total_size*100
i=1:1:size(I,2);
j=1:1:size(I,1);
dens_tot
dens_white
%plot 2d image and surace 3d plot
figure(1)
imshow(I);
figure(2)
mesh(i,j,z)
```

## Appendix B

**Table B.1: Shear test results**

Square #	Image #	X-coordinate	Y-coordinate	Before shear		After shear		Percent difference
				Total (Pixels)	Total (%)	Total (Pixels)	Total (%)	
1	1	101.0	9.9	1751	0.121	1853	0.128	0.007
	2	100.9	10.9	1471	0.102	1554	0.108	0.006
	3	102.1	7.7	12030	0.833	12314	0.853	0.020
	4	102.2	12.2	984	0.068	984	0.068	0.000
	5	102.2	5.5	2098	0.145	1998	0.138	-0.007
2	1	90.9	10.9	7325	0.507	7325	0.507	0.000
	2	91.0	8.8	1503	0.104	1587	0.110	0.006
	3	91.0	9.8	1246	0.086	1300	0.090	0.004
	4	91.0	8.7	1214	0.084	1294	0.090	0.006
	5	91.0	9.9	881	0.061	804	0.056	-0.005
							Average	0.004

**Table B.2: Capture test results for surface activation using IgG-Fab' fragments**

Depth ( $\mu\text{m}$ )	Flow rate (mL/min)	Shear Stress (Dyne/cm <sup>2</sup> )	<i>C.</i> <i>parvum</i> left	<i>C.</i> <i>parvum</i> retained	Blank (retained)	Captured	On filter			On slide		
							% captured	average	RSD (%)	% captured	average	RSD (%)
			100	100		33	16.5			10.23		
125	14	87	117	83	67	16	8	10.83	45	8.65	8.65	18
			117	83		16	8			7.08		
			117	83		83	42			7.87		
125	28	174	133	67	0	67	34	38.83	12	14.16	11.54	28
			117	83		83	42			12.59		
			83	117		50	25			4.72		
125	42	261	100	100	67	33	17	22.25	21	11.01	7.34	44
			83	117		50	25			6.29		
			67	133		66	33			9.44		
250	28	44	50	150	67	83	42	33.37	26	8.65	8.39	14
			83	117		50	25			7.08		
			117	83		0				1.57		
250	42	65	117	83	83	0	-	-	-	1.57	1.31	35
			167	33		-				0.79		

**Table B.3: Capture test results for surface activation using IgM-Fab' fragments**

Depth ( $\mu\text{m}$ )	Flow rate (mL/min)	Shear Stress (Dyne/cm <sup>2</sup> )	<i>C.</i> <i>parvum</i> left	<i>C.</i> <i>parvum</i> retained	Blank (retained)	Captured	On filter			On slide		
							% captured	average	RSD (%)	% captured	average	RSD (%)
			162	38		6	3			3.14		
125	14	87	150	50	32	18	9	12.01	90	3.14	2.88	16
			120	80		48	24			2.36		
			144	56		24	12			2.36		
125	28	174	102	98	32	66	33	25.03	45	2.36	2.36	0
			108	92		60	30			2.36		
			60	140		73	36			3.93		
125	42	261	66	134	ND	67	33	33.46	9	3.14	3.67	12
			72	128		61	30			3.93		
			114	86		19	9			3.14		
250	28	44	126	74	ND	7	3	15.44	103	3.14	3.41	13
			66	134		67	33			3.93		
			60	140		57	28			1.57		
250	42	65	114	86	ND	3	1	17.46	81	1.57	1.83	25
			72	128		45	22			2.36		

**Table B.4: Capture test results for surface activation using IgG -Fab fragments**

Depth ( $\mu\text{m}$ )	Flow rate (mL/min)	Shear Stress (Dyne/cm <sup>2</sup> )	C. <i>parvum</i> left	C. <i>parvum</i> retained	Blank (retained)	Captured	On filter			On slide		
							% captured	average	RSD (%)	% captured	average	RSD (%)
			174	26		26	13			5.50		
125	14	87	174	26	-	26	13	8.67	87	3.93	3.93	40
			210	-		0	0			2.36		
			186	14		14	7			2.36		
125	28	174	180	20	-	20	10	5.61	91	3.93	2.88	31
			210	-		0	0			2.36		

**Table B.5: Sample raw data of capture test at 1:8 dilution**

	Total	1	2	3	4	5	6	7	8	9	10	11	12	13	14	15	16	17	18	19	20	21	22	23	24	25	26	27	28	29	30
Row 1	13	0	0	1	0	0	0	1	0	1	0	1	2	0	1	0	0	1	0	0	0	0	0	0	0	0	0	0	0	0	2
Row 2	4	0	0	0	0	0	1	0	0	0	0	0	0	0	0	0	0	1	0	0	0	0	0	0	0	0	0	0	0	0	0
Row 3	2	0	0	0	0	0	0	0	0	0	1	0	0	0	0	0	0	0	0	0	0	1	0	0	0	0	0	0	0	0	0
Row 4	3	0	0	0	1	0	0	0	0	0	0	0	0	0	0	0	0	1	0	1	0	0	0	0	0	0	0	0	0	1	0
Row 5	2	0	0	0	0	0	0	0	0	0	0	0	0	0	0	1	0	0	0	0	0	1	0	0	0	0	0	0	0	0	0
Row 6	1	0	0	0	1	0	0	0	0	0	0	0	0	0	0	0	0	0	0	0	0	0	0	0	0	0	0	0	0	0	0
Total	32																														

	31	32	33	34	35	36	37	38	39	40	41	42	43	44	45	46	47	48	49	50	51	52	53	54	55	56	57	58	59	60	
Row 1	1	0	0	0	0	0	0	0	0	0	0	0	0	0	0	1	0	0	0	0	0	0	0	0	0	1	0	0	0	0	0
Row 2	0	0	0	0	0	0	0	0	1	0	0	0	0	0	0	0	0	0	0	0	0	0	0	0	0	0	0	0	1	0	0
Row 3	0	0	0	0	0	0	0	0	0	0	0	0	0	0	0	0	0	0	0	0	0										
Row 4	0	0	0	0	0	0	0	1	0	0	0	0	0	1	0	0	0	0	0	0	0	0	0	0	0	1	0	0	0	0	0
Row 5	0	0	0	0	0	0	0	0	0	0	0	0	0	0	0	0	0	0	0	1	0	0									
Row 6	0	0	0	0	0	0	0	0	0	1	0																				